Diss. ETH No.: 13287

Evaluation of Three Cocaine Analogues as PET Tracers for the Dopamine Transporter and Synthetic Approaches to [F-18]-DFMO

A thesis submitted to the

Swiss Federal Institute of Technology Zurich

For the degree of

Doctor of Natural Sciences

Presented by

Roland Daniel Schönbächler

Dipl. Chem. ETH Zurich

Born May 7th, 1970

Citizen of Einsiedeln/SZ

Accepted on the recommendation of

Prof. Dr. G. Folkers, examiner

Prof. Dr. P. A. Schubiger, co-examiner

1999

Acknowledgements

I would like to express my sincere gratitude to Professor Gerd Folkers for accepting me as a graduate student.

I would like to thank Professor P. August Schubiger for giving me the opportunity to conduct this interesting research project and for introducing me to the field of radiopharmacy.

My sincere thanks are due to Dr. Simon M. Ametamey who supervised this project. I profited greatly from his expertise in PET research and I am especially grateful for his enthusiasm, support, ideas and criticism.

My sincere thanks are due to all the PhD-students of the division of the "Center for Radioparmaceutical Sciences", especially Pascale Gucker for her encouragement, friendship and support during the time of my thesis and Joerg Spang and Marko Kokić for their friendship and numerous discussions.

I thank the past and present members in the division of the "Center for Radioparmaceutical Sciences", especially E. Sinnig, Dr. S. Samnick, M. Haeberli, R. Pellika, J. Jegge, A. Isenschmid, C. Vetter, Dr. M. Honer, S. Hengartner and D. Begel for their friendship, help and technical assistance, Dr. L. Allemann, M. Willmann and C. De Pasquale for their assistance with the animal experiments and Dr. G. Westera and Dr. J. Patt for the valuable discussions and technical help.

My thanks are further due to Professor Gustav K. von Schulthess, head of the Department of Nuclear Medicine of the University Hospital, and his co-workers T. Berthold, Dr. M. Arigoni, PD Dr. A. Buck, Dr. C. Burger, Dr. S. Kneifel and PD Dr. H.C. Steinert who showed great interest in my research project and contributed very much to the PET experiments and their evaluation.

I thank Dr. F.X. Vollenweider, at the Psychiatric University Hospital, and Dr. N. Khan, Dr. M. Vollenweider and Dr. R. Mettler for their medical support in this work.

Finally, I would like to thank my family and friends for their support.

Table of Contents

List of Abbreviations

5-HTT	serotonin transporter
ACE-Cl	1-chloroethyl chloroformate
BBB	blood-brain barrier
β-CPPIT	3β-(4'-chlorophenyl)-2β-(3'-phenylisoxazol-5'-yl)tropane
β-CIT	2β-carbomethoxy-3β-(4-iodophenyl)tropane
C_F	concentration of free ligand in tissue
C_{NS}	concentration of non-specifically bound ligand
C_P	tracer concentration in arterial plasma
C_S	concentration of specifically bound tracer
C_T	total concentration of ligand in tissue
d	deuteron
DAST	diethylaminosulfurtrifluoride
DAT	dopamine transporter
DFMO	α-difluoromethylornithine
DMF	dimethylformamide
DV	distribution volume
eq	equivalent
EOB	end of bombardment
FDG	2-fluoro-2-deoxy-glucose
FE-β-CPPIT	N-(2'-fluoroethyl-)-3β-(4'-chlorophenyl)-2β-(3'-phenylisoxazol-5'-yl)nortropane
FP-β-CPPIT	N-(2'-fluoropropyl-)-3β-(4'-chlorophenyl)-2β-(3'-phenylisoxazol-5'-yl)nortropane
FWHM	full width at half-maximum
HMPA	hexamethylphosphoramide
HPLC	high pressure liquid chromatography
ID	injected dose

i.v.	intravenous
K 2.2.2.	Kryptofix 2.2.2.®
LDA	lithium diisopropylamide
MeOH	methanol
MS	mass spectrometry
n	neutron
n.c.a.	no carrier added
NET	norepinephrine transporter
NMR	nuclear magnetic resonance
ODC	ornithine decarboxylase
p	proton
PET	positron emission tomography
p.i.	post-injection
ppm	parts per million
ROI	region of interest
rt	room temperature
SAM	S-adenosyl methionine
SPECT	single photon emission tomography
$t_{1/2}$	half-life
TEA	triethylamine
TFA	trifluoroacetic acid
THF	tetrahydrofuran
TLC	thin layer chromatography
vMAT	vesicular monoamine transporter

Summary

Positron emission tomography (PET) is an important diagnostic tool for the investigation of several diseases. The aim of this work was the synthesis, radiolabelling and the *in vivo* evaluation of new PET tracers for tumour diagnosis and for the quantification of the dopamine reuptake sites.

[F-18]-DFMO is a potential PET tracer for tumour diagnosis. Using ornithine as starting material, various attempts were made to prepare a suitable precursor for the fluorine-18 labelling of DFMO. Unfortunately, the synthetic methods investigated did not lead to the desired product.

The cocaine derivative, β-CPPIT, and two fluoroalkyl analogues were synthesised in order to get suitable tracers for imaging the dopamine transporter, which is implicated in degenerative brain disorders such as Parkinson's and Alzheimer's disease. β-CPPIT and its fluoroalkyl derivatives were prepared from cocaine and radiolabelled with carbon-11 or fluorine-18 in moderate yields. The *in vivo* properties of the tracers were evaluated in animal and human studies. In mice, [C-11]-β-CPPIT uptake in the striatum was 3.6fold higher than in the cerebellum (60 min p.i.) due to specific binding of the radiotracer to the DAT. To obtain information on the metabolism of [C-11]-β-CPPIT the metabolic fate of the radioligand in mice was also investigated. In the human PET study with six healthy volunteers, a high accumulation of [C-11]-β-CPPIT was observed in the striatum with a striatal-to-cerebellar ratio of 2.16 (60 min p.i.). In order to calculate the metabolite corrected input function of β-CPPIT, arterial blood samples were taken and analysed for metabolites. Kinetic modeling using a 1-tissue compartment model was performed to determine the rate constants for uptake (K_1) and release (k_2") and the volume of distribution (DV) of β-CPPIT in different brain areas. The results obtained were in analogy to the known distribution pattern of dopamine reuptake sites. For the *in vivo* evaluation of [F-18]-fluoroethyl- and [F-18]-fluoropropyl-β-CPPIT PET studies were performed in monkeys. Due to

high non-specific binding and rapid metabolism, [F-18]-FE-β-CPPIT and [F-18]-FP-β-CPPIT may not be suitable tracers for imaging the dopamine transporter. [C-11]-β-CPPIT, however, has proven to be a good candidate for imaging the dopamine reuptake sites using positron emission tomography. It therefore might be useful for the investigation of brain disorders related to alterations in the dopaminergic system.

Zusammenfassung

Die Positronen Emissions Tomographie (PET) ist ein wichtiges diagnostisches Hilfsmittel zur Untersuchung diverser Krankheiten. Ziel dieser Arbeit war es, neue PET-Liganden für die Tumordiagnostik einerseits und zur Quantifizierung der Dopamintransporter andererseits, zu synthetisieren, radioaktiv zu markieren und *in vivo* zu evaluieren.

[F-18]-DFMO ist ein potentieller PET-Tracer für die Tumordiagnostik. Ausgehend von Ornithin wurden diverse Methoden zur Synthese eines geeigneten Vorläufers für die [F-18]-Markierung von DFMO erprobt. Leider führten diese Versuche nicht zum gewünschten Produkt.

Zur bildlichen Darstellung des Dopamintransporters (DAT), welcher bei degenerativen Hirnerkrankungen wie z.B. Parkinson und Alzheimer eine wichtige Rolle spielt, wurden das Kokain-Derivat β-CPPIT und zwei fluorierte Analoga synthetisiert und mit Kohlenstoff-11 oder Fluor-18 radioaktiv markiert. Die *in vivo* Eigenschaften der PET-Liganden wurden in Tier- und Human-Studien evaluiert. Bei Mäusen wurde im Striatum, der Hirnregion höchster Dopamintransporter-Dichte, eine 3.6fache Traceraufnahme im Vergleich zum Cerebellum beobachtet (60 min p.i.), was auf die spezifische Bindung an den DAT zurückzuführen ist. Um Informationen über den Metabolismus von [C-11]-β-CPPIT zu erhalten, wurden in Mäusen auch Metabolitenstudien durchgeführt. In einer klinischen PET-Studie mit sechs gesunden Probanden konnte ebenfalls eine Anreicherung des [C-11]-β-CPPIT im Striatum beobachtet werden. Die Striatum zu Cerebellum-Ratio betrug 2.16 (60 min p.i.). Zur Korrektur der Input-Funktion, wurden arterielle Blutproben entnommen und der Anteil an radioaktiven Metaboliten im Plasma bestimmt. Die mittels tracer-kinetischer Analyse (2-Kompartiment-Modell) berechneten Distributions-volumina verschiedener Hirnregionen waren in Analogie zur bekannten Verteilung der Dopamintransporter im menschlichen Gehirn. Für die *in vivo* Evaluation von [F-18]-Fluorethyl- und [F-18]-Fluorpropyl-β-CPPIT wurden PET-

Studien in Affen durchgeführt. Diese Untersuchungen zeigten, dass [F-18]-FE- und [F-18]-FP-β-CPPIT aufgrund ihres schnellen Metabolismus und ihrer unspezifischen Bindung als PET-Tracer für den Dopamintransporter ungeeignet sind. [C-11]-β-CPPIT hingegen ist ein guter PET-Ligand für die bildliche Darstellung der Dopamintransporter und könnte Anwendung finden in der Diagnose von Hirnerkrankungen, welche mit einer Veränderung des dopaminergen Systems einhergehen.

1. Introduction

The aim of this work is the synthesis, radiolabelling and *in vivo* evaluation of new tracers for positron emission tomography: DFMO for tumour diagnosis and β-CPPIT for the quantification of the dopamine reuptake sites, respectively.

1.1. Positron emission tomography

Positron Emission Tomography (PET) is a quantitative imaging technique which allows the measurement of the regional concentration of a radiotracer in tissue. Examinations with PET radiopharmaceuticals give information about the uptake, biodistribution and secretion of the radiotracers in the organism and allow functional diagnostics of various diseases.

The most commonly used PET radionuclides are carbon-11 ($t_{1/2}$ = 20.4 min), nitrogen-13 ($t_{1/2}$ = 10.1 min), oxygen-15 ($t_{1/2}$ = 2.0 min) and fluorine-18 ($t_{1/2}$ = 110 min). As biomolecules mainly consist of stable isotopes of these elements, radiopharmaceuticals can be labelled with these PET radionuclides without effecting changes in their biochemical characteristics. Due to the stability of the bond formed and low steric hindrance arising from similarity in their van der Waals radius hydrogen is sometimes replaced by fluorine atom in organic molecules. Typical examples are [F-18]-tyrosine and [F-18]-fluoro-DOPA [1, 2].

PET radionuclides decay by positron emission. During the β^+-decay a proton is transformed into a neutron by emission of a positron and a neutrino. Immediately after the emission the positron collides with an electron. Such a collision results in two annihilation gamma ray photons each with an energy of 511 keV. The annihilation photons are emitted at an angle of nearly 180° [3]. The full width at half maximum (FWHM) of the emitted positron of the PET radionuclides is shown in table 1. The use of a coincidence camera for the

detection of the gamma ray emission leads to an improved resolution and sensitivity compared to Single Photon Emission Tomography (SPECT).

Another important property of the positron emitters is their short half-life (see table 1) which permits repeated studies in the same individual without radiation risks. However, the short half-lives of carbon-11, nitrogen-13 and oxygene-15 require an on site production of the radionuclides and the radioligands. Therefore, a cyclotron accelerator for isotope production and a special laboratory for radiolabelling have to be in the vicinity of the site of radioligand application [4].

1.2. Production of PET radionuclides

PET radionuclides are the products of nuclear reactions which are induced by the bombardment of stable isotopes with highly energetic protons or deuterons. The proton or deuteron is absorbed by the nucleus followed by the emission of a neutron or an α-particle. For the production of carbon-11 the target is filled with nitrogen containing traces of oxygen and bombarded with a proton beam. As soon as a proton hits a nitrogen nucleus the proton is taken up and an α-particle is emitted to give carbon-11. This process can be written as $^{14}N(p,\alpha)^{11}C$. Table 1 shows the nuclear reactions, the half-lives and the FWHM of some commonly used PET radionuclides.

radionuclide	**nuclear reaction** [3]	**half-life**	**FWHM** [5]
C-11	**$^{14}N(p,\alpha)^{11}C$** $^{11}B(p,n)^{11}C$	20.4 min	0.28 mm
N-13	**$^{16}O(p,\alpha)^{13}N$** $^{12}C(d,n)^{13}N$	10.1 min	0.39 mm
O-15	**$^{14}N(d,n)^{15}O$** $^{15}N(p,n)^{15}O$ *	2.1 min	1.05 mm
F-18	**$^{18}O(p,n)^{18}F$** * **(F^-)** **$^{20}Ne(d,\alpha)^{18}F$** **(F_2)**	110 min	0.22 mm

Table 1: Formation process, half-life and FWHM of carbon-11, nitrogen-13, oxygen-15 and fluorine-18. (Bold: most frequently used methods; *: enriched nuclides as target material)

1.3. PET radiopharmaceuticals in clinical use

PET radiopharmaceuticals have several different applications in nuclear medicine. The most important PET radiopharmaceuticals are listed in table 2.

radiotracer	measurement	literature
[C-11]-acetate	oxygen metabolism	[6-8]
[C-11]-flumazenil	benzodiazepine-receptor density	[9-11]
[C-11]-L-methionine	amino acid transport	[12-15]
[C-11]-McN-5652	serotonin transporter	[16-18]
[C-11]-raclopride	D_2-receptor-density	[19-22]
[N-13]-ammonia	perfusion	[23-26]
[O-15]-water	perfusion	[27-30]
[F-18]-FDG	glucose metabolism	[31-33]
[F-18]-6-fluoro-DOPA	dopamine metabolism	[1, 34, 35]
[F-18]-tyrosine	amino acid transport	[2, 36]

Table 2: Some important PET tracers and their use in nuclear medicine.

1.4. Radiopharmaceutical Aspects

The guidelines of several international groups of experts for the safety, quality assurance and quality control of short-lived radiopharmaceuticals have been summarised by Halldin and Nilsson [37, 38]. Short-lived radiopharmaceuticals have a special status among the pharmaceuticals based on the fact that they have to be produced under strict time limitations in the vicinity of the site of their use. Additionally, there is often not enough time between their production and their application to perform all accepted quality control testing. The six quality criteria which must be carried out for each individual preparation are described below (chapters 1.4.1 - 1.4.6).

According to GMP (Good Manufacturing Practice) production and quality assurance have to be fully documented with a general procedure and a batch protocol. Examples for working manuals, a batch protocol and a form for the quality control of β-CPPIT are shown in the appendix.

1.4.1. Radionuclide purity

PET radionuclides obtained by bombardment with protons or deuterons are normally contaminated with undesired radionuclides. Therefore, radionuclide purity has to be verified prior to application. For carbon-11 labelled radiopharmaceuticals radionuclide purity usually imposes negligible problems as impurities are eliminated during the synthetic pathway. Nevertheless, an investigation of this parameter is necessary during the set up phase. Radionuclide purity can be tested by checking the gamma ray spectra and the half-life of the product.

1.4.2. Chemical purity

Chemical identity, stereoisomeric purity and the absence of any undesired chemical compounds have to be checked to verify the chemical purity. This can normally be achieved by analytical HPLC with conditions different from the semi-preparative HPLC used for the purification of the radiotracer. The chemical purity can be verified by a comparison of the analytical HPLC-UV-chromatograms of product and standard.

1.4.3. Radiochemical purity

Radiochemical purity has to be verified to ensure the identity of the radiotracer (e.g. chemical structure of the labelled compound, position of labelling). Radiochemical purity can be checked with a radioactivity detector connected to the analytical HPLC under the same conditions used for the control of chemical purity. Routine radiochemical purity control has to be performed on every final product prior to application.

1.4.4. Specific radioactivity

The specific radioactivity is the ratio of the amount of radioactivity per mass of the radiotracer. It is usually expressed in Ci/mmol or GBq/µmol. The specific radioactivity can be calculated by comparison of the HPLC-UV-peak of the product and a standard. For quantitative PET receptor studies the specific radioactivity must be high (18.5-148 GBq/µmol) to minimise the influence of the unlabelled substance on the binding of the radiotracer and pharmacological effects.

1.4.5. Pharmaceutical quality

Prior to the first *in vivo* application of a PET radioligand a specified number of productions including quality control have to be performed. Tests for sterility, apyrogenicity and isotonicity must be evaluated and the pH of the formulated radioligand has to be in the acceptable range (pH 5-8). Isotonicity and pH of PET radiopharmaceuticals are tested for after each production. In contrast, sterility and apyrogenicity tests are performed after the application because the short half-life of the PET nuclides makes it impossible to wait for the results.

Due to the short half-life of carbon-11, sterilisation is generally achieved by the fastest method, the membrane filtration (pore size: 0.22 µm). For each radiotracer for human use the effectiveness of the sterilisation procedure are validated by an independent qualified professional using accepted procedures.

Pyrogens are bacterial endotoxins that cause fever. Usually they are bacterial by-products. It is required that pyrogen-free aqueous solutions, reagents and glassware are used. Apyrogenicity of the products are checked by an independent qualified professional using accepted procedures (e.g. Limulus amebocyte lysate-test). The test has to be performed frequently in routine production runs. If the synthesis is not regularly carried out, new tests must be performed before allowing a new administration to humans.

1.4.6. Stability and shelf-life

The stability and shelf-life of a radiotracer have to be checked during the evaluation of the compound. This control is normally achieved by HPLC-chromatography by analysing the stability of the compound over a period of at least three physical half-lives (see above: 1.4.2. and 1.4.3.). Further investigations of stability do not make sense as the tracers cannot be used later in any case because the specific radioactivity and the total amount of radioactivity becomes too low for *in vivo* application.

2. Synthetic Approaches to [F-18]-α-Difluoromethyl-ornithine ([F-18]-DFMO)

The various attempts to get a suitable precursor for no carrier added (n.c.a.) radiolabelling of DFMO **1** using [F-18]-fluoride are described in this chapter. Only the synthesis of ethyl-2-chlorofluoromethyl-2-methoxycarbonylamino-5-phthalimidopentanoate (**2**) led to the desired precursor which was then used for labelling experiments.

2.1. Introduction

As cancer is one of the major causes of death, tumour diagnosis is an important field in medicine. α-Difluoromethylornithine (**1**, figure 1) could be a potential PET tracer for tumour diagnosis if labelled with a positron emitting nuclide such as fluorine-18. In recent years, PET has become an important diagnostic tool to optimise the therapy of cancer patients for the following reasons:

- **Tumour detection at an early stage**: [F-18]-FDG-PET allows the detection of tumours larger than 0.5 cm. Therefore, tumours can be detected at an early stage which increases the probability of a successful therapy. With PET whole body imaging can be performed. Therefore, all organs can be examined for metastases with one PET scan. The exact knowledge of the stage of a tumour is important in choosing the ideal therapy.
- **Control of therapy**: PET as an imaging technique can also be used to follow treatment response. This information is essential for an optimisation of the therapy.
- **Monitoring**: After a tumour therapy the distinction between a scar and a residual can be made by PET with high specificity.

Malignant tumours consist of cells with features different from those of normal tissue. Because of the general loss of organ-specific cell functions, the search for suitable substances for tumour scintigraphy has not led to radiopharmaceuticals with tumour-selective enrichment. Tumour imaging can normally better be achieved with radiopharmaceuticals which are designed for the visualisation of changes in the regional physiology of the host tissue [39].

The most important PET tracer in routine clinical use for tumour imaging is [F-18]-2-fluoro-2-deoxy-glucose ([F-18]-FDG). It is used to measure the glucose metabolism which is increased in tumour cells. This is because tumour cells have a higher cell division and a higher energy consumption.

Amino acids such as [C-11]-methionine and [F-18]-fluorotyrosine have also found use as tumour imaging agents in humans [2, 12-15, 36] measuring the increased amino acid transport into brain tumours.

α-Difluoromethylornithine (DFMO, **1**, figure 1) is another amino acid which might serve as a PET tracer for tumour diagnosis if labelled with fluorine-18. DFMO has already been labelled with tritium and carbon-14 and used for studies of the enzyme ornithine decarboxylase (ODC) [40-49]. DFMO is an irreversible inhibitor of ODC [50]. This enzyme is involved in the rate-limiting step of the biosynthesis of the polyamines putrescine, spermidine and spermine (scheme 1) [51]. As the levels of these polyamines are increased in fast growing tissues such as tumours [52], ODC activity could be a marker for tumour growth rate [53]. It should therefore be possible to identify tumour tissue by quantifying ODC-activity using a labelled irreversible inhibitor such as [F-18]-DFMO. The mechanism by which DFMO inhibits ODC as proposed by Bey and co-workers is outlined in scheme 2 [54-56]. DFMO binds to the cofactor pyridoxalphosphate followed by decarboxylation of DFMO. Upon fluoride elimination the formed enimine **3** reacts with an amino acid of the active site of ODC which results in covalent binding and subsequent inactivation of ODC.

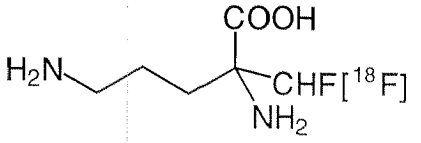

1

Figure 1: Structure of [F-18]-α-difluoromethylornithine (**1**)

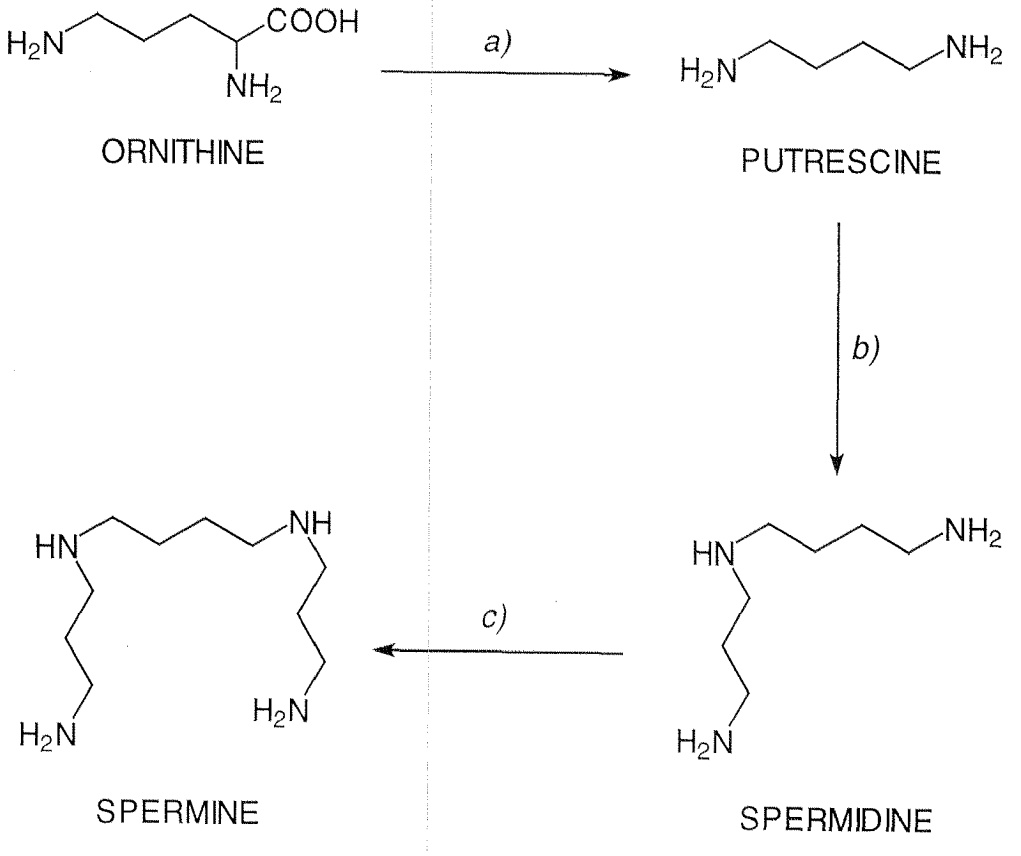

Scheme 1: Biosynthesis of the polyamines putrescine, spermidine and spermine starting from ornithine: *a)* ODC; *b)* decarboxylated SAM; *c)* decarboxylated SAM.

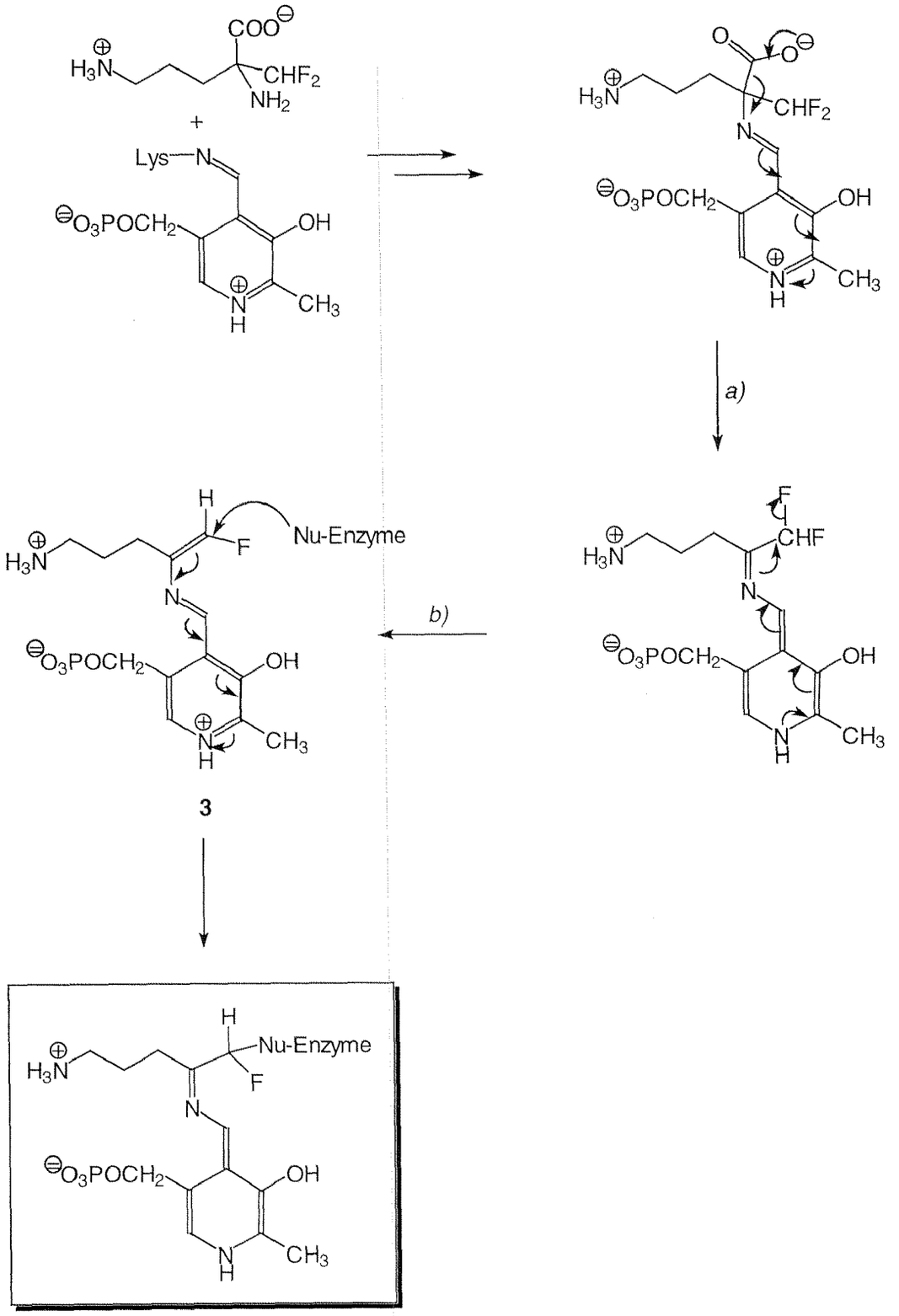

Scheme 2: Mechanism of the DFMO induced ODC inhibition proposed by Bey and co-workers [54-56]: *a)* – CO_2; *b)* – F^-.

The aim of this study was to substitute one of the fluorine atoms of DFMO by fluorine-18 in order to get a potential PET radiotracer for tumour diagnosis.

2.2. Precursor synthesis and radiolabelling

2.2.1. Methylation of ornithine

α-Bromo- and α-chlorofluoromethylornithine derivatives should be suitable precursors for the radiolabelling of DFMO with [F-18]-fluoride by a SN_2-reaction. An approach for the synthesis of these precursors is the methylation of ornithine with the corresponding halomethanes. This procedure is known from the literature for the synthesis of other α-halomethylornithine derivatives including DFMO [57].

Prior to the methylation reaction, the amino functions have to be protected to avoid methylation at the nitrogen atoms. These protecting groups must be stable under the conditions of methylation and furthermore, they should be easily cleavable. Therefore, the benzylidene protecting group was chosen. This Schiff base was obtained by reacting ornithinemethylester dihydrochloride (**4**) with benzaldehyde in the presence of triethylamine (scheme 3) in analogy to the method reported in the literature [57-59]. The resulting methyl-2,5-bis(benzylideneamino)pentanoate (**5**) was obtained in 69% yield.

The bis(para-nitro-benzylideneamino)pentanoate (**6**) was synthesised under similar conditions [60]. The introduction of the nitro function in the para-position should stabilise the anion formed during the methylation.

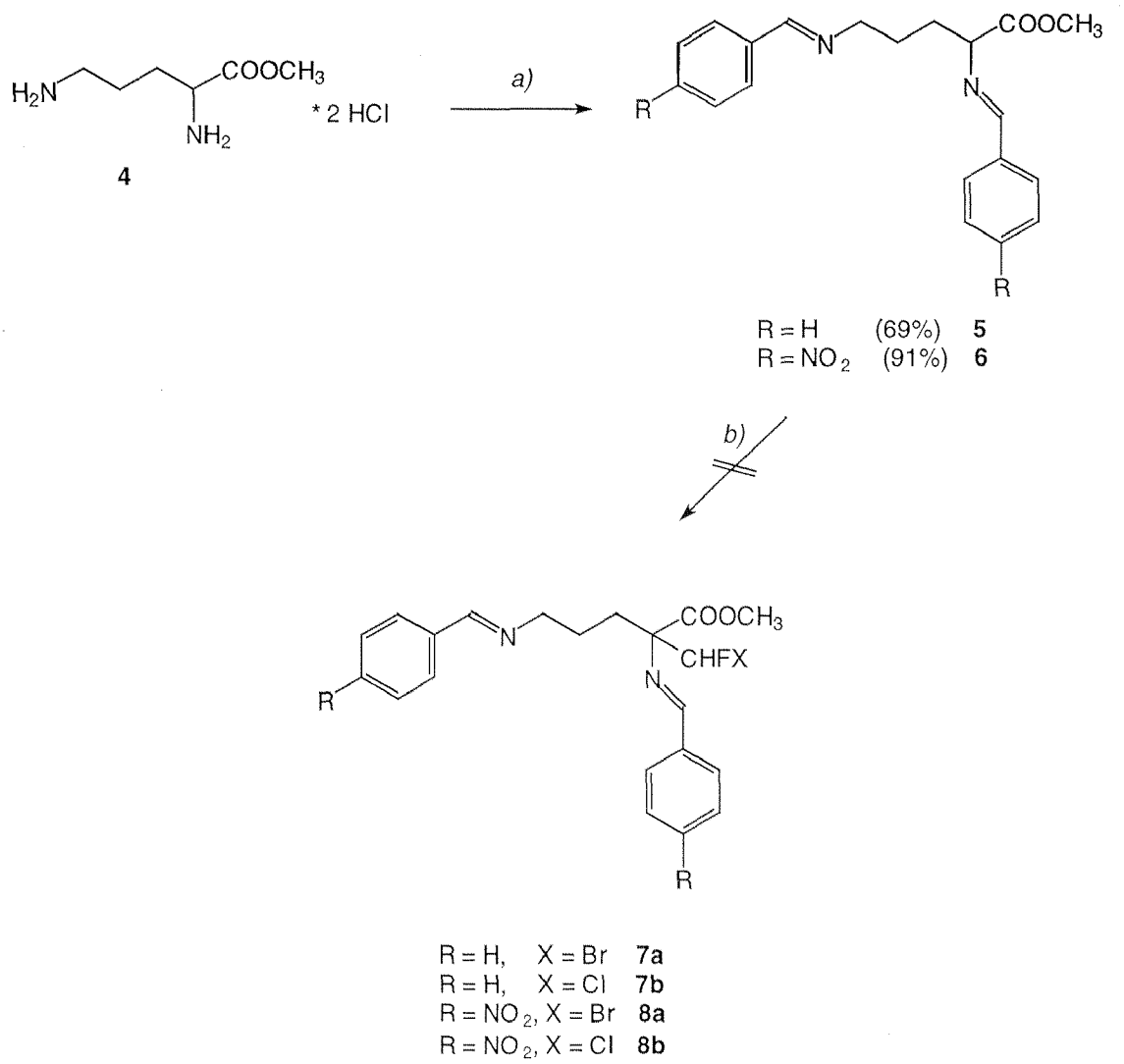

Scheme 3: Synthesis of the α-chlorofluoromethyl- and α-bromofluoromethyl precursors **7** and **8**: *a)* benzaldehyde or para-nitro-benzaldehyde, TEA; *b)* 1) base, 2) CHX_2F.

The methylation step was carried out under absolutely dry conditions by reacting the diimines **5** or **6** with sodium hydride at -78°C followed by the addition of a dihalofluoromethane (scheme 3) according to literature procedures [57-60]. Neither HPLC nor mass spectrometry indicated the formation of compounds **7** and **8**. Solvent, base and temperature variations did not lead to the desired compounds. Attempts to activate the intermediate anion by complexation of the counterion with a potassium-specific cryptand (Kryptofix

2.2.2.® (K 2.2.2., figure 2)), also failed. Some of the tested reaction conditions are shown in table 3.

educt	**base**	**methylhalide**	**solvent**	**temperature**
5	NaH (ca. 1.2 eq.)	$CHFBr_2$ (1.3 eq.)	THF	-78°C → rt (22h)
5	NaH	$CHFCl_2$	THF	rt → 40°C (72h)
5	LDA	$CHFCl_2$	THF	-78°C → 40°C (50h)
5	LDA	$CHFCl_2$	THF	rt (40h)
5	LDA	$CHFBr_2$	THF	rt (40h)
5	LDA	$CHFCl_2$	CH_3CN	rt (40h)
5	LDA	$CHFBr_2$	CH_3CN	rt (40h)
6	NaH (ca. 1.5 eq.)	$CHFBr_2$ (11.5 eq.)	DMF	0°C → rt (5h)
6	NaH (ca. 1.5 eq.)	$CHFBr_2$ (13.4 eq.)	THF	0°C → rt (72h) 50°C (45min)
6	NaH (ca. 1.4 eq.)	$CHFBr_2$ (16.3 eq.)	THF + HMPA	-20°C → rt (3h) rt (17h) 50°C (72h)
6	NaH (ca. 1.4 eq.)	$CHFBr_2$ (27.7 eq.)	THF	rt (160h) 50°C (20h)
6	NaH	$CHFCl_2$	THF	rt → 40°C (72h)
6	LDA	$CHFCl_2$	THF	78°C → 40°C (50h)
6	KO^tBu (ca. 1.2 eq)	$CHFBr_2$ (11.9 eq.)	CH_3CN	70°C (30min)

Table 3: Some of the tested reaction conditions for the methylation of the ornithine derivatives **5** and **6**

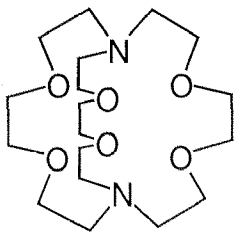

Figure 2: Structure of Kryptofix 2.2.2.®

In an attempt to verify whether the intermediate anion was formed at all, methylation was performed under similar conditions with iodomethane. Because the methylation gave the expected product, the failure of the methylation with the dihalofluoromethanes might be due to the low stability of the desired products or due to a steric hindrance.

2.2.2. Methylation of piperidinone derivatives

The possibility to use the piperidinone derivative **9** (scheme 4) was considered as an alternative. An advantage of using the piperidinone **9** compared to the aliphatic analogues is the absence of the methylester group which should reduce the radiosynthesis time of [F-18]-DFMO.

3-Amino-piperidinone (**9**) was obtained in a 91% yield by the intramolecular cyclisation of ornithine dihydrochloride (**4**) using sodium methanolate as base according to literature procedures [60-63]. The amino group of the piperidinone **9** was protected as imine. Unfortunately, the methylation reactions with dichlorofluoromethane and dibromofluoromethane under the conditions described above were also not succesful.

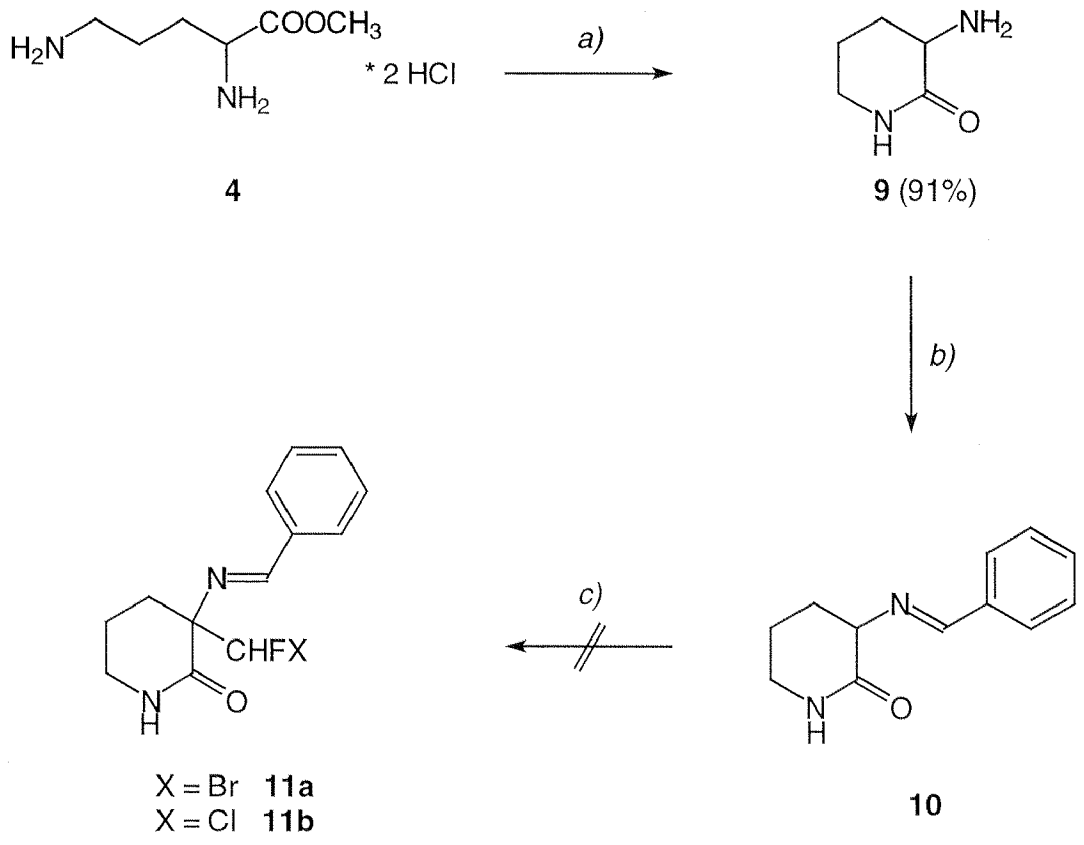

Scheme 4: Synthesis of the piperidinone precursor **215**: *a)* NaOMe; *b)* benzaldehyde, TEA; *c)* 1) base, 2) CHX_2F.

2.2.3. Fluorine-bromine exchange

The direct fluorine-bromine-exchange for an α-fluoromethyl amino acid has been described by Gerhardt and co-workers [64]. Under similar conditions the treatment of difluoromethylornithine dihydrochloride (**4**) with sodium hydroxide and hydrogen bromide gave no traces of the desired α-bromofluoromethyl-ornithine **12** (scheme 5). Mass spectra analysis showed only unreacted DFMO.

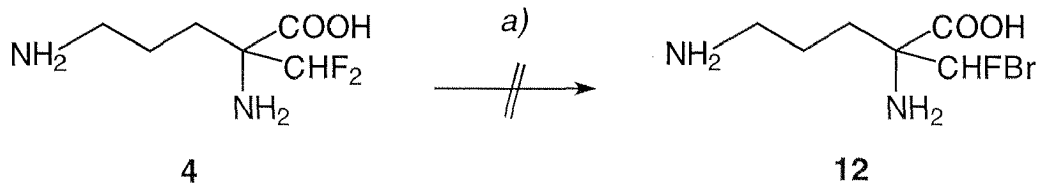

4 12

Scheme 5: Fluorine-bromine exchange: *a)* 1) NaOH, 2) HBr.

2.2.4. Ethyl-2-chlorofluoromethyl-2-methoxycarbonylamino-5-phthalimido-pentanoate (2)

The synthesis of the pentanoate **2** as a potential precursor was considered as an alternative for the direct fluorine-18 labelling. The substitution of the chloro atom by a fluoro functionality has been reported in the literature [65, 66]. Following the procedure reported by Schirlin and co-workers [67] the synthesis of precursor **2** was undertaken. Compound **14** was obtained in a 50% yield by reacting tert.-butyl-ethyl-malonate (**13**) with sodium hydride followed by the addition of bromo-phthalimido-propane under anhydrous conditions (schema 6). The resulting diester **14** was deprotonated with sodium hydride and alkylated with a large excess of dichlorofluoromethane at room temperature to give tert.-butylester **15** in 18% yield. Diester **15** was further converted to the carbamate **2** by treatment with trifluoroacetic acid (TFA) followed by a standard Curtius rearrangement sequence in 74% yield.

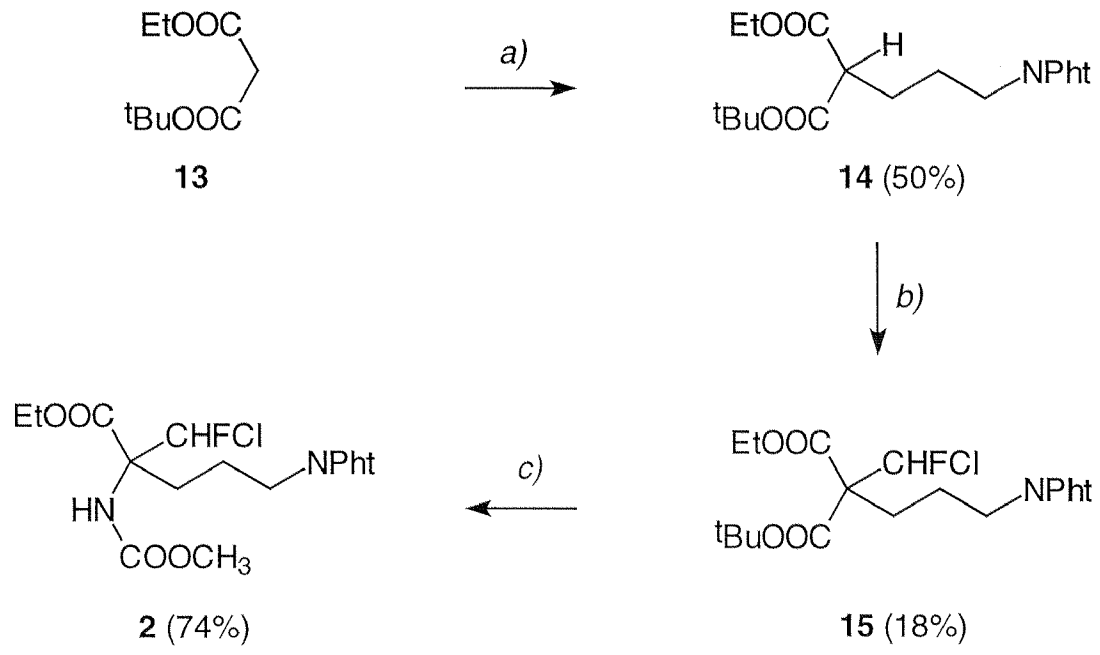

Scheme 6: Precursor synthesis according to a procedure described by Schirlin and co-workers [67]: *a)* 1) NaH, 2) $Br(CH_2)_3NPht$; *b)* 1) NaH, 2) CHFCl; *c)* 1) TFA, 2) $SOCl_2$, 3) NaN_3, 4) Δ.

Due to the asymmetry of the chlorofluoromethyl substituent four stereoisomers of the carbamate **2** are possible (figure 3). The two pairs of enantiomers (R,R;S,S and R,S;S,R) were obtained in a 1:1 mixture and were separated by flash chromatography. Each pair of enantiomers was used directly for the fluorine-18 radiolabelling experiments without any further separation because these can be separated after the radiolabelling more easily by HPLC using a chiral mobile phase [68, 69].

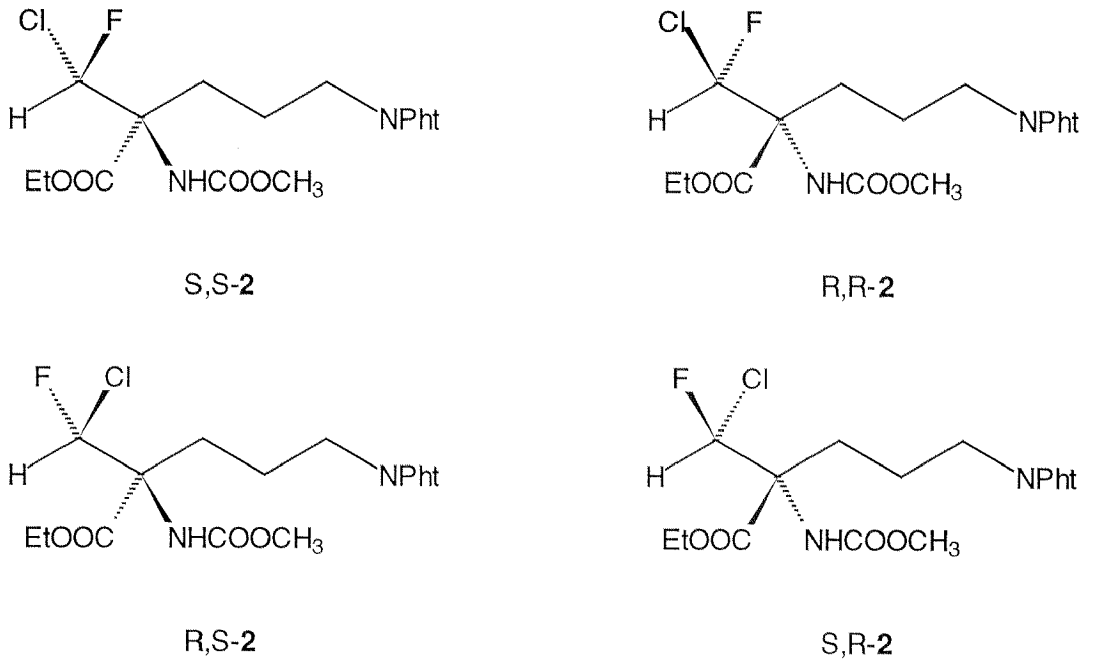

Figure 3: The four stereoisomers of ethyl-2-chlorofluoromethyl-2-methoxy-carbonylamino-5-phthalimidopentanoate (**2**).

The nucleophilic substitution of the chloro atom in compound **2** with [F-18]-fluoride was undertaken by using [F-18]-potassium fluoride and Kryptofix 2.2.2.® and standard n.c.a. fluorination reaction conditions [70] (scheme 7). The reaction was carried out in DMSO and reaction time and temperature were varied from 30-60 min and 120-160°C, respectively. After work up and analysis by HPLC and radio-TLC no [F-18]-DFMO (**1**) could be detected.

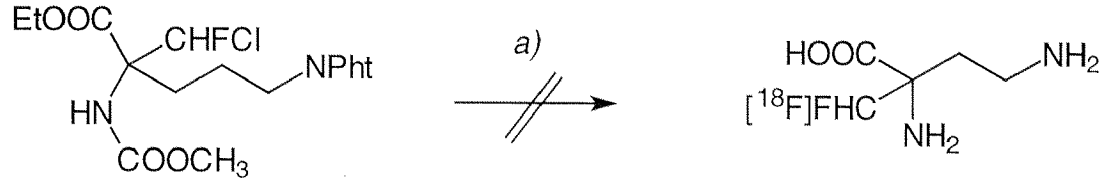

2-R,R;S,S or **2-R,S;S,R** **[F-18]-1**

Scheme 7: Radiolabelling of the chloro precursor **2** with Kryptofix 2.2.2.®: *a)* 1) [F-18]-KF, K 2.2.2.; 2) HCl.

The approach described by Angelini and co-workers [65, 66] was also tried. Antimony oxide was used instead of potassium carbonate and Kryptofix 2.2.2.® complex (scheme 8). Various reaction parameters such as reaction time and temperature were tested and in this case also no evidence for the radiolabelled product was found.

For the chlorine-fluorine exchange reaction Angelini co-workers reported a high temperature dependency of the yield. Unfortunately, at temperatures higher than 160°C decomposition of the starting materials occurred suggesting that pentanoate **2** is unsuitable as a precursor for the n.c.a. [F-18]-fluorination of DFMO.

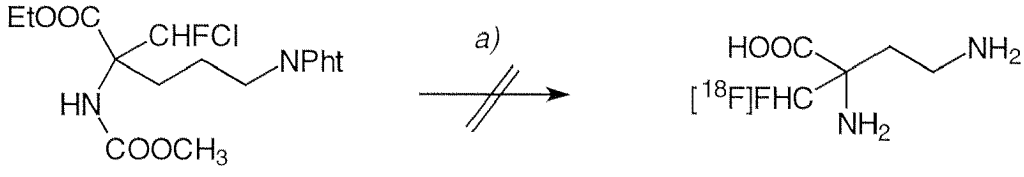

2-R,R;S,S or **2-R,S;S,R** **[F-18]-1**

Scheme 8: Radiolabelling of the chloro precursor **2** with antimony oxide: *a)* 1) Sb_2O_3, [F-18]-HF 2) HCl.

2.2.5. Ethyl-2-iodofluoromethyl-2-methoxycarbonylamino-5-phthalimido-pentanoate (16)

In order to obtain a better leaving group an attempt was made to synthesise the iodo analogue of compound **2** by a substitution reaction (scheme 9). The synthesis of iodo derivatives from their corresponding chloro analogues has been described elsewhere [71]. When the iodine displacement reaction was performed under standard reaction conditions, no product formation was observed. Next, varying reaction parameters such as temperature and sodium iodide concentration were investigated. Unfortunately, these conditions also did not effect the synthesis of compound **16**.

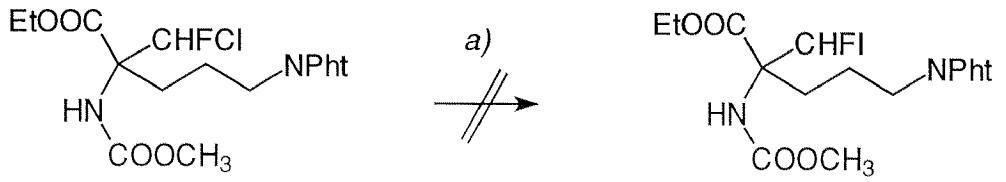

2 16

Scheme 9: Synthesis of precursor **16**: *a)* NaI.

2.3. Conclusion

Our attempts to prepare [F-18]-DFMO have been described. The synthetic approaches adapted were intended to lead to [F-18]-DFMO, which could be very useful for tumour imaging using PET. However, as described we were unable to prepare [F-18]-DFMO *via* SN_2-reaction. Therefore, no further investigations beyond these attempts were undertaken.

2.4. Experimental

2.4.1. General procedures

Diethylether and tetrahydrofuran (THF) were dried over sodium and benzophenone. Dibromo- and dichlorofluoromethane were obtained from ABCR, Karlsruhe, Germany; ornithine hydrochloride and ornithinemethylester dihydrochloride from Bachem. All the other chemicals were obtained from Fluka AG, Merck AG or Aldrich AG.

Column chromatography was performed on silica gel (Kieselgel 60, Merck). The solvent is noted in brackets.

For the radio-TLC silica gel plates (Kieselgel 60/UV_{254}, Merck) were used and analysed on a Berthold Tracemaster 20 automatic TLC-linear analyser

NMR-spectra were recorded on a Bruker AC-250 (^{1}H: 300 MHz) using TMS as an internal standard. The signals are reported in ppm (δ) downfield.

Mass spectra were recorded on a Trio 2000 Spectrometer (VG Organic, UK) using positive ion mode with electrospray as interface (ES^+).

2.4.2. Synthesis

2.4.2.1. Methyl-2,5,-bis(benzylideneamino)pentanoate (5) [58]

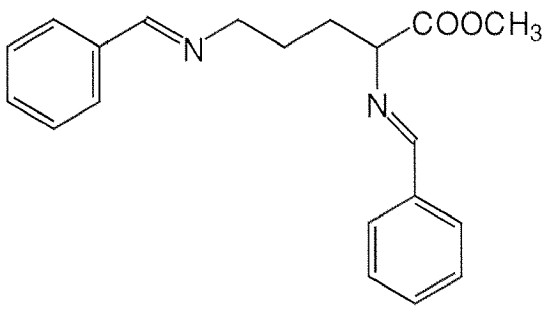

A solution of triethylamine (7.6 ml, 54.8 mmol) in dichloromethane (7 ml) was added slowly to a suspension of ornithinemethylester dihydrochloride (**4**) (6.0 g, 27.4 mmol) and freshly distilled benzaldehyde (5.8 g, 54.8 mmol) in dichloromethane (20 ml) at 0°C under vigorous stirring. The reaction mixture was stirred overnight at room temperature. After removal of the solvent the residue was taken up in anhydrous diethylether. The insoluble material was filtered off. The filtrate was washed three times with water and brine, dried over magnesium sulfate and concentrated under reduced pressure. 6.1 g (69%) of the pentanoate **5** were obtained. An analytical sample was further purified by recrystallisation from pentane.

MS: 323 (100, $C_{20}H_{23}N_2O_2^+$).

^{1}H-NMR ($CDCl_3$): 1.35 - 2.35 (m, 4 H), 3.5 - 3.8 (m, 2 H), 3.7 (s, 3H), 4.02 (b, t, 1 H, J = 6 Hz), 7.18 - 7.85 (m, 10 H), 8.21(s, 2 H).

2.4.2.2. Methyl-2,5,-bis(p-nitro-benzylideneamino)pentanoate (6) [60]

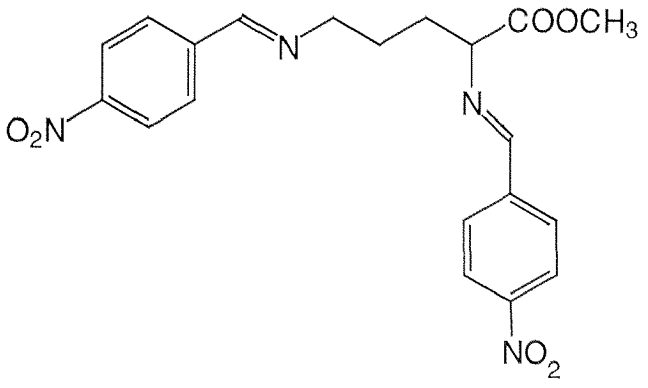

A solution of triethylamine (1.9 ml) in dichloromethane (3 ml) was added dropwise to a stirred suspension of ornithinemethylester dihydrochloride (**4**) (1,5 g, 6.8 mmol) and p-nitro-benzaldehyde (2.1 g, 13.7 mmol) in dichloromethane (20 ml) at 0°C. The reaction mixture was stirred overnight at room temperature. After the removal of the solvent, the crude product was redissolved in diethylether. The insoluble material was filtered off. The filtrate was washed three times with water and brine, dried over magnesium sulfate and concentrated under reduced pressure. 2.6 g (92%) of the pentanoate **6** were obtained.

MS: 413 (100, $C_{20}H_{21}N_4O_6^+$).

^{1}H-NMR ($CDCl_3$): 1.95 - 2.42 (m, 4 H), 2.92 - 3.05 (m, 2 H), 3.42 - 3.52 (m, 1 H), 3.88 (s, 3H), 7.15 - 7.19 (m, 4 H), 7.93 - 7.99 (m, 4 H) 8.15 (m, 2 H).

2.4.2.3. 3-Amino-2-piperidinone (9) [61]

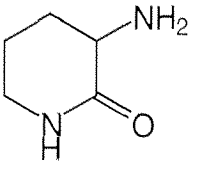

A solution of sodium (420 mg, 18.3 mmol) in MeOH (40 ml) was added dropwise to a vigorously stirred solution of ornithinemethylester dihydrochloride

(**4**) (2.0 g, 9.1 mmol) in MeOH (160 ml). After 15 min the reaction mixture was evaporated to dryness, redissolved in chloroform (80 ml) and stirred for additional 30 min. The insoluble material was filtered off and the filtrate was concentrated under reduced pressure. By cooling the resulting oil in the refrigerator light yellow crystals were formed (950 mg (91%)).

MS: 115 (100, $C_5H_{11}N_2O^+$).

^{1}H-NMR ($CDCl_3$): 1.52 - 1.99 (m, 5 H); 2.15 - 2.30 (m, 1 H); 3.25 - 3.39 (m, 3 H); 6.01 (s, b, 1H).

2.4.2.4. tert.-Butyl-ethyl-2-(3-phthalimidpropyl)malonate (14) [67]

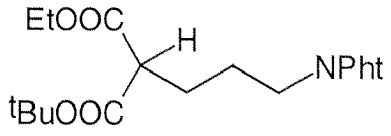

A mixture of tert.-butyl-ethyl-malonate (**13**) (4.0 ml, 30 mmol) and sodium hydride (1.2 g (60% suspension in oil), 30 mmol) in anhydrous THF (40 ml) was stirred at room temperature under nitrogen for 4 h before adding a solution of 1-bromo-3-phthalimidopropane (8.04 g, 30 mmol) in anhydrous THF (20 ml). After stirring for further 15 h at room temperature the reaction mixture was hydrolysed and extracted with diethylether. The combined organic layers were washed with brine and dried over anhydrous magnesium sulfate. Removal of the solvent under reduced pressure led to the crude product which was further purified by column chromatography (ethyl acetate : hexane = 1 : 1). 5.60 g (50%) of the diester **14** could be isolated.

MS: 398 (100, $C_{20}H_{25}NO_6Na^+$).

^{1}H-NMR ($CDCl_3$): 1.23 (t, 3 H, J = 7), 1.43 (s, 9 H), 1.70 - 2.00 (m, 4 H), 3.27 (t, 1H, J = 7), 3.68 (t, 2 H, J = 7), 4.14 (q, 2 H, J = 7), 7.71 (m, 4 H)

2.4.2.5. tert.-Butyl-ethyl-2-chlorofluoromethyl-2-(3-phthalimidopropyl)-malonate (15) [67]

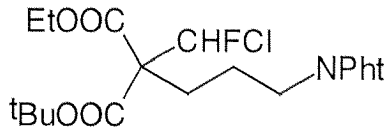

A mixture of tert.-butyl-ethyl-2-(3-phthalimidpropyl)malonate (**14**) (2.82 g, 7.5 mmol) and sodium hydride (0.29 g (60% suspension in oil), 7.5 mmol) in anhydrous THF (50 ml) was stirred under nitrogen at room temperature for 2 h. After cooling to -30°C dichlorofluoromethane (Freon 21, 13 ml) was added. The mixture was stirred for 15 h at room temperature, hydrolysed and extracted with diethylether. The combined organic layers were washed with brine and dried over anhydrous magnesium sulfate. The solvent was removed under reduced pressure. The resulting oil was further purified by column chromatography (ethyl acetate : hexane = 2 : 8). 0.6 g (18%) of the diester **15** were obtained as white crystals.

MS: 466 (33, $C_{21}H_{25}NO_6{}^{37}ClFNa^+$); 464 (100, $C_{21}H_{25}NO_6{}^{35}ClFNa^+$).

^{1}H-NMR ($CDCl_3$):1.23 (t, 3 H, J = 7), 1.43 (s, 9 H), 1.65 - 2.30 (m, 4 H), 3.67 (t, 2 H, J = 7), 4.19 (q, 2 H, J = 7), 6.60 (d, 1 H, J_{HF} = 48), 7.73 (m, 4 H)

2.4.2.6. Ethyl-2-chlorofluoromethyl-2-methoxycarbonylamino-5-phthalimidopentanoate (2) [67]

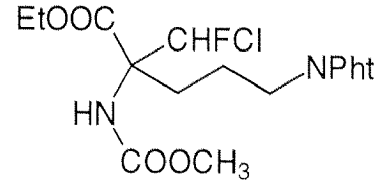

A mixture of the diester **15** (0.3 g, 0.67 mmol) and TFA (3 ml) was stirred at 0°C for 30 min. The solvent was removed under reduced pressure. The obtained

crude ethyl 2-chlorofluoromethyl-2-(3-phthalimidopropyl)malonate was redissolved in thionyl dichloride (5 ml). The resulting mixture was heated at reflux for 2 h. The removal of the solvent under reduced pressure led to the crude acyl chloride which was redissolved in acetone (2.5 ml) before adding a solution of sodium azide (104 mg, 1.6 mmol) in water (0.35 ml). After stirring for further 45 min at 0°C water (2 ml) was added. The mixture was extracted with diethylether. The combined organic layers were dried over anhydrous magnesium sulfate and concentrated under reduced pressure to give the crude acyl azide. A solution of the azide in anhydrous methanol (10 ml) was heated under reflux for 5 h. After the removal of the solvent under reduced pressure the crude carbamate **2** was purified by column chromatography (ethyl acetate : hexane = 2 : 8) which led to the separation of the two pairs of enatiomers of the carbamate **2** as pure crystalline materials.

1st eluted pair of enantiomers (R,R;S,S: 114.4 mg; 41%):

MS: 439 (33, $C_{18}H_{20}N_2O_6{}^{37}ClFNa^+$), 437 (100, $C_{18}H_{20}N_2O_6{}^{35}ClFNa^+$).

^{1}H-NMR ($CDCl_3$): 1.35 (t, 3 H, J = 7), 1.40 -2.85 (m, 4 H), 3.60 - 3.70 (m, 5 H), 4.30 (q, 2 H, J = 7), 5.95 (s, b, 1 H), 6.55 (d, 1 H, J_{HF} = 48), 7.75 (m, 4 H).

2nd eluted pair of enantiomers (R,S;S,R: 90.3 mg; 33%):

MS: 439 (40, $C_{18}H_{20}N_2O_6{}^{37}ClFNa^+$), 437 (100, $C_{18}H_{20}N_2O_6{}^{35}ClFNa^+$).

^{1}H-NMR ($CDCl_3$): 1.28 (t, 3 H, J = 7), 1.45 -2.90 (m, 4 H), 3.55 - 3.65 (m, 5 H), 4.25 (q, 2 H, J = 7), 5.85 (s, b, 1 H), 6.50 (d, 1 H, J_{HF} = 49), 7.78 (m, 4 H).

3. Synthesis and Evaluation of [C-11]-, [F-18]-FE- and [F-18]-FP-β-CPPIT

3.1. Introduction

Carbon-11 labelled 3β-(4'-chlorophenyl)-2β-(3'-phenylisoxazol-5'-yl)tropane ([C-11]-β-CPPIT, **17**) and the fluorine-18 labelled fluoroethyl- and fluoropropyl analogues **18** and **19** were synthesised as potential PET tracers for the dopamine transporter (DAT).

Dopamine has been identified as a neurotransmitter in the 50's [72]. It was found in high concentrations in the basal ganglia and in the substantia nigra of the mammalian brain [73, 74]. Dopamine is released from the presynaptic neuron into the synaptic cleft where it binds to specific receptors. Five receptor subtypes (D_1 - D_5) have been identified to date [75] (figure 4). Dopamine is either metabolised or transported back into the presynaptic nerve by a specific transporter, the DAT. The gene for the DAT has been cloned and the full length encoded protein sequence has been expressed in cultured cells [76, 77].

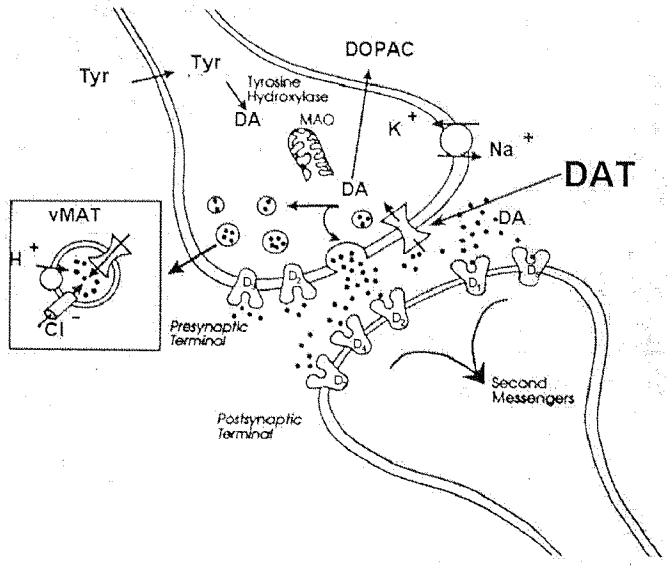

Figure 4: Schematic drawing of a dopaminergic synapse [78]. (D_1-D_5: dopamine receptor subtypes; DA: dopamine; MAO: monoamine oxidase).

Many brain disorders are related to alterations of the dopaminergic system. As the DAT is located presynaptically on dopaminergic nerve terminals [76, 77, 79], it can be used as a suitable marker for neurological diseases related to dopaminergic neurones. A markedly reduced density of the DATs has been demonstrated in the basal ganglia of post-mortem brains from patients with degenerative brain disorders such as Parkinson's, Huntington's and Alzheimer's diseases and recently in the living human brain [80-83].

The stimulant and reinforcing properties of cocaine have been ascribed to its ability to inhibit the DAT [84]. Cocaine itself has been labelled with carbon-11 and used for PET studies in humans [85, 86]. Because the affinity of cocaine is rather low (IC_{50} = 89.1 nM [87]), attempts have been made to identify more potent antagonists for the DAT. Consequently, several compounds based on the cocaine structure, have been examined *in vitro*. Most of these derivatives displayed higher affinities and were therefore radiolabelled with carbon-11 or fluorine-18 for PET or with iodine-123 for SPECT [88-95]. An undesired property accompanying striatal uptake of most of these cocaine analogues has been the high to moderate binding to the serotonin transporter (5-HTT) and the norepinephrine transporter (NET) [91, 96, 97]. Recently, the synthesis and the *in vitro* biological evaluation of the new cocaine analogue β-CPPIT (figure 5), with improved selectivity for the DAT has been published [98]. The IC_{50} value for the DAT of 1.28 nM combined with 5-HTT/DAT and NET/DAT ratios of 1891 and 393, respectively have been reported (see table 4) [98]. Compared to the commonly used β-CIT **20** (2β-carbomethoxy-3β-(4-iodophenyl)-tropane), β-CPPIT is 630-fold more selective for the DAT. In contrast to existing DAT radioligands, this new analogue bears the isoxazole heterocyclic group at the C-2β-position of the tropane ring. Due to the absence of the metabolically labile 2β-ester function, β-CPPIT is expected to be stable against the action of esterases. Another tropane analogue lacking the ester group at the 2β-position has been synthesised and radiolabelled with carbon-11 [99]. However, to date no *in vivo* data on this new tropane derivative has been published.

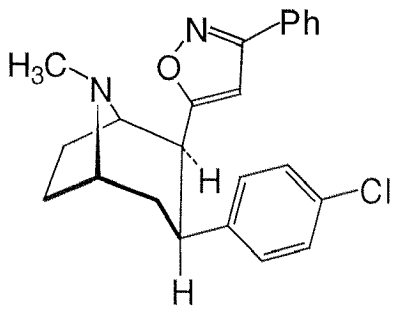

β-CPPIT

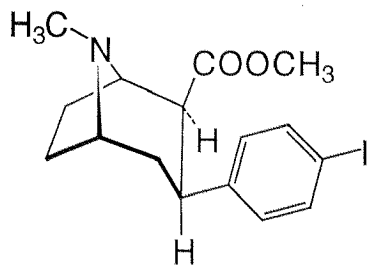

β-CIT

Figure 5: Structures of β-CPPIT and β-CIT

	cocaine [87]	**β-CIT [87]**	**β-CPPIT [98]**
Dopamine (DAT)	89.1 ± 4.8	1.26 ± 0.04	1.28 ± 0.18
Serotonin (5-HTT)	1045 ± 89	4.21 ± 0.34	2420 ± 136
Norepinephrine (NET)	3298 ± 293	36.0 ± 2.7	504 ± 29
5-HTT / DAT	12	3	**1891**
NET / DAT	37	29	**393**

Table 4: *In vitro* IC_{50}-values of cocaine and derivatives [nM] and the corresponding ratios (from literature).

A disadvantage of carbon-11 labelled compounds like [C-11]-β-CPPIT is their short physical half-life (20.4 min), which results in a short time frame for PET measurement. This problem can be overcome by the use of fluorine-18 labelled analogues (fluorine-18: $t_{1/2}$ = 110 min). Therefore, to increase the time frame of the PET studies the [F-18]-fluoroethyl and [F-18]-fluoropropyl analogues of β-CPPIT were synthesised.

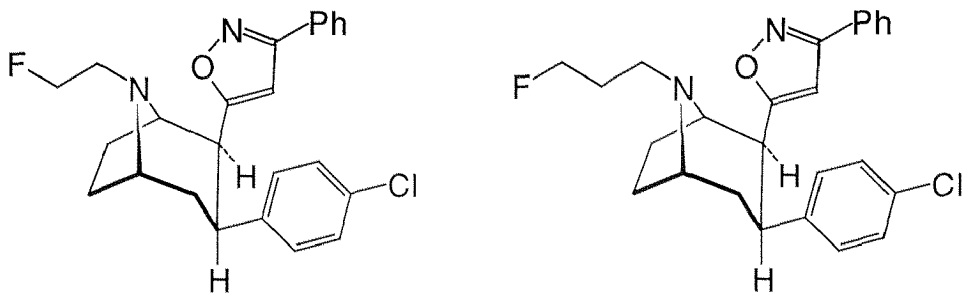

FE-β-CPPIT FP-β-CPPIT

Figure 6: Structures of FE-β-CPPIT and FP-β-CPPIT

3.2. Results

3.2.1. Synthesis of [C-11]-β-CPPIT

3.2.1.1. Precursor synthesis

The synthetic pathway leading to β-CPPIT (**17**) and to the desmethyl compound **21** is outlined in scheme 10. Anhydroecgonine methyl ester (**23**) was obtained in a 75% yield by refluxing cocaine hydrochloride (**22**) in concentrated hydrochloric acid as reported by Swahn and co-workers [100]. The intermediate **24** was prepared according to the literature procedure [100]. The α- and β-adducts of compound **24** arising from the conjugate addition were separated by flash chromatography. The yields of the α- and β-isomers were 14% (α) and 30% (β) which are comparable to the reported literature yields [100]. Unlabelled β-CPPIT (**17**) was obtained in a 54% yield by treating the β-isomer of the methylester **21** with the dilithium salt of acetophenone oxime according to the method described by Kotian and co-workers [98]. The β-configuration of the C-2 substituent was assigned on the basis of the NMR coupling constant [98]. Attempts to prepare the precursor **21** from β-CPPIT by the general procedure [92, 101] using 2,2,2-trichloroethyl chloroformate and zinc-acetic acid reduction failed. Presumably, the trichloroethyl carbamate formed during the reaction is

sterically hindered to undergo reductive cleavage. β-CPPIT was, however, demethylated successfully to desmethyl-β-CPPIT (**21**) with a yield of 67% by conversion to its carbamate using 1-chloroethyl chloroformate (ACE-Cl) followed by hydrolysis in methanol [102, 103].

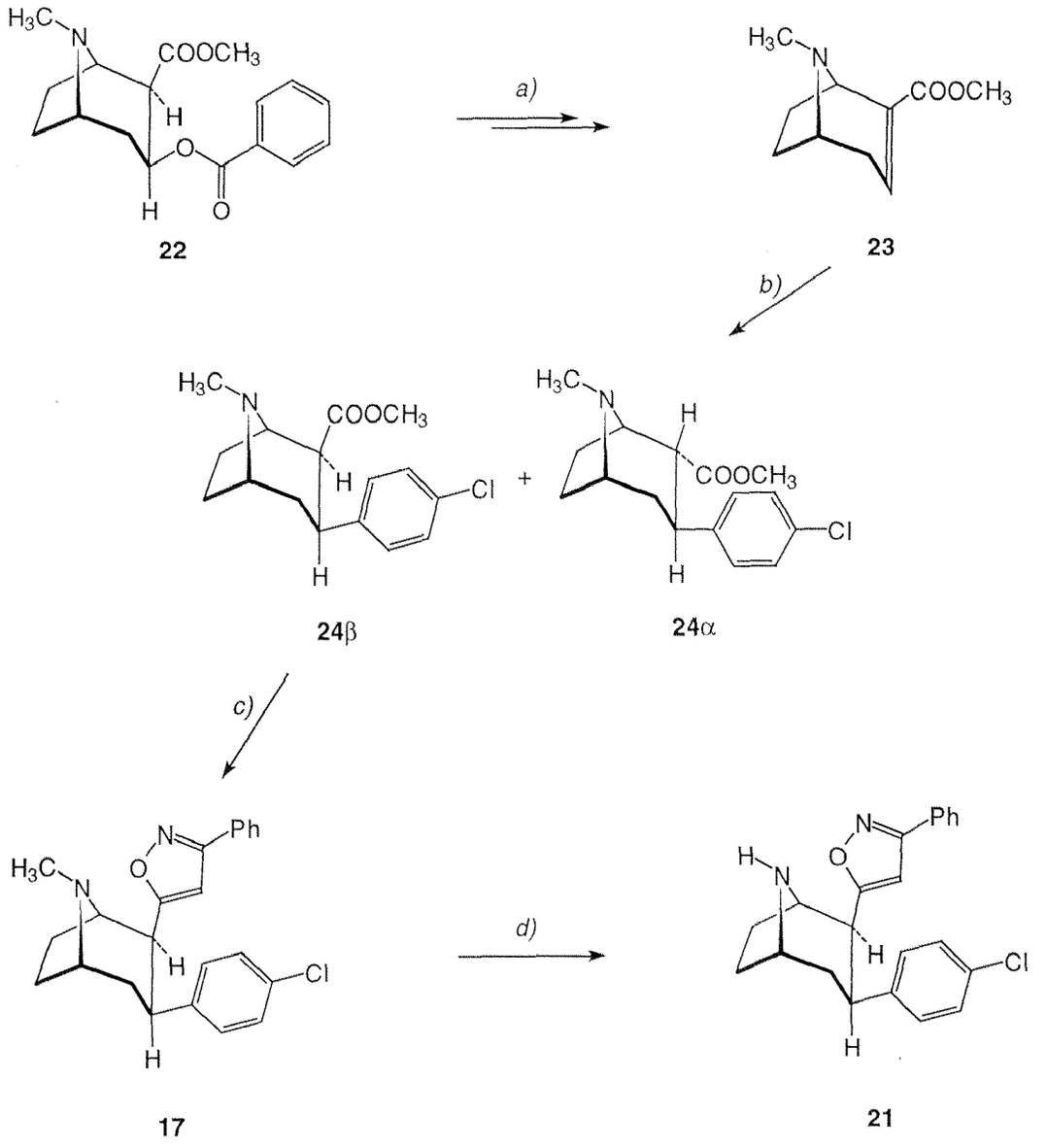

Scheme 10: Synthesis of β-CPPIT (**17**) and desmethyl β-CPPIT (**21**) starting from cocaine (**22**): *a)* 1) HCl (conc.), 2) HCl/MeOH; *b)* 4-ClPhMgBr; *c)* 1) acetophenone oxime, n-BuLi, 2) H_2SO_4; *d)* 1-chloroethyl chloroformate (ACE-Cl), MeOH.

3.2.1.2. [C-11]-Radiolabelling

The radiolabelling of β-CPPIT was achieved by the reaction of the desmethyl precursor **21** with [C-11]-iodomethane. Two different methods for the synthesis of [C-11]-iodomethane were employed. At the Paul Scherrer Institute (PSI) [C-11]-iodomethane was obtained by the bombardment of nitrogen (containing 200 ppm oxygen) with 17 MeV protons. The resulting [C-11]-carbon dioxide was reduced with lithium aluminium hydride to [C-11]-methanol and further converted to [C-11]-iodomethane by the addition of hydroiodic acid (57%) [104]. For human studies, the labelling procedure had to be established at the University Hospital in Zurich (USZ) where a different method is used for the [C-11]-iodomethane production. The first step was again the bombardment of nitrogen (containing 400 ppm oxygen) with 16.5 MeV protons. The [C-11]-carbon dioxide was then reduced to [C-11]-methane over a nickel catalyst and hydrogen. [C-11]-Iodomethane was finally obtained by the reaction of the [C-11]-methane with iodine at a temperature of 720°C [105, 106].

The radiolabelling of [C-11]-β-CPPIT was accomplished by the N-methylation of the desmethyl precursor **21** with [C-11]-iodomethane (scheme 11). [C-11]-β-CPPIT was separated from unreacted material and radioactive impurities by semi-preparative HPLC (Figure 7, panel A) and formulated in a 0.9% NaCl-solution containing ethanol (10%) and Tween 80® (0.1%). Tween 80® (polyoxyethylene(20)sorbitan monooleate) is a dissolving agent which was added to increase the solubility of the radiotracer. The total synthesis time was on average 60 minutes (counted from EOB) and the radiochemical yield ranged between 60 and 70% (decay corrected from [C-11]-iodomethane). The final product contained 0.5 - 5 µg of β-CPPIT and had a specific activity of 2000 - 2700 Ci/mmol (74 - 100 TBq/mmol) at EOS (end of synthesis). The radiochemical purity of [C-11]-β-CPPIT was greater than 99% (Figure 7, panel B).

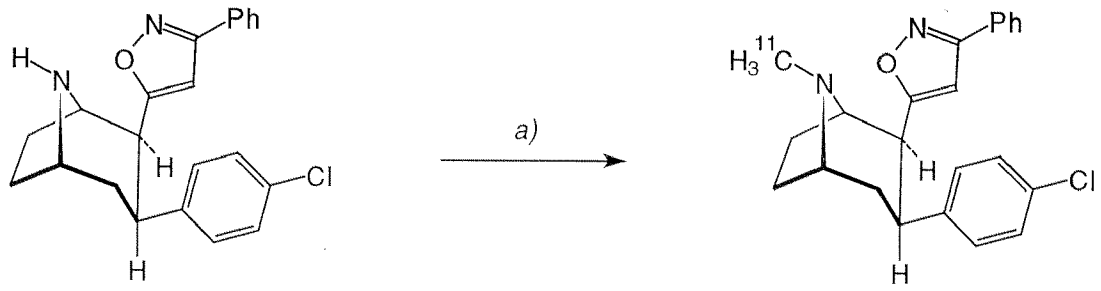

21 **[C-11]-17**

Scheme 11: Radiolabelling of [C-11]-β-CPPIT: *a)* [C-11]-iodomethane, DMF

To confirm that the [C-11]-methylation occurs at the nitrogen in position 8 of the tropane ring, [C-13]-β-CPPIT was synthesised under the same conditions by reacting the desmethyl compound **21** with carbon-13 enriched iodomethane. It was purified according to the procedure for the [C-11]-compound and characterised by ^{13}C-NMR and MS using positive ion mode and electrospray as interface. The ^{13}C signal at 46.7 ppm corresponded to the N-methyl group of authentic β-CPPIT. Mass spectrometry showed molecular ion peaks at m/z 379 (M+1) and 380 (M+1) for authentic β-CPPIT and carbon-13 enriched β-CPPIT, respectively.

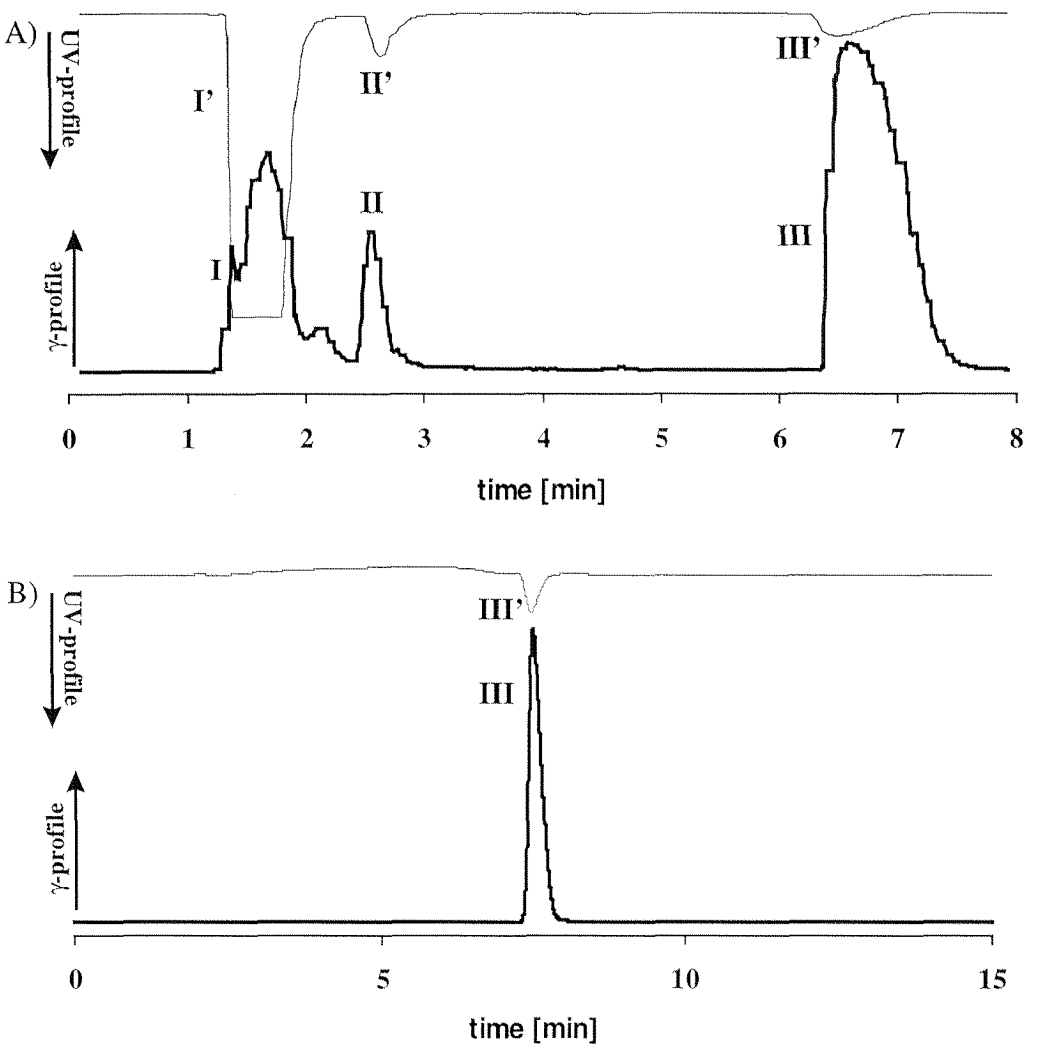

Figure 7: A) Semi-preparative HPLC of the crude reaction mixture (system A); B) analytical HPLC of [C-11]-β-CPPIT (system B). I and II: unknown, I': DMF, II': precursor, III: [C-11]-β-CPPIT, III': β-CPPIT

3.2.2. Synthesis of [F-18]-FE- and FP-β-CPPIT

3.2.2.1. Synthesis of precursor and reference compound

To obtain suitable precursors for [F-18]-FE- and [F-18]-FP-β-CPPIT the bromoethyl- and bromopropyl derivatives (**25** and **26**) were synthesised by

reacting the nortropane **21** with 1,2-dibromoethane or 1,3-dibromopropane in the presence of triethylamine (scheme 12). Although the formation of the products could be observed by mass spectrometry, they were too unstable to be isolated.

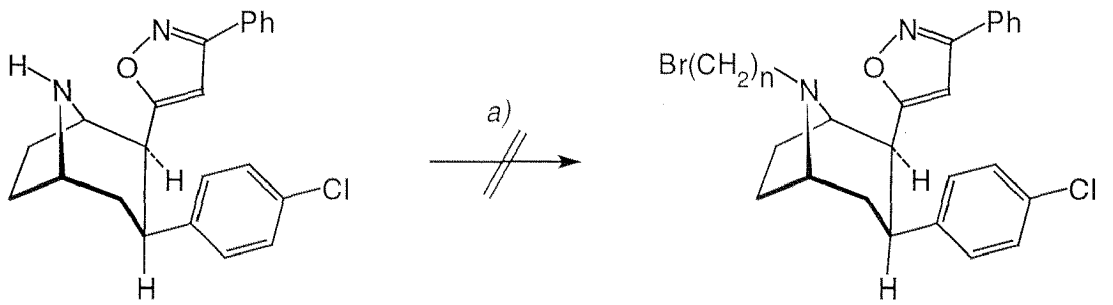

21

n=2: 25
n=3: 26

Scheme 12: Synthesis of the bromo precursors **25** and **26**: *a)* $Br(CH_2)_n)Br$

An alternative approach considered was the use of the mesylate precursors **29** and **30** (scheme 13). In analogy to a published procedure [107, 108] the hydroxy alkyl derivatives **27** and **28** were obtained by the alkylation of the nortropane **21** with the corresponding bromo alcohols in quantitative yields. The alcohols **27** and **28** were treated with an excess of methanesulfonic anhydride to obtain the mesylate precursors **29** and **30** which were used for the radiolabelling with [F-18]-fluoride without further purification.

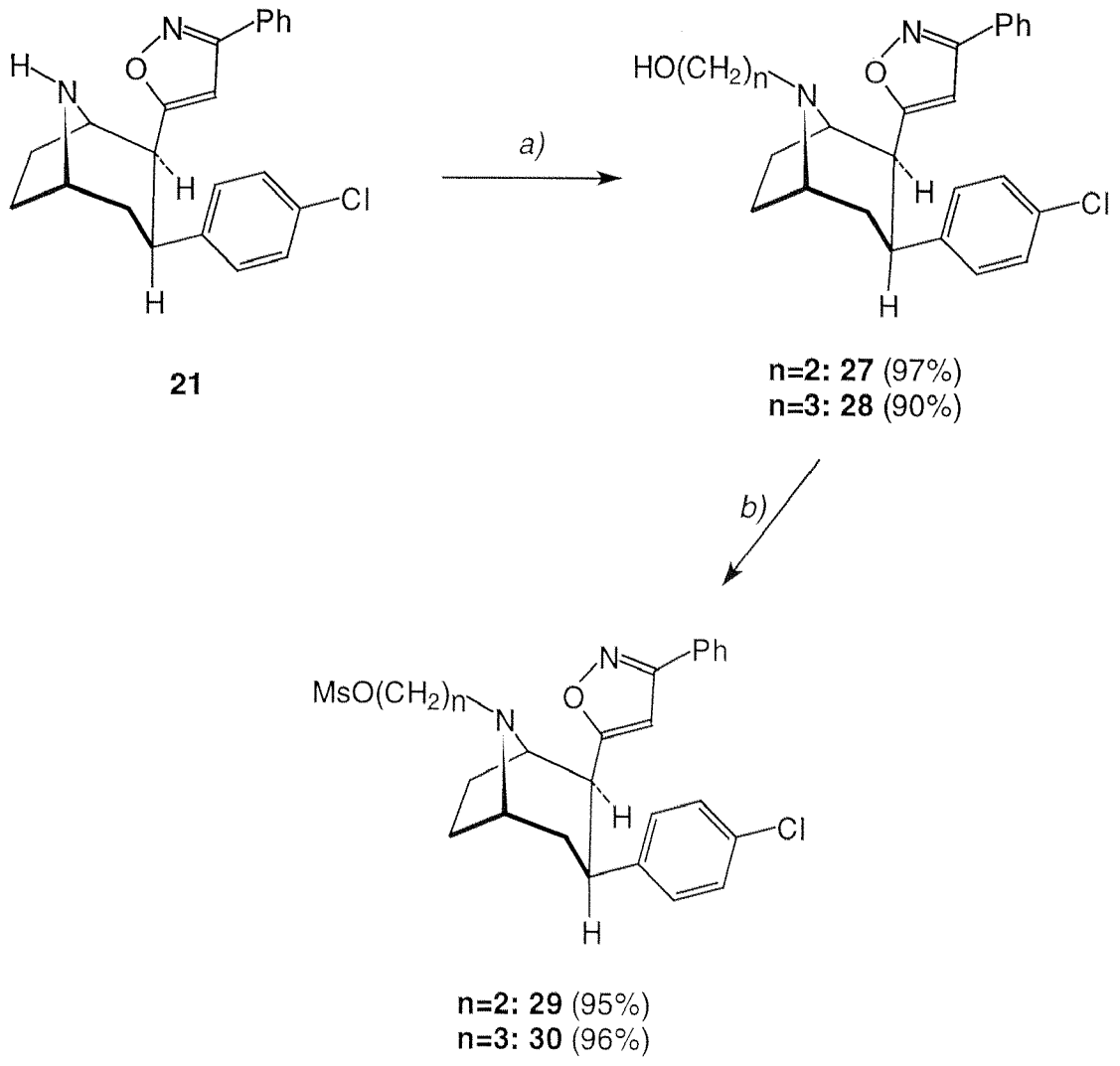

Scheme 13: Synthesis of the mesylate precursors for FE- and FP-β–CPPIT: *a)* $Br(CH_2)_nOH$; *b)* methanesulfonic anhydride.

Authentic FP-β-CPPIT **19** was obtained by reacting nortropane **21** with 1-fluoro-3-bromopropane and triethylamine in analogy to a literature procedure [108, 109] in a 60% yield (scheme 14). Because 1-fluoro-2-bromoethane is commercially not available, the fluoroethyl analogue **18** was synthesised by a different route using the fluorinating agent diethylaminosulfur trifluoride (DAST) [110].

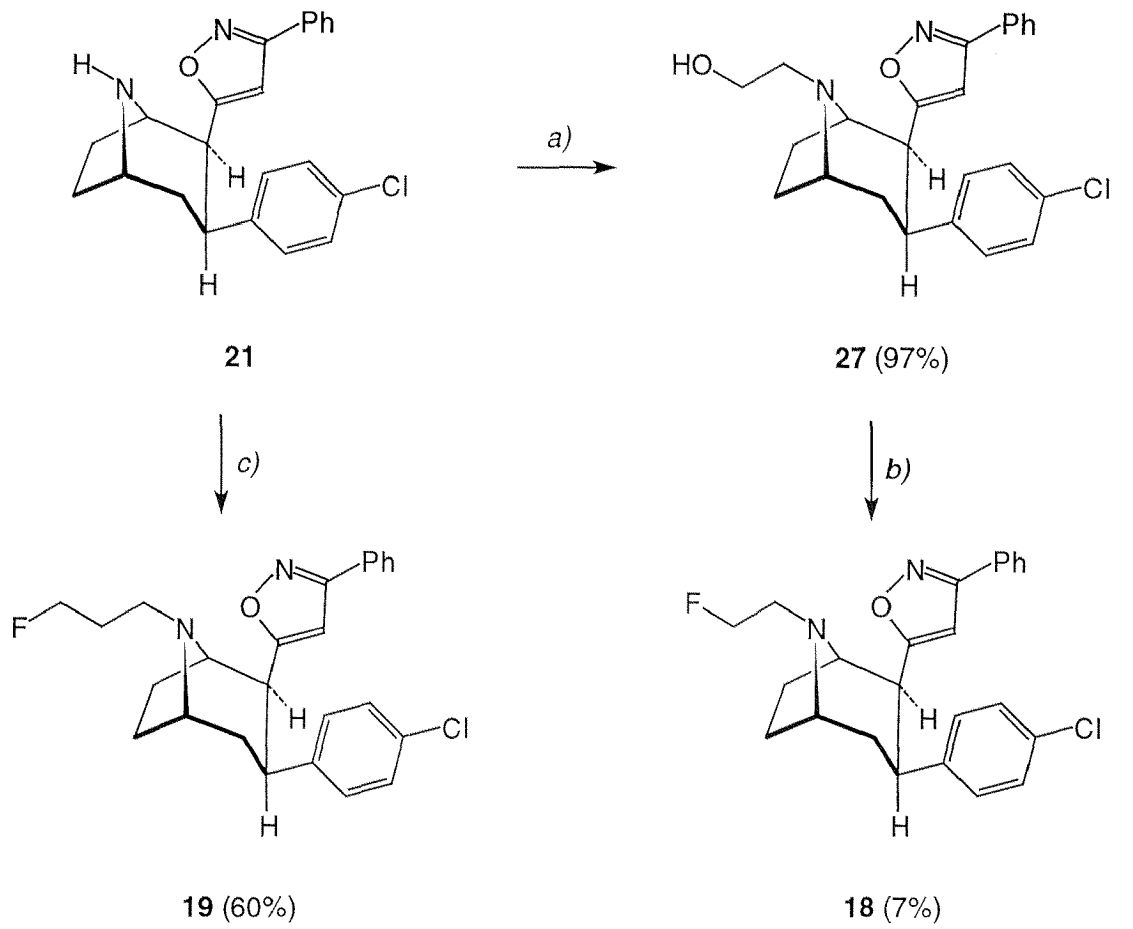

Scheme 14: Synthesis of the unlabelled standards of FE- and FP-β-CPPIT: *a)* $BrCH_2CH_2OH$; *b)* DAST; *c)* $F(CH_2)_3Br$.

3.2.2.2. [F-18]-Radiolabelling

The fluorine-18 radiolabelling of FE-β-CPPIT **18** was carried out by nucleophilic n.c.a. radiofluorination of the mesylate **29** in acetonitrile using [F-18]-potassium fluoride and Kryptofix 2.2.2.®-complex as the fluorinating agent (scheme 15) [70, 108]. After the separation of unreacted fluorine-18 with a Sep-Pak® cartridge, the product was purified by semi-preparative reversed phase HPLC. A typical HPLC chromatogram is shown in figure 8, panel A. The total synthesis time was on average 150 minutes (counted from EOB). The radiochemical yield

of [F-18]-FE-β-CPPIT was 15%. Analytical HPLC showed a radiochemical purity greater than 99% (Figure 8, panel B). The product was formulated in a solution containing Tween 80® (0.1%), ethanol (10%) and 0.15 M phosphate buffer (pH 7.4) (90%).

The [F-18]-FP-CPPIT **19** was obtained under similar reaction conditions. The radiochemical yield was low and ranged from 1% to 10%. Radiochemical purity was greater than 99%.

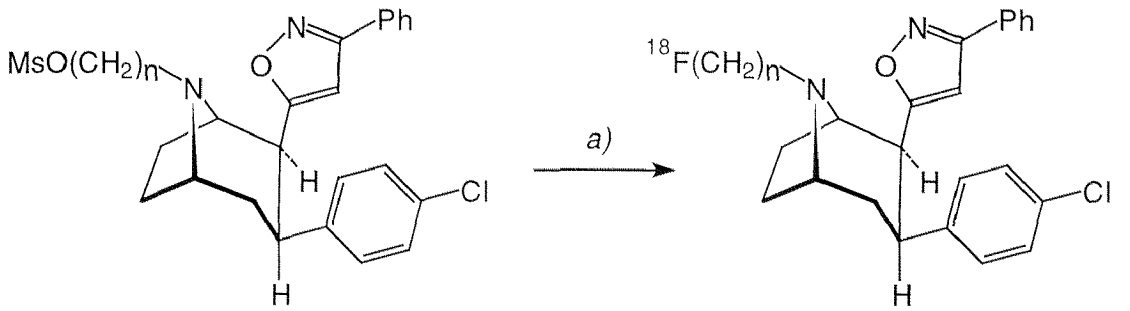

n=2: 29
n=3: 30

n=2: 18
n=3: 19

Scheme 15: Radiolabelling of [F-18]-FE- and [F-18]-FP-β-CPPIT: *a)* [F-18]-KF, Kryptofix 2.2.2.®, CH_3CN, 100°C, 45 min.

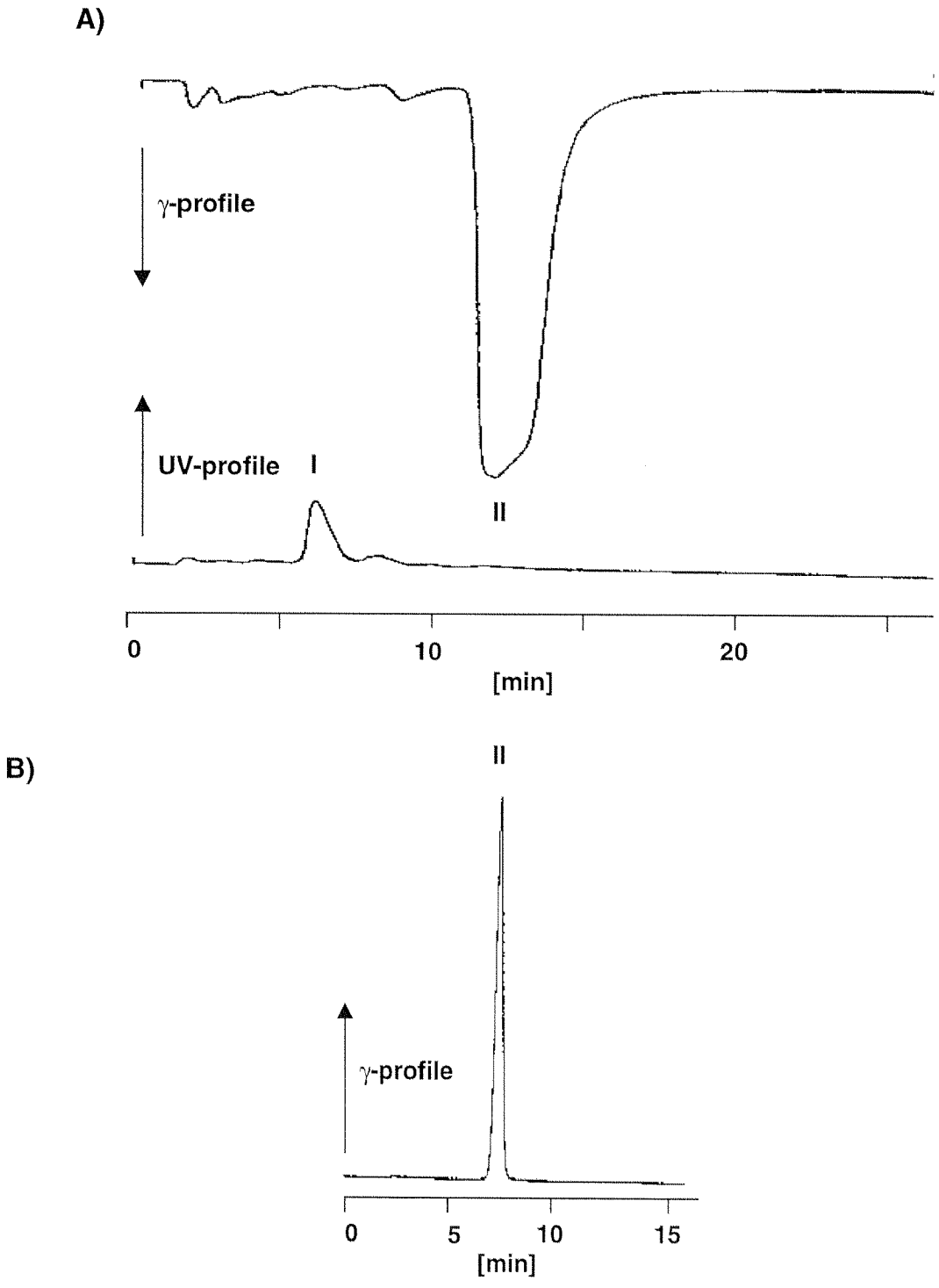

Figure 8: A) Semi-preparative HPLC (system C) of the crude reaction mixture of [F-18]-FE-β-CPPIT; B) γ-profile of the analytical HPLC of [F-18]-FE-β-CPPIT (system D). I: precursor; II: [F-18]-FE-β-CPPIT.

3.2.3. *In vitro* evaluation of [C-11]-β-CPPIT and its [F-18]-fluoroalkyl analogues

3.2.3.1. Lipophilicity

Lipophilicity represents the affinity of a molecule or a moiety for a lipophilic environment. It is commonly measured by its distribution behaviour in a biphasic system, either liquid-liquid (e.g., partition coefficient in 1-octanol/water) or solid-liquid (e.g. retention on reversed phase HPLC or TLC) systems. In 1959, Gaudette and Brodie [111] realised both the possibility for using a partition coefficient to model lipophilic character, and the relevance of lipophilicity to pharmacokinetic processes. They found a parallel between the heptane/buffer partition coefficient of certain drugs, and their rate of entry into cerebrospinal fluid.

The partition coefficient (P) is a widely measured property of a radiopharmaceutical. It can be used to estimate the blood-brain barrier (BBB) penetration of a radioligand [112]. The $logP_{7.4}$-values of β-CPPIT and the fluoroethyl and fluoropropyl derivatives were determined using the shake flask method and are shown in table 5 [113, 114].

tracer	$logP_{7.4}$	$logP_{7.4}$ of the corresponding CIT derivative [115]
[C-11]-β-CPPIT	2.13 ± 0.11	1.13 ± 0.08
[F-18]-FE-β-CPPIT	2.92 ± 0.14	1.68 ± 0.01
[F-18]-FP-β-CPPIT	2.54 ± 0.39	1.49 ± 0.01

Table 5: Determined $logP_{7.4}$-values of [C-11]-β-CPPIT and its fluorinated derivatives and logP-values of the corresponding β-CIT derivatives from literature [115].

The higher logP-value of the fluoroethyl compound (2.92) in comparison to the fluoropropyl β-CPPIT (2.54) is in accordance with the logP-values of the fluorinated β-CIT derivatives (table 5). The lower lipophilicity of the fluoropropyl compounds may be explained by the longer alkyl side chain which results in a higher basicity of the nitrogen in position 8 of the tropane structure and therefore in a higher percentage of protonated compound at pH 7.4. The increased water solubility leads to a lower octanol-water partition coefficient.

3.2.3.2. *In vitro* stability in human plasma

To investigate the *in vitro* stability of [C-11]-β-CPPIT, human plasma was incubated with 100 MBq of the radiotracer at 37°C for one hour (3 half-lives). After precipitation of plasma proteins with acetonitrile, the supernatant was analysed with HPLC. No metabolites could be detected.
The determination of stability of [F-18]-FE- and [F-18]-FP-β-CPPIT in plasma was performed under analogous conditions, but with an incubation time of six hours. HPLC analysis indicated only parent compound and no additional peaks could be detected. These results indicate a high *in vitro* plasma stability of the three radiotracers.

3.3. *In vivo* evaluation in animals

3.3.1. Biodistribution of [C-11]-β-CPPIT in mice

The suitability of [C-11]-β-CPPIT as a dopamine transporter antagonist was evaluated in mice. After intravenous (i.v.) injection, [C-11]-β-CPPIT showed good BBB penetration consistent with the logP value of 2.13. The highest uptake of radioactivity was observed in the striatum, a region known to contain a high density of the DAT (table 6). The retention of radioactivity in the striatum

between 10 and 40 min p.i. was nearly constant. In accordance with the DAT density distribution [116, 117] the cerebellum and the frontal cortex showed low radioactivity uptake values (table 6). The clearance of radioactivity from the cerebellum was fast. As a result of the slower washout of the radioactivity from the striatal region the striatum-to-cerebellum ratio increased with time and reached a maximum of 3.5 at 60 min p.i. In the frontal cortex, a region with low DAT density [117], the [C-11]-β-CPPIT uptake was just slightly higher than in the cerebellum resulting in a target-to-non-target ratio of 1.5 at 60 min p.i.. The frontal cortex is known to have a low DAT density [117] and a considerable concentration of serotonin reuptake sites [118].

In peripheral organs [C-11]-β-CPPIT showed a high accumulation in the lung (50% ID/g at 5 min p.i.) which was washed out rapidly reaching a concentration of 4% ID/g at 90 min p.i. (table 6). A similar course of lung uptake has been reported also for [C-11]-β-CIT in Cynomolgus monkeys [97]. A considerable lung uptake was also observed for other amines [119]. A marked uptake of 12% ID/g (5 min p.i.) was measured in the liver at 5 min p.i.. In contrast to the lung the radioactivity in the liver decreased slowly to 8% ID/g at 90 min p.i.. The activity in blood remained constant (1% ID/g) throughout the experiment.

organ	5 min	15 min	30 min	60 min	90 min
striatum	14.11 ± 1.34	13.27 ± 2.35	12.59 ± 3.00	9.96 ± 3.49	4.66 ± 0.98
frontal cortex	15.80 ± 0.60	12.80 ± 1.64	7.87 ± 1.39	4.29 ± 1.30	2.81 ± 0.75
cerebellum	12.21 ± 0.71	9.69 ± 1.50	5.28 ± 0.82	2.75 ± 0.95	1.77 ± 0.21
blood	0.98 ± 0.21	0.82 ± 0.14	0.88 ± 0.54	0.73 ± 0.19	1.11 ± 0.19
lung	50.58 ± 2.19	24.65 ± 6.39	10.34 ± 1.23	5.46 ± 0.71	4.26 ± 0.70
liver	11.75 ± 2.48	10.08 ± 0.30	8.87 ± 1.83	7.66 ± 1.99	7.98 ± 1.30

Table 6: Distribution of radioactivity [% ID/g] after i.v. application of 10 MBq [C-11]-β-CPPIT in mice (n=3).

The *in vivo* specificity of [C-11]-β-CPPIT was demonstrated in blocking studies (figure 9, table 7). The uptake of [C-11]-β-CPPIT in the striatum was reduced to almost the level of cerebellum by preinjecting the dopamine reuptake antagonist GBR 12909 (5 mg/kg) (figure 10). Radioactivity uptake in the brain was not affected by the preinjection of citalopram (5 mg/kg), desipramine (5 mg/kg) and ketanserin (2.5 mg/kg). These results suggest that [C-11]-β-CPPIT is selective and could be useful as a PET tracer for imaging the dopamine transporter.

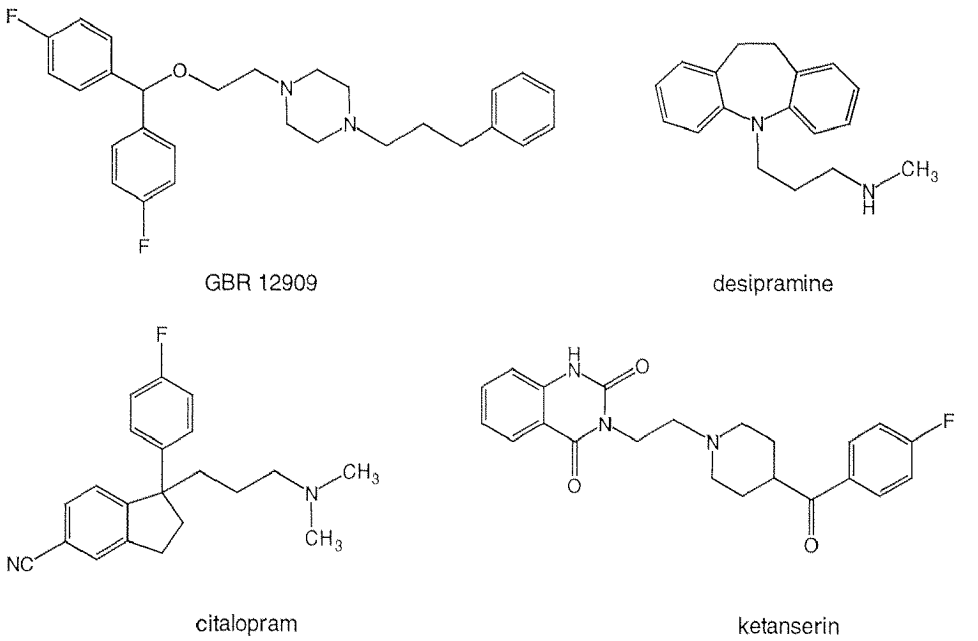

Figure 9: Structures of GBR 12909, desipramine, citalopram and ketanserin.

uptake inhibitor	binding site	pretreatment	concentration
GBR 12909	DAT	15 min	5 mg/kg
citalopram	5-HTT	5 min	5 mg/kg
desipramine	NET	15 min	5 mg/kg
ketanserin	vMAT	15 min	2.5 mg/kg

Table 7: Concentration and injection time of the antagonists GBR 12909, citalopram, desipramine and ketanserin in mice.

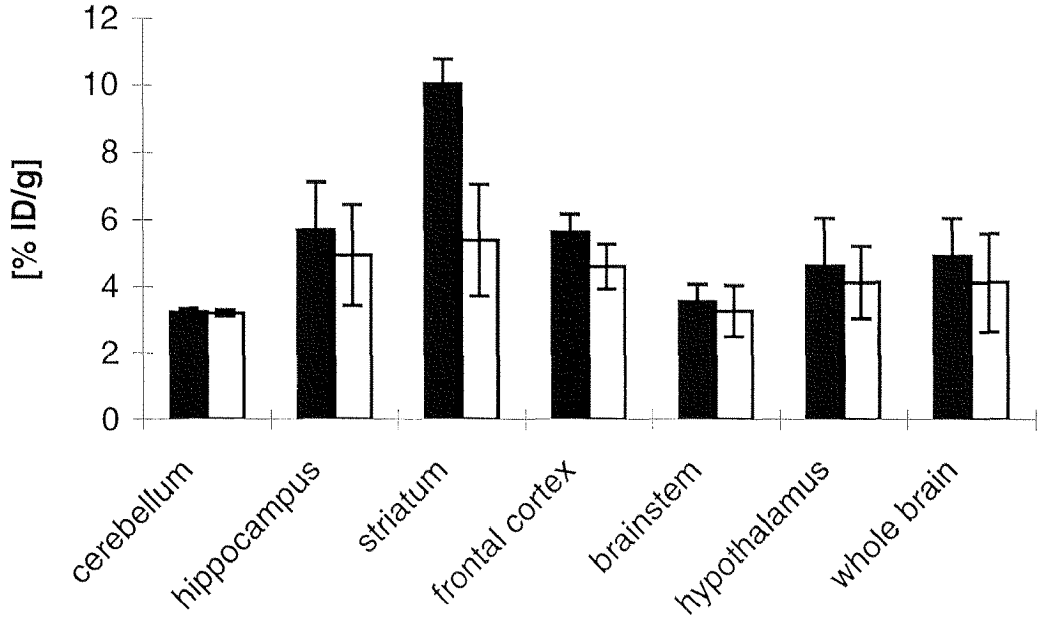

Figure 10: Blockade study in mice (n=3) with GBR 12909 (5 mg/kg; 15 min prior to [C-11]-β-CPPIT): ■ control, □ GBR 12909.

To determine whether radioactive metabolites of [C-11]-β-CPPIT, which would interfere with the [C-11]-β-CPPIT binding, were present in the brain, metabolite studies were performed in mice brain homogenates. Additionally, a method for the quantification of radioactive metabolites in plasma was evaluated in order to determine the metabolite corrected input function in human PET studies. For the separation of [C-11]-β-CPPIT from its radioactive metabolites brain homogenates and plasma samples were extracted with heptane in analogy to the method described by Mathis and co-workers [120]. The recovery of radioactivity of this extraction was > 95% for both brain homogenates and plasma.

In plasma 49 ± 11% of [C-11]-β-CPPIT at 15 min p.i. and 58 ± 7% at 30 min p.i. were metabolised (n=4). HPLC and radio-TLC analysis revealed the radioactive metabolites to be more polar than β-CPPIT with an HPLC-retention time of 8.2 min for [C-11]-β-CPPIT and 1.8 - 2.5 min for the radioactive

metabolites. In the brain homogenates at 15 and 30 min p.i 95% of the radioactivity was identified as [C-11]-β-CPPIT with radio-TLC and HPLC by co-elution with reference compound (figure 11). These results confirm that radioactive metabolites are neither formed within the brain nor penetrate the blood-brain barrier.

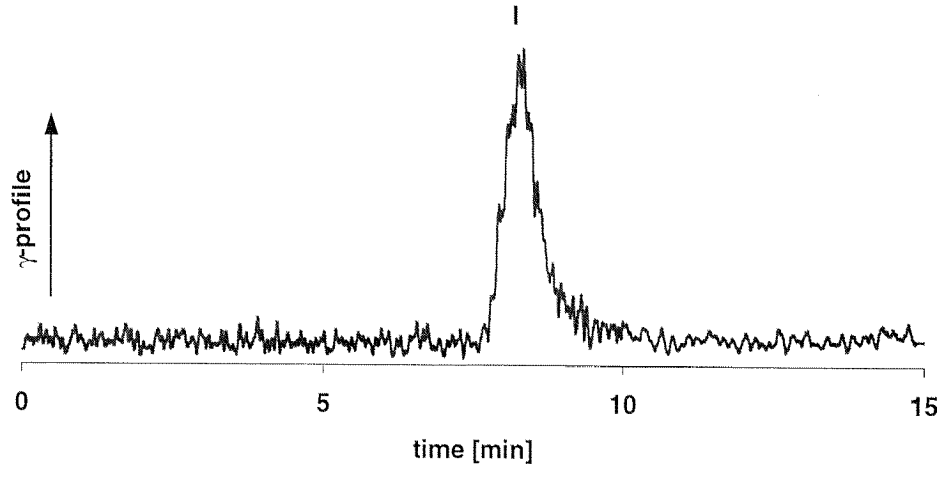

Figure 11: HPLC-chromatogram (system F) of the organic phase after brain homogenate extraction 15 min p.i.. I: [C-11]-β-CPPIT.

Prior to the human studies toxicological studies were performed in mice and rats by Biological Research Laboratories, Füllinsdorf, Switzerland. No clinical signs of toxicity of β-CPPIT at a maximum concentration of 0.1 mg/kg were observed. As the routinely applied doses of [C-11]-β-CPPIT for PET studies in humans are more than six orders of magnitude lower, it can be assumed that β-CPPIT can safely be used as a radioligand in humans.

3.3.2. PET studies with [F-18]-FE- and [F-18]-FP-β-CPPIT in Rhesus monkeys

For the purpose of increasing the time frame of the PET studies of carbon-11 labelled radiotracers several research groups have used with success the [F-18]-fluoroethyl and fluoropropyl groups as bioisosteric substitutes for the methyl group [88, 107, 121, 122]. Following the same concept, it was decided to prepare the fluorine-18 labelled fluoroethyl and fluoropropyl analogues of β-CPPIT and to evaluate their usefulness as DAT imaging agents directly in the monkey.

The PET studies of [F-18]-FE- and [F-18]-FP-β-CPPIT were carried out in female Rhesus monkeys. A 94 min PET scan of the brain was performed after i.v. application of 95 MBq of [F-18]-FE-β-CPPIT or 154 MBq of [F-18]-FP-β-CPPIT.

A rapid uptake of radioactivity was observed initially. In all the brain areas investigated (striatum, frontal cortex and cerebellum) the time-activity curves reached a maximum in the time interval between 10 and 20 min p.i. and decreased slowly with time (figure 12). At the end of the scan the radioactivity uptake in the brain region examined were identical indicating high non-specific binding of the fluorine-18 labelled fluoroethyl derivative. Similar uptake kinetics were observed for the fluoropropyl analogue.

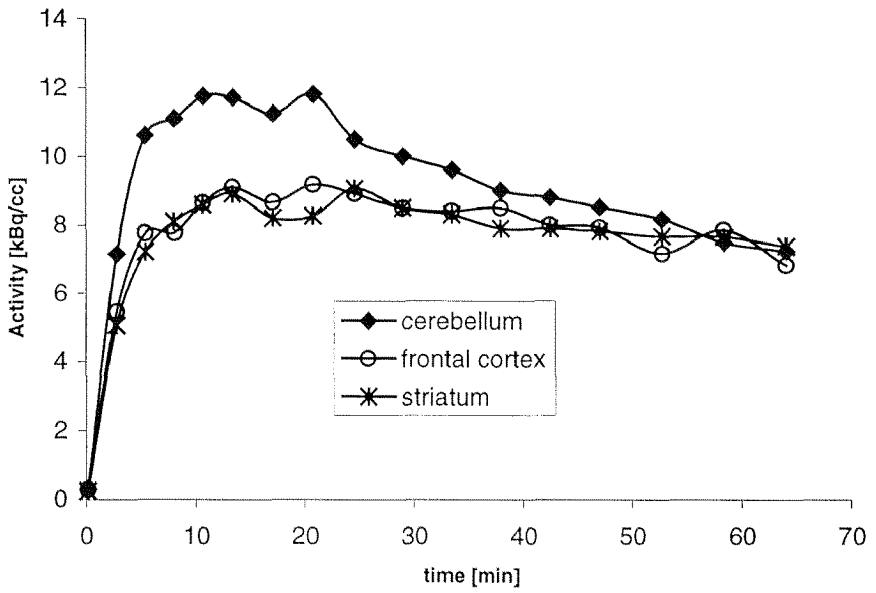

Figure 12: Time-activity curves of [F-18]-FE-β-CPPIT after i.v. application of 95 MBq into rhesus monkey: ◆ cerebellum, O frontal cortex, ✳ striatum.

To investigate the metabolism of [F-18]-FE- and [F-18]-FP-β-CPPIT venous blood samples were taken at 5, 15, 30, 60 and 90 min p.i.. HPLC and radio-TLC analyses showed a rapid metabolism of both radiotracers (figure 13). The metabolite identified by co-injection was [F-18]-fluoride. The relative amounts are shown in table 8.

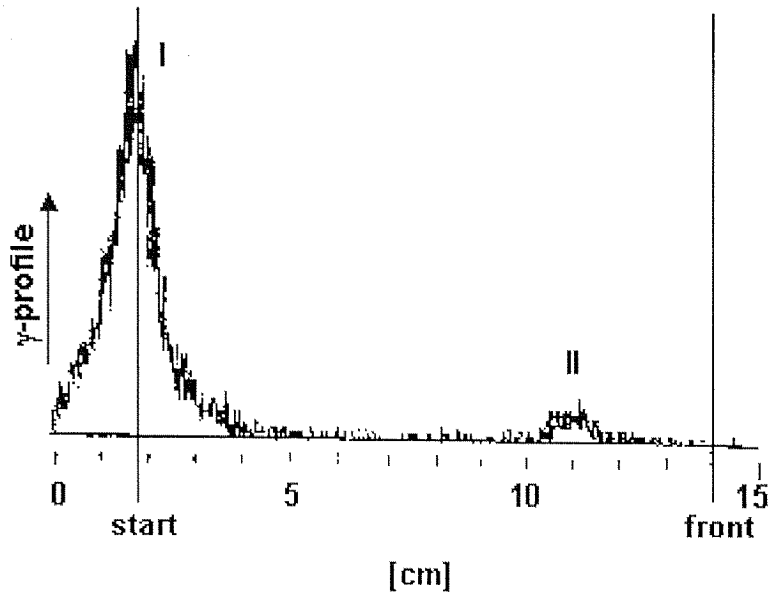

Figure 13: Radio-TLC of the metabolite studies with [F-18]-FP-β-CPPIT 15 min p.i.. I: fluoride, II: [F-18]-FP-β-CPPIT

time p.i.	[F-18]-FE-β-CPPIT				[F-18]-FP-β-CPPIT			
	HPLC		radio-TLC		HPLC		radio-TLC	
	tracer	fluoride	tracer	fluoride	tracer	fluoride	tracer	fluoride
5 min	100%	0%	94%	6%	5%	95%	5%	95%
30 min	42%	58%	22%	78%	0%	100%	0%	100%
60 min	5%	95%	5%	95%	0%	100%	0%	100%

Table 8: Percentage of non-metabolised tracer and [F-18]-fluoride in plasma.

The PET experiments showed that the N-fluoroalkyl analogues of β-CPPIT are not suitable as PET ligands for the DAT indicating the difficulty in predicting *in vivo* binding of analogues.

3.4. PET study with [C-11]-β-CPPIT in humans

The results of the *in vivo* studies with [C-11]-β-CPPIT in mice (chapter 3.3.1.) encouraged us to evaluate this radioligand in humans. Six healthy volunteers (4 male and 2 female; age: 23 ± 2; body weight 64 ± 5 kg) were investigated. 90 min PET scans of the brain were performed with an average dose of 381 ± 90 MBq and a specific activity of 3337 ± 802 Ci/mmol.

3.4.1. Distribution pattern in plasma and brain

Arterial blood samples were taken during the PET scan in order to calculate the metabolite-corrected input function. Blood radioactivity quickly dropped after the end of the [C-11]-β-CPPIT application (i.v. infusion over 5 min) and remained constant until the end of the scan (figure 15). The percentage of non-metabolised [C-11]-β-CPPIT in the arterial plasma was determined using the extraction method mentioned above (chapter 3.3.1.) The recovery of the radioactivity was greater than 93%. Figure 14 shows the percentage of radioactivity in plasma corresponding to [C-11]-β-CPPIT. The fraction of metabolites increased from 5% at 5 min p.i. to 54% at the end of the scan (90 min p.i.).

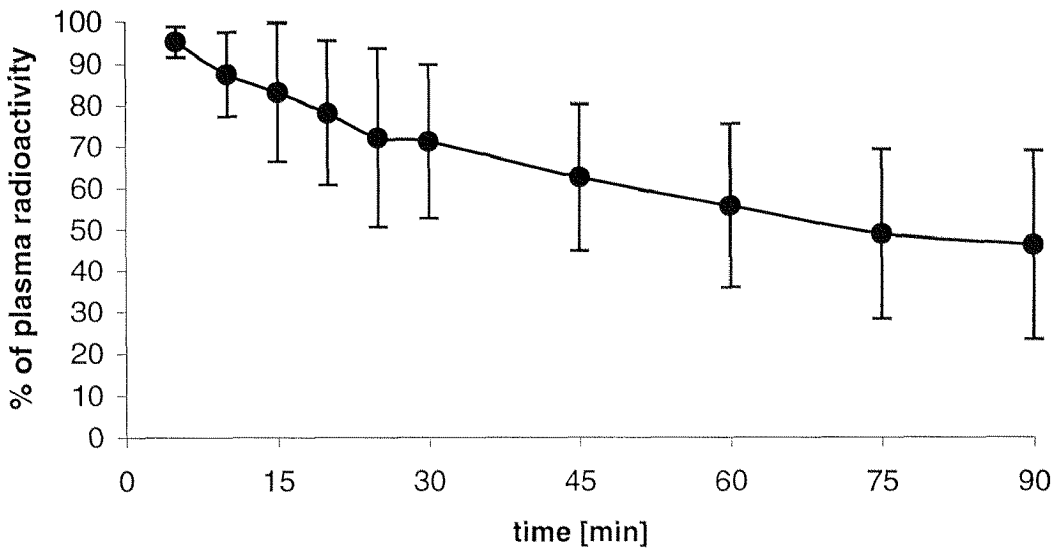

Figure 14: Mean of the percentage of radioactivity in plasma corresponding to the parent tracer [C-11]-β-CPPIT (n=6).

The highest brain uptake of radioactivity was observed in the striatum (putamen and caudate) where the activity reached a maximum at 45 min p.i. and remained at a constant level until the end of the scan (figure 15). The striatum-to-cerebellum ratio increased linearly with time (figure 16) and was 2.16 ± 0.17 (n=6) at 60 min p.i.. The thalamus-to-cerebellum ratio was 1.34 ± 0.09 (n=6) at 60 min p.i., whereas the ratios for the cortical regions did not exceed 1.09 ± 0.04 (n=6). The selectivity of [C-11]-β-CPPIT for the dopamine transporter over the 5-HTT transporter was approximately 2.

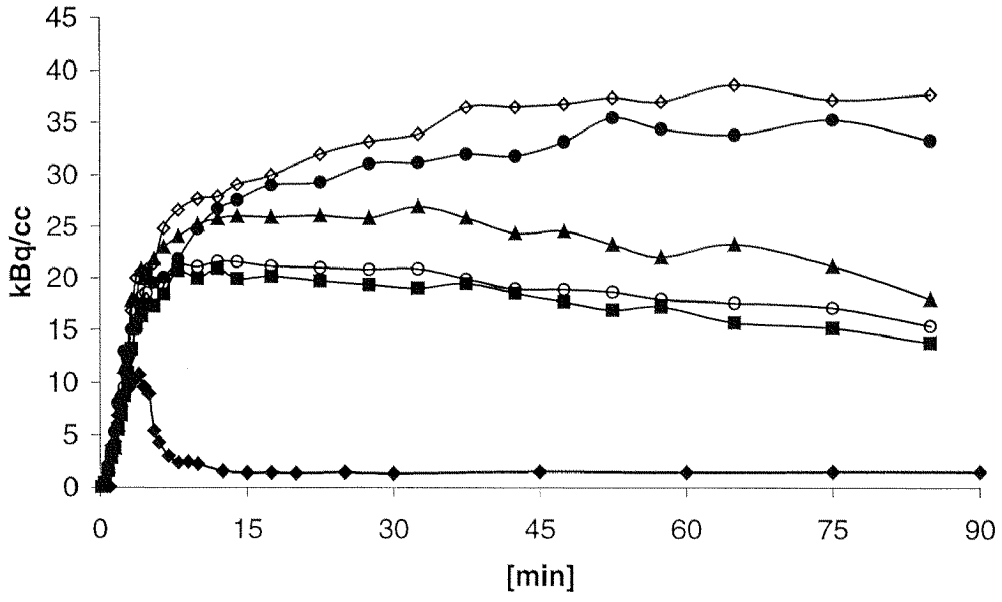

Figure 15: Radioactivity in brain regions and plasma of a healthy female volunteer after i.v. application of 438 MBq [C-11]-β-CPPIT: ✧ putamen; ● caudate; ▲ thalamus; O frontal cortex; ■ cerebellum; ◆ plasma.

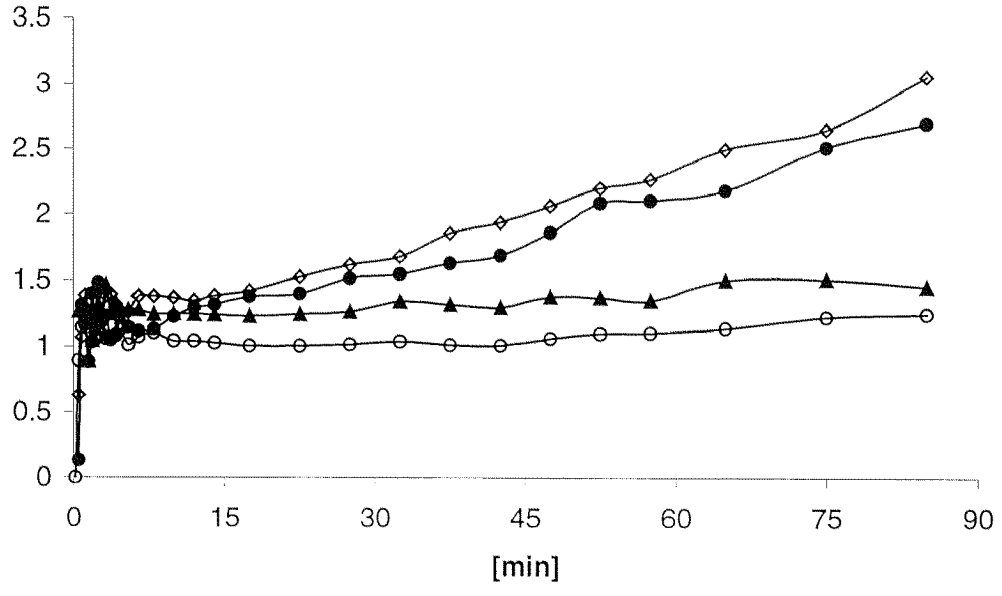

Figure 16: Ratios of radioactivity in different brain regions compared to the cerebellum (healthy female volunteer) after i.v. application of 438 MBq [C-11]-β-CPPIT: ✧ putamen; ● caudate; ▲ thalamus; O frontal cortex.

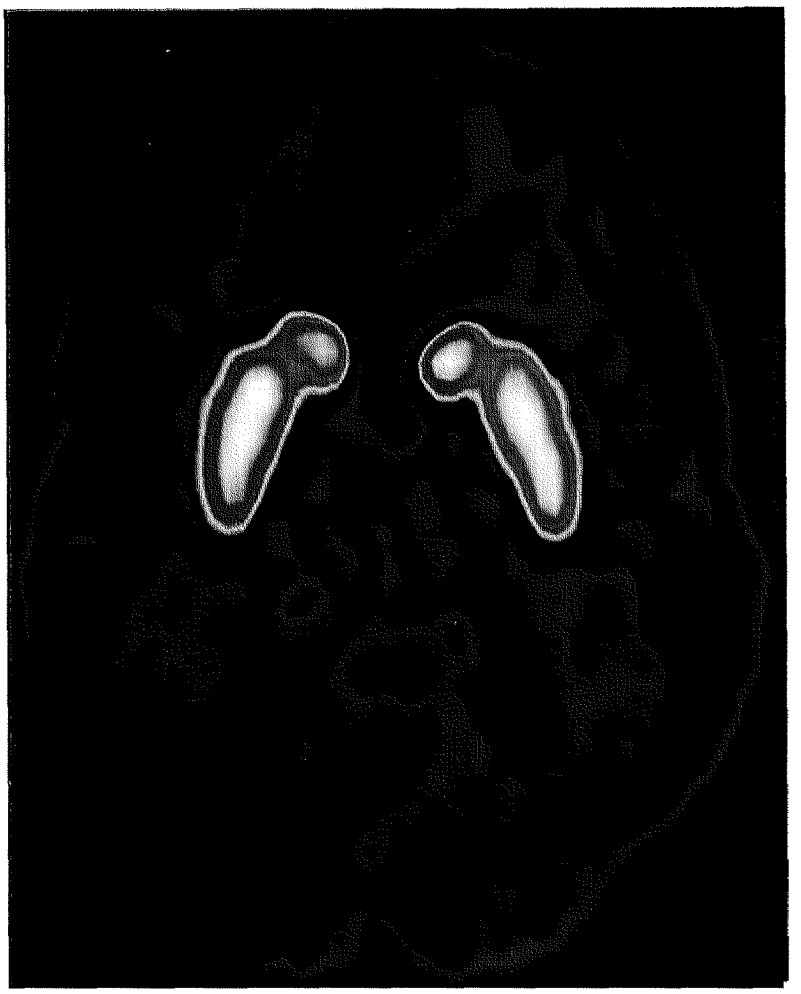

Figure 17: Axial PET image of one volunteer showing the distribution of [C-11]-β-CPPIT at the level of the basal ganglia (at 60 min p.i.).

3.4.2. Kinetic modeling

Regions of interest (ROIs) were defined over the occipital (medial and radial), frontal (medial and lateral), temporal (medial and lateral) parietal and cerebellar cortex, striatum (caudate and putamen), thalamus and pons. To analyse radioligand binding in these ROIs several compartment models were tested based on the dynamic PET data and the metabolite corrected input function.

To describe the time course of the uptake of a ligand in tissue, a model is required which distinguishes between the different components contributing to the externally detected signal [123-126]. Figure 18 illustrates a 3-tissue compartment model.

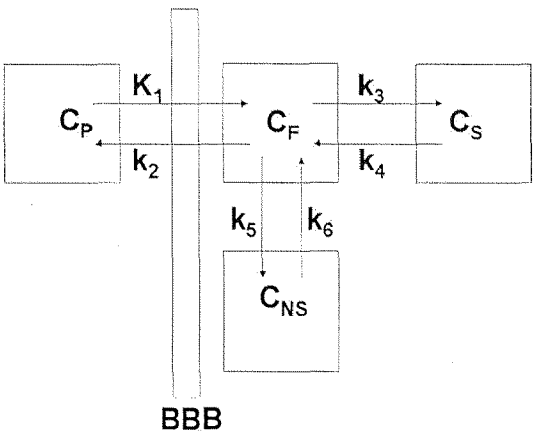

Figure 18: Generalised neuroreceptor model; 3-tissue compartment kinetic model configuration with six rate parameters (K_1-k_6).

The generalised kinetic model with three tissue compartments consists of C_P, the arterial plasma concentration, C_F, the concentration of free ligand in tissue, C_S, the concentration of specifically bound tracer and C_{NS}, the concentration of non-specifically bound ligand which is not available for binding to the specific receptors under investigation.

K_1 and k_2 represent the BBB transport rate constants, k_3 and k_4 designate the rates of binding and release from specific binding sites, while k_5 and k_6 describe the transport between free and non-specifically bound compartments. The 3-tissue compartment model can be reduced to a 2-tissue compartment model (figure 19, panel A), where the compartments for free (C_F) and non-specifically bound (C_{NS}) ligand are combined under the assumption of rapid equilibration between the compartments, which makes them kinetically indistinguishable. This simplification can be applied if the values of k_5 and k_6 from the 3-tissue compartment model are high compared to K_1 and k_2. A further reduction to a 1-tissue compartment model (figure 19, panel B) is possible if

additionally, the values for k_3 and k_4 are high compared to the BBB transport rates K_1 and k_2, thus allowing a rapid equilibrium between free and specifically bound components. The distribution volume (DV) is a kinetic parameter corresponding to the ratio of tissue (C_T) and plasma (C_P) concentrations at equilibrium. For the single-compartment model this ratio corresponds to the ratio of K_1 and k_2".

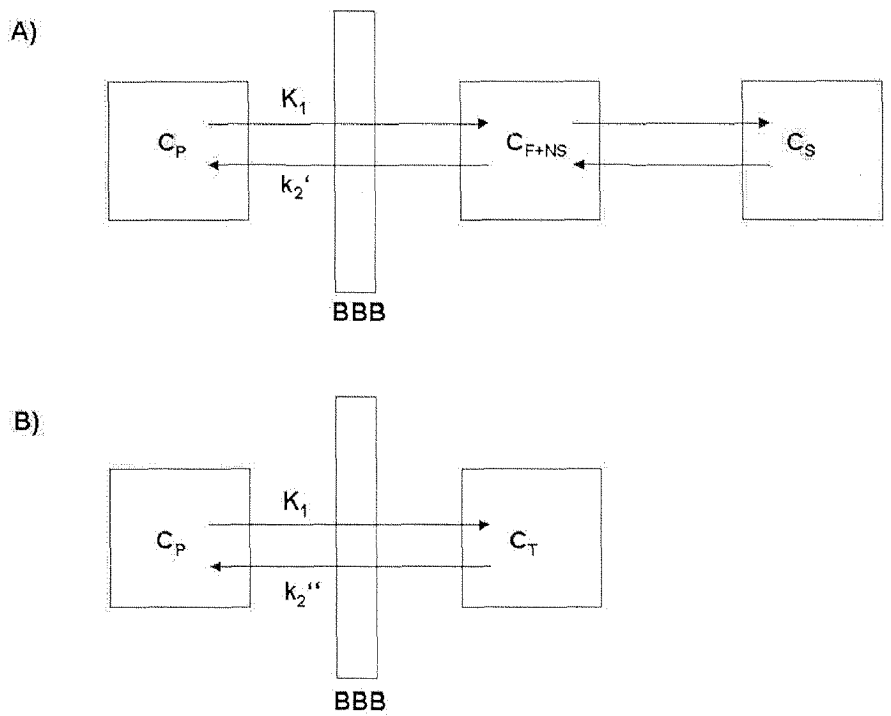

Figure 19: 2-tissue compartment model (panel A) and 1-tissue compartment model (panel B): $C_T = C_F + C_{NS} + C_S$.

The 2-tissue and the 1-tissue compartment models were compared for kinetic modeling of [C-11]-β-CPPIT. The 1-tissue compartment model provided more robust kinetic variables (K_1, k_2" and DV). Table 9 shows the mean and standard deviation of the distribution volumes (DV) and the BBB transport rates K_1 and k_2" of the six volunteers. The tracer was highly extracted as seen by the high DVs. The DV of the putamen and the caudate are 33.3 ml/ml_{tissue} and 32.2 ml/ml_{tissue} respectively. These values are a factor 3.5 higher than the cerebellar

DV (9.4 ml/ml_{tissue}). Compared to the cerebellum a higher DV-value was also obtained in the thalamus (12.7 ml/ml_{tissue}), whereas in the other brain regions the DVs were slightly increased (9.6 - 10.5 ml/ml_{tissue}). Comparable DVs were observed in a PET study with [F-18]-FP-β-CIT by Kazumata and co-workers [122].

ROI	K_1 [$ml/ml_{tissue}/min$]	k_2'' [1/min]	DV (K_1/k_2'') [ml/ml_{tissue}]
putamen	0.276 ± 0.050	0.009 ± 0.001	33.3 ± 10.6
caudate	0.259 ± 0.040	0.009 ± 0.002	32.1 ± 11.5
thalamus	0.270 ± 0.054	0.022 ± 0.002	12.8 ± 3.3
temporal-lateral cortex	0.223 ± 0.038	0.022 ± 0.003	10.5 ± 2.7
parietal cortex	0.222 ± 0.040	0.022 ± 0.003	10.5 ± 2.7
temporal-medial cortex	0.163 ± 0.032	0.016 ± 0.002	10.3 ± 2.7
occipital-medial cortex	0.245 ± 0.034	0.025 ± 0.004	10.0 ± 2.6
frontal-medial cortex	0.234 ± 0.042	0.024 ± 0.004	10.0 ± 2.5
frontal-lateral cortex	0.226 ± 0.038	0.023 ± 0.003	10.0 ± 2.4
occipital-radial cortex	0.263 ± 0.051	0.027 ± 0.004	9.8 ± 2.5
pons	0.213 ± 0.048	0.023 ± 0.003	9.6 ± 2.4
cerebellum	0.229 ± 0.043	0.025 ± 0.002	9.4 ± 2.2

Table 9: Kinetic parameters (mean and standard deviation) of the ROIs in human (n=6)

3.5. Conclusion and Outlook

Many degenerative brain disorders such as Parkinson's and Alzheimer's disease are related to a loss of dopaminergic neurones. In order to get a diagnostic tool for the dopaminergic system [C-11]-β-CPPIT, [F18]-FE-β-CPPIT

and [F-18]-FP-β-CPPIT were synthesised and evaluated as potential selective PET tracers for the DAT.

The precursor for [C-11]-β-CPPIT was obtained *via* a four step synthesis starting from cocaine in an overall yield of 8%. The synthesis and purification steps were straightforward and the product showed high stability with no decomposition after storage at room temperature for more than one year. The radiolabelling was achieved by the N-methylation of the desmethyl compound with [C-11]-iodomethane in a radiochemical yield of 60-70%. The labelling method gave reproducible results with high chemical and radiochemical purity.

Biodistribution studies in mice confirmed the specificity and selectivity of [C-11]-β-CPPIT for the dopamine transporter and its suitability as a PET tracer. The results of the PET study in six healthy volunteers were consistent with the findings in mice. The investigated group of subjects showed homogeneous results with regard to time-activity curves, metabolism and kinetic parameters. The enrichment of the tracer in the striatum, the region with the highest DAT density, gave a striatum-to-cerebellum ratio of 2.16 ± 0.17 (60 min p.i.).

Farde and co-workers reported a blood-to-plasma ratio of 2 for [C-11]-β-CIT [97]. This ratio might result from the binding of the tracer to the serotonin transporter on the platelet membrane [97]. In the present study, the blood-to-plasma ratio was only 0.7 - 0.9 indicating a lower affinity of [C-11]-β-CPPIT to the serotonin transporter.

The course of the metabolism was similar for [C-11]-β-CPPIT and β-CIT. The percentage of radioactive metabolites of [C-11]-β-CPPIT in plasma (54% at 90 min p.i.) was comparable to the results reported by Scanley and co-workers for [I-123]-β-CIT (60% at 90 min p.i.) [94].

In contrast to β-CIT [97] where the striatal uptake increased with time, the striatal time-activity curve of β-CPPIT reached a maximum at 45 min p.i. and remained at a constant level until the end of the scan. The striatum-to-cerebellum ratio increased continuously during the whole period of the PET study. The uptake of radioactivity in the thalamus was considerably lower for β-CPPIT than for β-CIT [97] indicating a lower serotonin transporter affinity.

To confirm specificity and selectivity of the [C-11]-β-CPPIT binding to the human DAT, blockade- or displacement studies have to be performed. Especially, further investigations of the affinity of [C-11]-β-CPPIT to the human serotonin transporter would be of interest because radioactivity in the thalamus is normally ascribed to 5-HTT binding. To analyse radioligand binding several compartment models were tested. The 1-tissue compartment model provided the most robust kinetic variables. All data processing steps such as ROI delineation, time-activity curve generation and kinetic model fitting were performed using a software package dedicated for PET data quantitation (Pmod, [127]). Preliminary calculations with a reference model using the white matter as reference region have shown that kinetic modeling may be performed without determination of the metabolite-corrected input function, which would markedly reduce the required time and costs of a PET examination.

In summary, the findings in this work suggest that [C-11]-β-CPPIT is a suitable PET tracer for the human DAT. Future studies in patients with Parkinson's or Alzheimer's disease, schizophrenia or depression will show, whether neurodegenerative processes can be visualised using [C-11]-β-CPPIT and PET.

3.6. Experimental

3.6.1. General Procedures

Cocaine hydrochloride was obtained from Hänseler AG, Herisau, Switzerland and 4-chlorophenylmagnesium bromide was obtained from Aldrich Chemie, Buchs, Switzerland. Diethylether and tetrahydrofuran were dried over sodium and benzophenone.

Thin layer chromatography (TLC) was performed on silica gel plates Kieselgel 60/UV_{254}, Merck) and column chromatography on silica gel (Kieselgel 60, Merck).

The NMR-spectra were recorded on a Bruker AC-250 (^{1}H: 300 MHz; ^{13}C: 75 MHz) or on a Bruker AMX 500 (^{13}C: 125 MHz) using TMS as an internal standard. The signals are reported in ppm (δ) downfield.

Mass spectra were recorded on a Trio 2000 Spectrometer (VG Organic, UK) using positive ion mode with electrospray as interface (ES^+).

Melting points were determined on a Büchi 530 apparatus (Büchi, Switzerland) and are uncorrected.

For radio-TLC silica gel plates (Kieselgel 60/UV_{254}, Merck) were used and analysed on a Berthold Tracemaster 20 automatic TLC-linear analyser.

For isocratic HPLC separations six different systems were used:

System A (semi-preparative): Consisting of a Merck-Hitachi L-6000A pump, a LabSource H.S. valve 7000e with a 5 ml loop, a Merck-Hitachi L-4000A UV detector (at 254 nm), a NaI scintillation detector and a Phenomenex column, Luna, C18, (10 x 250 mm, 5μm) with 0.01M ammonium formate : CH_3CN = 20 : 80 as solvent at a flow rate of 8 ml/min.

System B (analytical): Consisting of a Merck-Hitachi D-7100 pump, a 100 μl loop, a Merck-Hitachi D-7200 autosampler, a NaI scintillation detector, a Merck-Hitachi L-7400 UV detector (at 254 nm), a Phenomenex column, Luna, C18, (4.6 x 250 mm, 5 μm) with 0.1% TEA : CH_3CN = 15 : 85 as solvent at a flow rate of 1.5 ml/min.

System C (semi-preparative): Consisting of a Waters 510 pump, a valco 6-port valve with 5 ml loop, a KNAUER UV detector (at 254 nm), a Geiger-Müller counter LND 714 with an Eberline RM-14 instrument and a Phenomenex Bondclone C18 column (250 x 10 mm) with 0.1% TEA : CH_3CN = 45 : 55 as solvent at a flow rate of 8 ml/min.

System D (analytical): Consisting of a Rheodyne injector with 100 ml loop, a Merck-Hitachi L 6200 pump, a NaI scintillation detector (Scintillation Meter type 540, Mini Instruments Ltd, Burnham on Crouch/UK), a Merck-Hitachi L-4000 UV detector (at 254 nm), a Merck-Hitachi D-2500 Chroma integrator, a Bondclone 10, C18 column (300 x 3.9 mm) with 0.1% TEA : CH_3CN = 35 : 65 as solvent at a flow rate of 2 ml/min.

System E (analytical): In analogy to system D with a μBondapak C18 column (300 x 4.6 mm) with 0.1% TEA : CH_3CN = 30 : 70 as solvent at a flow rate of 2 ml/min.

System F (semi-preparative): In analogy to system A with a Phenomenex Bondclone C18 column (10 x 250 mm) MeOH : water buffered with phosphoric acid and 0.2% TEA, pH 7.2 = 2:1 as solvent at a flow rate of 8 ml/min.

3.6.2. Synthesis of precursors and reference compounds

3.6.2.1. Anhydroecgonine methyl ester (23) [100]

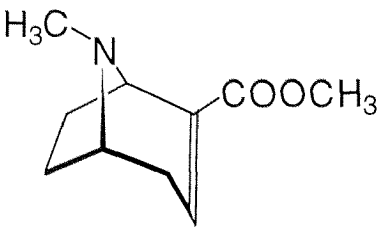

Cocaine hydrochloride (**22**) (20.0 g, 59 mmol) was refluxed in concentrated hydrochloric acid (200 ml) for 20 h. The reaction mixture was allowed to cool to room temperature, kept in a refrigerator at 4°C for 2 h and the benzoic acid was removed by filtration. The filtrate was concentrated, MeOH (80 ml) was added and the solvent was evaporated. The oily residue was triturated several times with portions of diethylether (3 x 50 ml) and filtered to remove traces of benzoic acid. The residue was dried at room temperature under reduced pressure for 30 min before adding a saturated solution of hydrogen chloride gas in MeOH (250 ml). After standing for 3 days at room temperature the MeOH was removed. The residue was made alkaline (pH 11-12) with 4M NaOH, extracted with diethylether and dried over sodium sulfate. The solvent was evaporated and the residue was distilled in vacuum (120°C, 1 mbar) to give 8.16 g (45 mmol, 75%) of the ester **23** as a yellow oil ([100]: 75%).

^{1}H-NMR ($CDCl_3$): 1.31 - 1.41 (m, 1 H); 1.64 - 1.72 (m, 2 H); 1.92 - 2.07 (m, 2 H); 2.19 (s, 3 H); 2.40 - 2.50 (m, 1 H); 3.08 (m, 1 H); 3.58 (s, 3 H); 3.61 - 3.63 (m, 1 H); 6.65 - 6.67 (m, 1 H).

MS: 182 (100%, $C_{10}H_{16}NO_2^+$).

3.6.2.2. 2β-Carbomethoxy-3β-(4'-chlorophenyl)tropane (24) [100, 101]

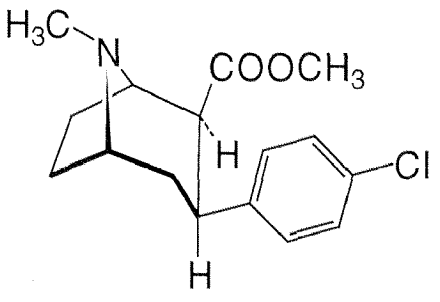

A solution of anhydroecgonine methyl ester (**23**) (3.7 g, 20 mmol) in dry diethylether (100 ml) was dropped to a vigorously stirred solution of 4-chlorophenylmagnesium bromide (1 M; 40 ml) in dry diethylether (120 ml) at -45 to -50°C (temperature of the reaction mixture). The reaction mixture was kept between -45 and -50°C for further 2 h, then cooled to -78°C and treated with a solution of TFA (4.6 g, 40 mmol) in dry diethylether (30 ml) during 5 min. The mixture was allowed to warm to 0°C and diluted with distilled water (100 ml). The aqueous phase was acidified to pH 1 with concentrated hydrochloric acid, separated from the organic phase, made alkaline with concentrated ammonium hydroxide and extracted with diethylether. The combined organic phases were dried over sodium sulfate, filtered, evaporated and purified by flash chromatography (diethylether : TEA = 9 : 1) to give 1.8 g (30%) of the β-isomer of the tropane **24** and 0.8 g (14%) of the α-isomer ([100]: 15% α; 41% β).

^{1}H-NMR ($CDCl_3$): 1.64 - 1.82 (m, 4 H); 2.10 - 2.22 (m, 1 H); 2.28 (s, 3 H); 2.56 - 2.68 (m, 1 H); 2.91 - 2.96 (m, 1 H); 2.98 - 3.07 (m, 1 H); 3.42 - 3.46 (m, 1 H); 3.57 (s, 3 H); 3.59 - 3.64 (m, 1 H); 7.22 - 7.32 (m, 4 H).

MS: 318 (13%, $C_{16}H_{20}NO_2{}^{37}ClNa^+$); 316 (34%, $C_{16}H_{20}NO_2{}^{35}ClNa^+$); 296 (32%, $C_{16}H_{21}NO_2{}^{37}Cl^+$); 294 (100%, $C_{16}H_{21}NO_2{}^{35}Cl^+$).

3.6.2.3. 3β-(4'-Chlorophenyl)-2β-(3'-phenylisoxazol-5'-yl)tropane (β-CPPIT, 17) [98]

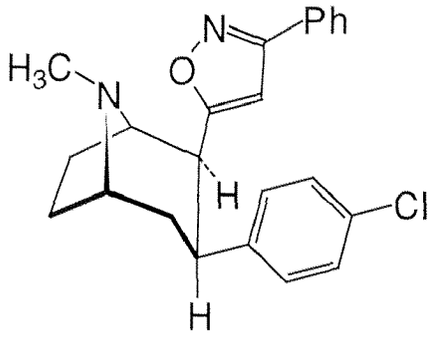

A solution of n-butyllithium in hexane (1.6 M, 3.9 ml) was dropped under vigorous stirring at 0°C under nitrogen to a solution of acetophenone oxime (0.42 g, 3.12 mmol) in dry THF (11 ml). After 1 hour stirring at 0°C a solution of the ester **24** (0.50 g, 1.71 mmol) in THF (4 ml) was added slowly. The suspension was allowed to warm to room temperature and stirred for further 19 h. The reaction mixture was poured into a stirred solution of concentrated sulfuric acid (1.4 g) in THF (7 ml) and distilled water (2 ml) and refluxed for 70 min. After cooling to room temperature the reaction mixture was made alkaline with saturated potassium carbonate solution and extracted with dichloromethane. The combined organic phases were dried over sodium sulfate. The solvent was removed to give 0.84 g of crude isoxazole **17**. Purification by column chromatography (hexane : diethylether : TEA = 80 : 18 : 2) gave 0.35 g (0.92 mmol, 54%) of the pure isoxazole **17** [98]: 50%).

^{1}H-NMR ($CDCl_3$): 1.66 - 1.78 (m, 3 H); 2.12 - 2.30 (m, 3 H); 2.31 (s, 3 H); 3.22 - 3.35 (m, 2 H); 3.35 - 3.48 (m, 2 H); 6.84 (s, 1 H); 6.94 - 6.98 (d, 2 H, J = 8.4 Hz); 7.12 - 7.16 (d, 2 H, J = 8.5 Hz); 7.40 - 7.47 (m, 3 H); 7.77 - 7.80 (m, 2 H).

^{13}C-NMR ($CDCl_3$, 75 MHz): 42.6 N(CH_3)

MS: 403 (26, $C_{23}H_{23}N_2O^{37}ClNa^+$); 401 (98, $C_{23}H_{23}N_2O^{35}ClNa^+$); 381 (33, $C_{23}H_{24}N_2O^{37}Cl^+$); 379 (100, $C_{23}H_{24}N_2O^{35}Cl^+$).

Mp.: 110 - 112°C

3.6.2.4. 3β-(4'-Chlorophenyl)-2β-(3'-phenylisoxazol-5'-yl)nortropane (21)

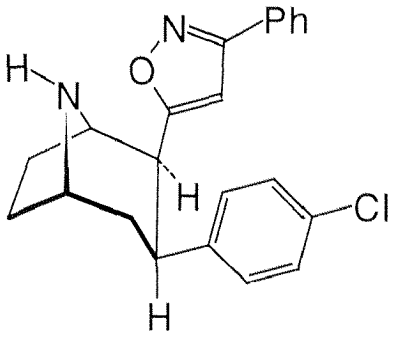

1-Chloroethyl chloroformate (0.1 ml, 0.9 mmol) was added to a solution of the tropane **17** (101 mg, 0.27 mmol) in 1,2-dichloroethane (2.5 ml). The reaction mixture was refluxed at 94°C for 70 h. The resulting suspension was concentrated under reduced pressure. The residue was dissolved in MeOH (1.5 ml) and refluxed (80°C) for 5 h. After removal of the solvent the residue was dissolved in dichloromethane (2 ml) and saturated sodium hydrogen carbonate solution (5 ml). The mixture was extracted with dichloromethane (5 x 10 ml). The combined organic phases were dried over sodium sulfate and concentrated under reduced pressure to give 105 mg of the crude nortropane **21**. Purification by column chromatography (hexane : diethylether : TEA = 50 : 45 : 5) gave 66 mg (0.18 mmol, 67%) of the pure nortropane **21**.

MS: 367 (32; $C_{22}H_{22}N_2O^{37}Cl^+$); 365 (100; $C_{22}H_{22}N_2O^{37}Cl^+$).

^{1}H-NMR ($CDCl_3$): 1.70 - 2.40 (m, 7 H); 3.29 - 3.50 (m, 2 H); 3.74 - 3.86 (m, 2 H); 6.21 (s, 1 H); 6.98 - 7.03 (d, 2 H, J = 8.5 Hz); 7.12 - 7.18 (d, 2 H, J = 8.5 Hz); 7.39 - 7.44 (m, 3 H); 7.68 - 7.73 (m, 2 H).

Elemental analysis calculated for $C_{22}H_{21}N_2OCl$: C: 72.42%, H: 5.80%, N: 7.68%, O: 4.38%, Cl: 9.72%; found: C: 72.27%, H: 5.79%, N: 7.76%.

Mp.: 80 - 84°C

3.6.2.5. N-(2'-Hydroxyethyl)-3β-(4'-chlorophenyl)-2β-(3'-phenylisoxazol-5'-yl)nortropane (27)

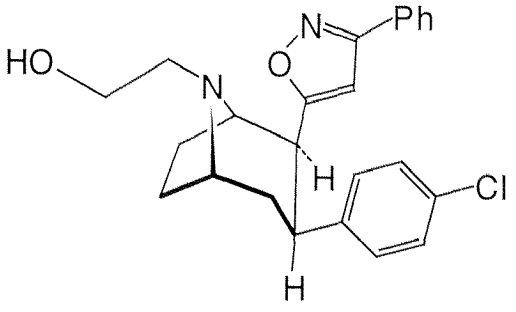

A solution of the nortropane **21** (32.2 mg, 88 µmol), TEA (40 µl, 280 µmol) and 2-bromoethanol (37 µl, 260 µmol) in acetonitrile (3 ml) was stirred at 35°C for 90 h. During the reaction time a further portion of 2-bromoethanol (18.5 µl, 130 µmol) was added. The reaction mixture was concentrated under reduced pressure. The product was separated by preparative TLC (diethylether : TEA = 95 : 5).

^{1}H-NMR ($CDCl_3$): 1.30 - 2.31 (m, 8 H); 2.49 - 3.06 (m, 4 H); 3.24 - 3.66 (m, 3 H); 6.28 (s, 1 H); 6.98 - 7.05 (d, 2 H, J = 8.5); 7.12 - 7.18 (d, 2 H, J = 8.5); 7.35 - 7.43 (m, 3 H); 7.65 - 7.75 (m, 2 H)

MS: 411 (34, $C_{24}H_{26}N_2O_2{}^{37}Cl^+$); 409 (100, $C_{24}H_{26}N_2O_2{}^{35}Cl^+$).

3.6.2.6. N-(2'-Mesyloxyethyl)-3β-(4'-chlorophenyl)-2β-(3'-phenylisoxazol-5'-yl)nortropane (29)

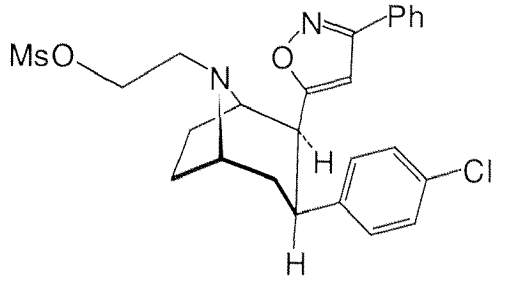

The alcohol **27** (16.3 mg, 33.5 µmol) and methanesulfonic anhydride (58.3 mg, 335 µmol) were dissolved in dichloromethane (2 ml) and stirred for 90 h. During the reaction time a further portion methanesulfonic anhydride (29.1 mg, 167 µmol) was added. The reaction mixture was diluted with phosphate buffer (0.15 M, 20 ml) and extracted with dichloromethane. The combined organic layers were dried over magnesium sulfate and concentrated under reduced pressure. The resulting yellow oil (18.9 mg, 95%) was used for the radiolabelling without further purification and no ^{1}H-NMR data was collected. MS: 489 (43, $C_{25}H_{28}N_2O_4{}^{37}ClS^+$); 487 (100, $C_{25}H_{28}N_2O_4{}^{35}ClS^+$); 391 (22).

3.6.2.7 N-(2'-Fluoroethyl)-3β-(4'-chlorophenyl)-2β-(3'-phenylisoxazol-5'-yl)nortropane (18)

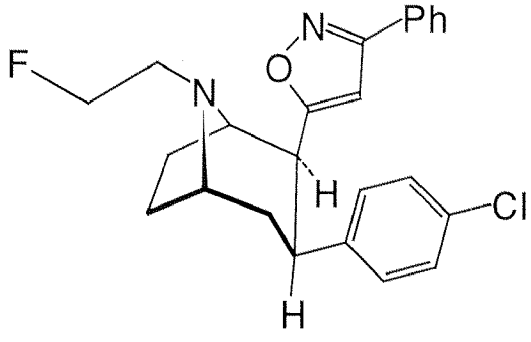

Diethylaminosulfurtrifluoride (DAST) (3.2 µl, 24.5 µmol) was diluted with dichloromethane (0.5 ml) and cooled down to -78°C in a dry ice acetone bath. A solution of the alcohol **27** in dichloromethane was added dropwise under vigorous stirring. The cooling-bath was removed and the light yellow solution was stirred for 30 h. During this time a second portion of DAST (24.5 µmol, 3.2 µl) was added. The reaction mixture was concentrated under reduced pressure and the product was separated by preparative TLC (diethylether : TEA : hexane = 63.3 : 3.3 : 33.3; R_f: 0.33). 1.5 g (7%) of the fluoroethyltropane **18** were isolated.

^{1}H-NMR ($CDCl_3$): 1.29 - 2.30 (m, 8 H); 2.47 - 2.76 (m, 3 H); 3.12 - 3.23 (m, 1 H); 4.45 - 4.73 (dt, 2 H, J_{HF} = 47.4 Hz, J = 5.6 Hz); 6.63 (s, 1 H); 6.98 - 7.06 (d, 2 H, J = 8.5); 7.10 - 7.18 (d, 2 H, J = 8.5); 7.37 - 7.49 (m, 3 H); 7.71 - 7.79 (m, 2 H)

MS:435 (34, $C_{24}H_{24}N_2OF^{37}ClNa^+$); 433 (100, $C_{24}H_{24}N_2OF^{35}ClNa^+$); 413 (13, $C_{24}H_{25}N_2OF^{37}Cl^+$); 411 (41, $C_{24}H_{25}N_2OF^{35}Cl^+$).

3.6.2.8. N-(3'-Hydroxypropyl)-3β-(4'-chlorophenyl)-2β-(3'-phenylisoxazol-5'-yl)nortropane (28)

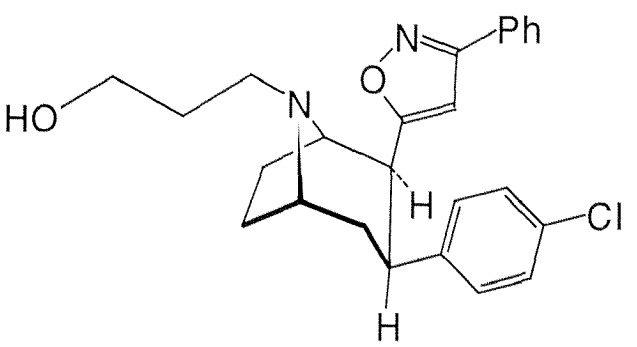

The nortropane **21** (29.6 mg, 81 µmol), TEA (40 µl, 280 µmol) and 3-bromopropanol (40 µl, 457 µmol) were dissolved in acetonitrile (3 ml) and stirred for 70 h at 35°C. After evaporation of the solvent the crude product was redissolved in dichloromethane and separated by preparative TLC (diethylether : TEA = 95 : 5; R_f: 0.23). The product was eluted of the silica gel with dichloromethane. 31.0 mg (90%) of the alcohol **28** could be obtained as a colorless oil.

^{1}H-NMR ($CDCl_3$): 1.35 - 2.29 (m, 10 H); 2.44 - 3.02 (m, 4 H); 3.29 - 3.70 (m, 3 H); 6.41 (s, 1 H); 6.92 - 7.02 (d, 2 H, J = 8.3); 7.09 - 7.19 (d, 2 H, J = 8.3); 7.31 - 7.42 (m, 3 H); 7.66 - 7.78 (m, 2 H)

MS: 447 (18, $C_{25}H_{27}N_2O_2{}^{37}ClNa^+$); 445 (54, $C_{25}H_{27}N_2O_2{}^{35}ClNa^+$); 425 (35, $C_{25}H_{28}N_2O_2{}^{37}Cl^+$); 423 (100, $C_{25}H_{28}N_2O_2{}^{35}Cl^+$).

3.6.2.9. N-(3'-Mesyloxypropyl)-3β-(4'-chlorophenyl)-2β-(3'-phenylisoxazol-5'-yl)nortropane (30)

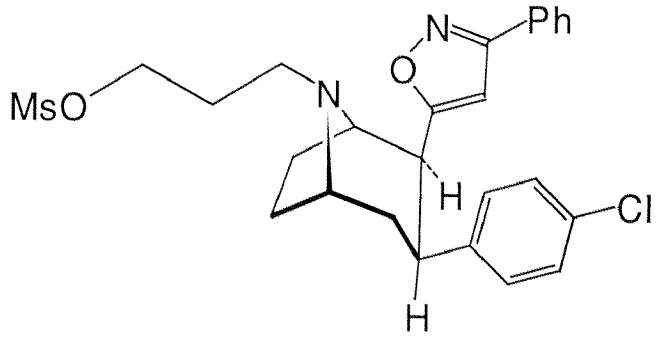

The alcohol **28** (31 mg, 73 µmol) and methanesulfonic anhydride (129 mg, 740 µmol) were dissolved in dichloromethane (4 ml) and stirred at 35°C for 90 h. The reaction mixture was diluted with phosphate buffer (0.15 M, 30 ml) and extracted with dichloromethane. The combined organic layers were dried over sodium sulfate and concentrated under reduced pressure. Due to the low stability the resulting mesylate **30** (35.5 mg; 96%, yellow oil) was used for the radiolabelling without further purification and no ^{1}H-NMR data was collected.
MS: 503 (36, $C_{26}H_{30}N_2O_4S^{37}Cl^+$); 501 (100, $C_{26}H_{30}N_2O_4S^{35}Cl^+$)

3.6.2.10 N-(3'-Fluoropropyl)-3β-(4'-chlorophenyl)-2β-(3'-phenylisoxazol-5'-yl)nortropane (19)

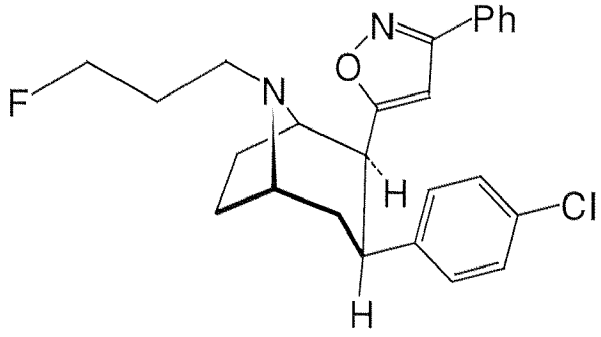

A solution of the nortropane **21** (7.0 mg, 19 µmol), TEA (15 µl, 108 µmol) and 3-bromo-1-fluoropropanol (8 µl) in acetonitrile (2 ml) was stirred for 90 h at 35°C. After evaporation of the solvent the crude product was redissolved in dichloromethane and separated by preparative TLC (diethylether : TEA = 95 : 5; R_f: 0.71). The product was eluted from the silica gel with dichloromethane. After evaporation of the solvent 4.9 mg (60%) of FP-β-CPPIT **19** could be isolated.

^{1}H-NMR ($CDCl_3$): 1.32 - 2.33 (m, 10 H); 2.42 – 2.71 (m, 3 H); 3.21 - 3.32 (m, 1 H); 4.38 - 4.65 (dt, 2 H, J_{HF} = 47.5 Hz, J = 5.8 Hz); 6.68 (s, 1 H); 6.94 - 7.03 (d, 2 H, J = 8.5); 7.08 - 7.16 (d, 2 H, J = 8.5); 7.38 - 7.49 (m, 3 H); 7.69 - 7.80 (m, 2 H)

MS: 449 (34, $C_{25}H_{26}N_2OF^{37}ClNa^+$); 447 (100, $C_{25}H_{26}N_2OF^{35}ClNa^+$); 427 (33, $C_{25}H_{27}N_2OF^{37}Cl^+$); 425 (98, $C_{25}H_{27}N_2OF^{35}Cl^+$).

3.6.3. Radiolabelling and [C-13]-labelling

3.6.3.1. Radiosynthesis of [C-11]-iodomethane

At the University Hospital in Zurich (USZ) [C-11]-CO_2 was produced *via* the $^{14}N(p,\alpha)^{11}C$ reaction using the 16.5 MeV cyclotron. [C-11]-CH_3I was prepared from [C-11]-CO_2 in a two step reaction sequence involving the catalytic (Ni) reduction of [C-11]-CO_2 to [C-11]-CH_4 and the subsequent gas phase iodination of [C-11]-CH_4 with I_2 at 720^{0}C to give [C-11]-CH_3I according to the standard procedure described in the literature [105, 106]. Yields up to 50% (decay-corrected from [C-11]-CH_4) were obtained with a preparation time of approximately 12 min. At the Paul Scherrer Institute (PSI) [C-11]-CH_3I was obtained by the bombardment of nitrogen (containing 100 - 200 ppm oxygen) with 17 MeV protons using the classical method described by Crouzel and co-workers [104].

3.6.3.2. [C-11]-3β-(4'-Chlorophenyl)-2β-(3'-phenylisoxazol-5'-yl)tropane ([C-11]-β-CPPIT, [C-11]-17)

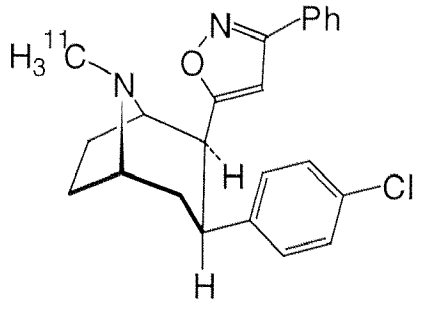

The nortropane **21** (0.5 mg, 1.4 μmol) was dissolved in dry DMF (300 μl). The reacti-vial containing the solution of the precursor was then positioned in a quartz lamp-heated vessel, and [C-11]-CH_3I was added to the solution *via* a slow stream of helium. Following the complete addition of the [C-11]-iodomethane, the flow of helium was stopped and the reacti-vial was heated to 120°C for 10 min. The purification of the crude product was achieved by HPLC (system A). After evaporation of the mobile phase, the residue was dissolved in a mixture of Tween 80® (0.1%), ethanol (10%) and 0.9% NaCl-solution (90%) and filtered through a Millipore filter (0.22 μm). The radiochemical yield was in the range of 60 - 70% (decay corrected from [C-11]-CH_3I)

3.6.3.3. [C-13]-3β-(4'-Chlorophenyl)-2β-(3'-phenylisoxazol-5'-yl)tropane ([C-13]-β-CPPIT, [C-13]-17)

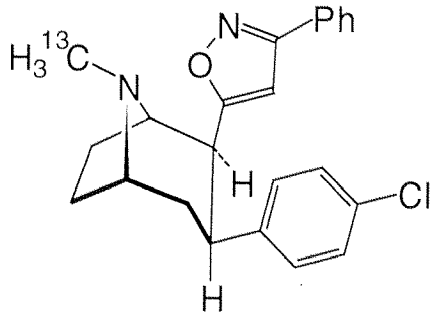

The [C-13]-methylation was achieved by reacting the desmethyl-compound **21** with [C-13]-CH_3I under the same conditions as described above (120°C, 10 min). The product was purified by HPLC (system A) and examined by ^{13}C-NMR and mass spectrometry.

^{13}C-NMR ($CDCl_3$, 125 MHz): 42.68 (N-CH_3).

MS: 380 (M+1, 100).

3.6.3.4. [F-18]-N-(3'-Fluoroethyl)-3β-(4'-chlorophenyl)-2β-(3'-phenylisoxazol-5'-yl)nortropane ([F-18]-FE-β-CPPIT, [F-18]-18)

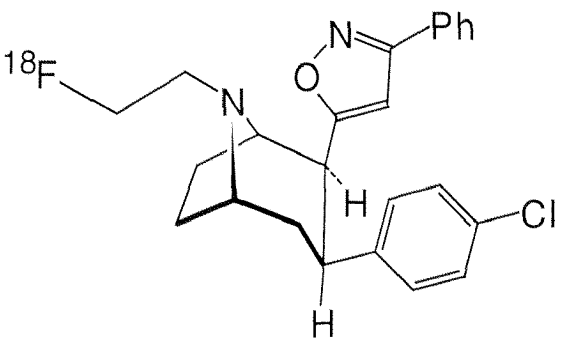

[F-18]-Fluoride was produced by irradiation of 2.5 ml 98% enriched [O-18]-water by the $^{18}O(p,n)^{18}F$ reaction as described previously [128, 129]. The aqueous [F-18]-fluoride (7.8 GBq) was placed into a reacti-vial containing K_2CO_3 (3 mg). After evaporation to dryness under a stream of nitrogen at 100°C a solution of Kryptofix 2.2.2.® (9 mg) in acetonitrile was added. The solvent was removed under reduced pressure followed by azeotropic evaporation with acetonitrile (3 x 1 ml). The mesylate precursor **29** was dissolved in acetonitrile (1 ml) and added. After stirring the mixture for 1 h at 100°C the reaction mixture was diluted with water and passed through a Sep-Pak® C18-cartridge (Millipore Corp.). The cartridge first was washed with water and the product was eluted with diethylether into a new reacti-vial. The organic solvent was removed under reduced pressure. [F-18]-FE-β-CPPIT was purified by HPLC (system C). After the evaporation of the mobile phase, the [F-18]-FE-β-CPPIT was formulated in

a solution containing Tween 80® (0.1%), ethanol (10%) and 0.15 M phosphate buffer (90%) and filtered through a Millipore filter (0.22 µm). The radiochemical yield was 15%.

3.6.3.5. [F-18]-N-(3'-Fluoropropyl)-3β-(4'-chlorophenyl)-2β-(3'-phenyl-isoxazol-5'-yl)nortropane ([F-18]-FP-β-CPPIT, 19)

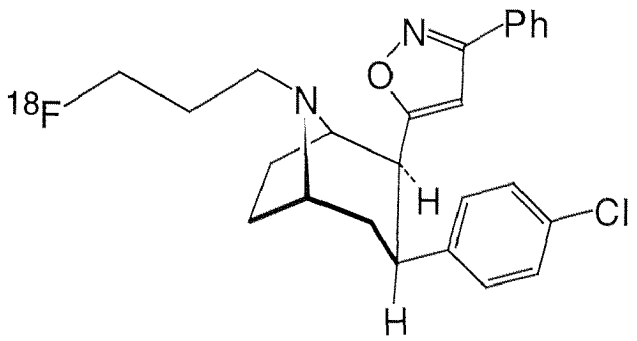

[F-18]-radiolabelling of FP-β-CPPIT was achieved in analogy to the fluoroethyl derivative by a n.c.a. fluorination of the mesylate precursor **30**. The radiochemical yield was in the range of 1 - 10%.

3.6.4. LogP-Determination

The lipophilicity of β-CPPIT and its fluoroalkyl analogues was estimated by the shake flask method described by Strijckmans co-workers [114] using a mixture of octanol and phosphate buffer (0.15 M). The radiotracers (100 kBq) were shaken vigorously for 1 min in a test tube containing 1 ml of octanol and 1 ml of the phosphate buffer. The mixture was centrifuged for 5 min at 3000 rpm. 100 µl of each phase were taken off and the radioactivity of each sample was measured in a γ-counter. 600 µl of the octanol phase were transferred to another test tube containing 400 µl of octanol and 1 ml of phosphate buffer. The

mixture was further shaken and centrifuged. This procedure was repeated several times. The radioactivity ratios of organic and aqueous phase (P) were calculated and the partition coefficient (log $P_{7.4}$) determined.

3.6.5. *In vitro* stability

To investigate the stability of [C-11]-β-CPPIT in human plasma, 100 MBq of the radiotracer were added to 5 ml human blood. The plasma was separated by centrifugation (3000 rpm, 5 min) and incubated for 1 h (3 x $t_{1/2}$ of [C-11]) at 37°C. For protein precipitation a plasma sample (0.6 ml) was treated with acetonitrile (1.2 ml). After centrifugation (3000 rpm, 2 min) the supernatant was analysed by HPLC (system E) and radio-TLC (silicagel, diethylether : TEA = 95 : 5).

The same procedure was used for the determination of the *in vitro* plasma stability of the [F-18]-fluoroalkyl derivatives. The only differences were the increased incubation time of 6 h (3 x $t_{1/2}$ of [F-18]) and the use of a different analytical HPLC system (system D).

3.6.6. Biodistribution of [C-11]-β-CPPIT in mice

The biodistribution of [C-11]-β-CPPIT was determined in female mice (ICR, ca. 20 g, originating from the Institut für Labortierkunde, Universität Zürich). Each animal received a tail vein injection of 3 MBq of [C-11]-β-CPPIT, dissolved in a solution containing Tween 80® (1%), ethanol (9%) and 0.15 M phosphate buffer (pH 7.4) (90%). The specific activity of [C-11]-β-CPPIT was in the range of 2000 - 3000 GBq/mmol at the time of injection. At 5, 15, 30, 60 or 90 min p.i. groups of three mice each were sacrificed. Striatum, frontal cortex, cerebellum, blood, lung and liver were dissected and weighed. The tissue radioactivity was measured in a γ-counter and the percentage ID/g was calculated.

3.6.7. Blockade studies of [C-11]-β-CPPIT in mice

The blockade studies were performed in female mice (ICR, ca. 20 g, obtained from the Institut für Labortierkunde, Universität Zürich). Various uptake inhibitors were injected prior to the tracer application in groups of three animals into the tail vein (citalopram, prior 5 min, 5 mg/kg; GBR 12909, prior 15 min, 5 mg/kg; ketanserin, prior 15 min, 2.5 mg/kg and desipramine, prior 15 min, 5 mg/kg). Each animal received a tail vein injection of 3 MBq of [C-11]-β-CPPIT, dissolved in a solution containing Tween 80® (1%), ethanol (9%) and 0.15 M phosphate buffer (pH 7.4) (90%). The specific activity of [C-11]-β-CPPIT was in the range of 2000 - 3000 GBq/mmol at the time of injection. At 60 min p.i. [C-11]-β-CPPIT the mice were sacrificed and their brains dissected.

3.6.8. Metabolite studies of [C-11]-β-CPPIT in mice

The metabolite studies were carried out in female mice (NMRI, 25 - 30 g, originating from Biological Research Laboratories, Füllinsdorf, Switzerland). The mice were anaesthetised with methoxyflurane and kept under narcosis during the incubation time. The administered dose was 10 MBq of [C-11]-β-CPPIT and injected through the tail vein. At the time of injection [C-11]-β-CPPIT had a specific activity of 50 - 60 GBq/μmol. The mice were sacrificed after 15 or 30 min.

For determination of radiolabelled metabolites the blood samples were taken and centrifuged at 3000 rpm for 5 min. The plasma fractions (210 μl) were treated with phosphate buffer (pH 7.4) (60 μl) and extracted twice with heptane (270 μl). The aqueous and organic phases were measured in a γ–counter and analysed with HPLC (system F) and radio-TLC (silicagel, diethylether : TEA = 9 : 1).

The brains were washed with distilled water and homogenised with 1 ml phosphate buffer (pH 7.4) using a Potter Elveshjem homogeniser while cooling

with ice-water. 500 µl of the homogenate were measured in a γ-counter and then extracted twice with 500 µl heptane. The organic and aqueous phases were analysed for metabolites with HPLC and radio-TLC in analogy to the blood samples.

3.6.9. Toxicological study of [C-11]-β-CPPIT in mice and rats

The toxicological studies were performed by Biological Research Laboratories, Füllinsdorf, Switzerland in mice (NMRI (SPF)) and rats (Hanlbm: WIST (SPF)). Groups of three female and three male animals were treated with β-CPPIT at 0.1 mg/kg body weight by i.v. injection into the tail vein. β-CPPIT was suspended in a solution containing Tween 80® (1%), ethanol (9%) and 0.15 M phosphate buffer (pH 7.4) (90%) at a concentration of 0.1 mg/ml and administered in a volume of 1 ml/kg body weight. The animals were examined for clinical signs four times during day 1 and once daily during days 2-15. Mortality and viability were recorded together with clinical signs at the same time intervals. Body weights were recorded on days 1 (prior to administration) 8 and 15. All animals were necropsied and examined macroscopically.

3.6.10. PET studies with [F-18]-FE- and [F-18]-FP-β-CPPIT in monkeys

3.6.10.1. PET brain imaging

The PET scans were performed in female rhesus monkeys (Macaca mulatta) weighing approximately 6 kg. Anaesthesia was induced by Nembutal® and maintained with a mixture of N_2O and O_2. Before each study, the monkey was deprived of food for 12 h. The studies were conducted according to the regulations for animal research from the Veterinary Health Authorities of Cantons Zurich and Aargau, Switzerland.

The PET brain imaging was performed on a Ecat PRT-2 scanner. [F-18]-FE-β-CPPIT (95 MBq) or [F-18]-FP-β-CPPIT (154 MBq), respectively, were injected i.v.. Simultaneously, the PET scan was started according to the following protocol: 5 x 2 min, 3 x 3 min, and 15 x 5 min (total: 94 min).

3.6.10.2. Metabolite studies

For metabolite studies venous blood samples were taken at 5, 15, 30 and 60 min p.i.. The blood samples were centrifuged at 3000 rpm for 5 min. The plasma proteins were precipitated by treating the plasma (0.6 ml) with acetonitrile (1.2 ml). After centrifugation (3000 rpm, 2 min) the supernatant was evaporated to dryness. The residue was redissolved in the HPLC solvent and analysed with HPLC (system D) and radio-TLC (diethylether/TEA 95/5)

3.6.11. PET study with [C-11]-β-CPPIT in humans

3.6.11.1. Study subjects

Six healthy volunteers (4 male and 3 female) with a mean age of 23 (range: 21-27) were recruited and physically examined including electrocardiogram and blood analyses. The volunteers were also screened by psychiatric interview to assure that they had neither personal nor family histories of major psychiatric disorders. Subjects with a history of illicit drug abuse were excluded from the study. All subjects gave written informed consent. The study was approved by the local and the National Ethics Committees and by the Swiss Federal Health Office (BAG).

3.6.11.2. PET brain imaging

PET imaging was performed on a GE Advance PET scanner (General Electrics, Waukesha, Wisconsin, U.S.A.) with an axial field of 14.45 cm, divided into 35 slices each with a slice thickness of 4.25 mm. After the placement of a radial artery and a cubital vein catheter, the subjects were positioned supine in the scanner. Prior to the injection of the radioligand a 10 min transmission scan with a ^{68}Ge pin source of 400 MBq activity was performed to correct for attenuation. Following i.v. injection (slow bolus over 5 min with an infusion pump) of 381 ± 90 MBq [C-11]-β-CPPIT a dynamic PET scan was initiated according to the following protocol: 31 frames in 90 min (9x20 sec, 4x30 sec, 2x60 sec, 4x120 sec, 9x300 sec, 3x600 sec). The specific radioactivity at the time of injection was on average 124 ± 30 GBq/µmol (3337 ± 802 Ci/mmol).

3.6.11.3. Blood sampling and determination of labelled metabolites in plasma

Arterial blood samples were collected every 30 sec for the first 6 min, and then at the following time points: 6, 7, 8, 9, 10, 12.5, 15, 17.5, 20, 25, 30, 45, 60, 75, and 90 min p.i.. An aliquot of each sample was measured in a γ-counter and the plasma was analysed to correct the input function for metabolised radioligand activity. Following centrifugation, 1 ml of plasma was extracted as described in chapter 3.6.8.. The fractions were counted in a γ-counter and some samples were additionally analysed with radio-TLC (silicagel; diethylether : TEA = 90 : 10) to confirm the absence of metabolites in the organic phase and the absence of the parent compound [C-11]-β-CPPIT in the aqueous phase.

3.6.11.4. Data analysis

Reconstruction was performed using filtered backprojection (Hanning filter, cut-off: 4 mm transaxial; Ramp filter, cut-off: 8.5 mm axial) and a 128x128 pixel output matrix. Attenuation correction based on the above mentioned transmission scan. The plasma data (well counter units, cpm) were expressed in scanner units by performing a calibration measurement using a 20 cm cylindrical phantom. ROIs were defined over the occipital (medial and radial), frontal (medial and lateral), temporal (medial and lateral), parietal and cerebellar cortex, striatum (caudate and putamen), thalamus and pons and the corresponding tissue time-activity curves were calculated.

To analyse radioligand binding several compartmental models were tested. The 1-tissue compartment model provided the most robust kinetic variables. Parameters of radioligand uptake (K_1), release (k_2) and distribution volume ($DV=K_1/k_2$) were obtained using least squares fitting.

All required data processing steps such as ROI delineation, time-activity curve generation and kinetic model fitting were performed using a software package dedicated for PET data quantitation (Pmod, [127]).

4. References

1. Barrio J.R., Huang S.C., Melega W.P., Yu D.C., Hoffman J.M., Schneider J.S., Satyamurthy N., Mazziotta J.C. and Phelps M.E., *6-[^{18}F]fluoro-L-dopa probes dopamine turnover rates in central dopaminergic structures.* J. Neurosci. Res., 1990. **27**: p. 487-493.
2. Wienhard K., Herholz K., Coenen H.H., Rudolf J., Kling P., Stöcklin G. and Heiss W.D., *Increased amino acid transport into brain tumors measured by PET of L-(2-^{18}F)fluorotyrosine.* J. Nucl. Med., 1991. **32**: p. 1338-1346.
3. Bauer R., *Physikalisch-technische Grundlagen der Positronen-Emissions-Tomography (PET).* Der Nuklearmediziner, 1994. **17**: p. 177-189.
4. von Schulthess G.K., Westera G. and Schubiger P.A., *Positronenemissionstomographie (PET) - grundsätzliche Überlegungen.* Schweiz. Rundschau Med., 1993: p. 901-904.
5. Burger C. and von Schulthess G.K., *Gamma rays: Nuclear medicine*, in *Functional imaging*, von Schulthess G.K. and Hennig J., Editors. 1998, Lippincott-Raven: Philadelphia. p. 157-216.
6. Walsh M.N., Geltman E.M., Brown M.A., Henes C.G., Weinheimer C.J., Sobel B.E. and Bergmann S.R., *Noninvasive estimation of regional myocardial oxygen consumption by positron emission tomography with carbon-11 acetate in patients with myocardial infarction.* J. Nucl. Med., 1989. **30**: p. 1798-1808.
7. Henes C.G., Bergmann S.R., Walsh M.N., Sobel B.E. and Geltman E.M., *Assessment of myocardial oxidative metabolic reserve with positron emission tomography and carbon-11 acetate.* J. Nucl. Med., 1989. **30**: p. 1489-1499.

8. Rubin P.J., Lee D.S., Davila Roman V.G., Geltman E.M., Schechtman K.B., Bergmann S.R. and Gropler R.J., *Superiority of C-11 acetate compared with F-18 fluorodeoxyglucose in predicting myocardial functional recovery by positron emission tomography in patients with acute myocardial infarction.* Am. J. Cardiol., 1996. **78**: p. 1230-1235.

9. Richardson M.P., Koepp M.J., Brooks D.J. and Duncan J.S., *^{11}C-flumazenil PET in neocortical epilepsy.* Neurology, 1998. **51**: p. 485-492.

10. Koepp M.J., Labbe C., Richardson M.P., Brooks D.J., Van Paesschen W., Cunningham V.J. and Duncan J.S., *Regional hippocampal [^{11}C]flumazenil PET in temporal lobe epilepsy with unilateral and bilateral hippocampal sclerosis.* Brain, 1997. **120**: p. 1865-1876.

11. Richardson M.P., Koepp M.J., Brooks D.J., Fish D.R. and Duncan J.S., *Benzodiazepine receptors in focal epilepsy with cortical dysgenesis: an ^{11}C-flumazenil PET study.* Ann. Neurol., 1996. **40**: p. 188-198.

12. Fujiwara T., Matsuzawa T., Kubota K., Abe Y., Itoh M., Fukuda H., Hatazawa J., Yoshioka S., Yamaguchi K. and Ito K., *Relationship between histologic type of primary lung cancer and carbon-11-L-methionine uptake with positron emission tomography.* J. Nucl. Med., 1989. **30**: p. 33-37.

13. Leskinen Kallio S., Nagren K., Lehikoinen P., Ruotsalainen U., Teras M. and Joensuu H., *Carbon-11-methionine and PET is an effective method to image head and neck cancer.* J. Nucl. Med., 1992. **33**: p. 691-695.

14. Nuutinen J., Leskinen S., Lindholm P., Soderstrom K.O., Nagren K., Huhtala S. and Minn H., *Use of carbon-11 methionine positron emission tomography to assess malignancy grade and predict survival in patients with lymphomas.* Eur. J. Nucl. Med., 1998. **25**: p. 729 -735.

15. Herholz K., Holzer T., Bauer B., Schroder R., Voges J., Ernestus R.I., Mendoza G., Weber Luxenburger G., Lottgen J., Thiel A., Wienhard K. and Heiss W.D., *^{11}C-Methionine PET for differential diagnosis of low-grade gliomas.* Neurology, 1998. **50**: p. 1316-1322.

16. McCann U.D., Szabo Z., Scheffel U., Dannals R.F. and Ricaurte G.A., *Positron emission tomographic evidence of toxic effect of MDMA ("Ecstasy") on brain serotonin neurons in human beings.* Lancet, 1998. **352**: p. 1433-1437.

17. Szabo Z., Kao P.F., Scheffel U., Suehiro M., Mathews W.B., Ravert H.T., Musachio J.L., Marenco S., Kim S.E. Ricaurte G.A. Wong D.F., Wagner Jr. H.N. and Dannals R.F., *Positron emission tomography imaging of serotonin transporters in the human brain using [^{11}C](+)McN5652.* Synapse, 1995. **20**: p. 37-43.

18. Suehiro M., Scheffel U., Dannals R.F., Ravert H.T., Ricaurte G.A. and Wagner H.N., Jr., *A PET radiotracer for studying serotonin uptake sites: carbon-11-McN-5652Z.* J. Nucl. Med., 1993. **34**: p. 120-127.

19. Hietala J., Nagren K., Lehikoinen P., Ruotsalainen U. and Syvalahti E., *Measurement of striatal D_2 dopamine receptor density and affinity with [^{11}C]-raclopride in vivo: a test-retest analysis.* J. Cereb. Blood Flow Metab., 1999. **19**: p. 210-217.

20. Farde L., Hall H., Pauli S. and Halldin C., *Variability in D2-dopamine receptor density and affinity: a PET study with [^{11}C]raclopride in man.* Synapse, 1995. **20**: p. 200-208.

21. Rinne J.O., Laihinen A., Rinne U.K., Nagren K., Bergman J. and Ruotsalainen U., *PET study on striatal dopamine D2 receptor changes during the progression of early Parkinson's disease.* Mov. Disord., 1993. **8**: p. 134-138.

22. Rinne J.O., Hietala J., Ruotsalainen U., Sako E., Laihinen A., Nagren K., Lehikoinen P., Oikonen V. and Syvalahti E., *Decrease in human striatal dopamine D2 receptor density with age: a PET study with [^{11}C]raclopride.* J. Cereb. Blood Flow Metab., 1993. **13**: p. 310-314.

23. Lancellotti P., Melon P.G., de Landsheere C.M., Degueldre C., Kulbertus H.E. and Pierard L.A., *The role of early measurement of nitrogen-13 ammonia uptake for predicting contractile recovery after acute myocardial infarction.* Int. J. Card. Imaging., 1998. **14**: p. 261-267.

24. Yonekura Y., Tamaki N., Senda M., Nohara R., Kambara H., Konishi Y., Koide H., Kureshi S.A., Saji H., Ban T., Kawai C. and Torizuka K., *Detection of coronary artery disease with ^{13}N-ammonia and high-resolution positron-emission computed tomography.* Am. Heart J., 1987. **113**: p. 645-654.

25. Hara T., Michihata T., Yokoi F., Sakamoto S., Masuoka T. and Iio M., *Quantitative measurement of regional myocardial blood flow in patients with coronary artery disease by intravenous injection of ^{13}N-ammonia in positron emission tomography.* Eur. J. Nucl. Med., 1990. **16**: p. 231 -235.

26. Gerber B.L., Melin J.A., Bol A., Labar D., Cogneau M., Michel C. and Vanoverschelde J.L., *Nitrogen-13-ammonia and oxygen-15-water estimates of absolute myocardial perfusion in left ventricular ischemic dysfunction.* J. Nucl. Med., 1998. **39**: p. 1655-1662.

27. Yamamoto Y., de Silva R., Rhodes C.G., Araujo L.I., Iida H., Rechavia E., Nihoyannopoulos P., Hackett D., Galassi A.R. Taylor C.J.V., Lammertsma A.A., Jones T. and Maseri A., *A new strategy for the assessment of viable myocardium and regional myocardial blood flow using ^{15}O-water and dynamic positron emission tomography.* Circulation, 1992. **86**: p. 167-178.

28. Iida H., Miura S., Shoji Y., Ogawa T., Kado H., Narita Y., Hatazawa J., Eberl S., Kanno I. and Uemura K., *Noninvasive quantitation of cerebral blood flow using oxygen-15-water and a dual-PET system.* J. Nucl. Med., 1998. **39**: p. 1789-1798.

29. Burchert W., Schellong S., van den Hoff J., Meyer G.J., Alexander K. and Hundeshagen H., *Oxygen-15-water PET assessment of muscular blood flow in peripheral vascular disease.* J. Nucl. Med., 1997. **38**: p. 93-98.

30. Muller R.A., Behen M.E., Rothermel R.D., Chugani D.C., Muzik O., Mangner T.J. and Chugani H.T., *Brain mapping of language and auditory perception in high-functioning autistic adults: a PET study.* J. Autism. Dev. Disord., 1999. **29**: p. 19-31.

31. Huitink J.M., Visser F.C., van Lingen A., Groeneveld A.B., Bax J.J., van Leeuwen G.R., Visser G.M., Van Loon M.J., Teule G.J. and Visser C.A., *Feasibility of planar fluorine-18-FDG imaging after recent myocardial infarction to assess myocardial viability.* J. Nucl. Med., 1995. **36**: p. 975-981.

32. Bax J.J., Visser F.C., van Lingen A., Cornel J.H., Fioretti P.M. and van der Wall E.E., *Metabolic imaging using F18-fluorodeoxyglucose to assess myocardial viability.* Int. J. Card. Imaging, 1997. **13**: p. 145-155.

33. Reske S.N., Bares R., Büll U., Guhlmann A., Moser E. and Wannenmacher M.F., *Klinische Wertigkeit der Positronen-Emissions-Tomographie (PET) bei onkologischen Fragestellungen: Ergebnisse einer interdisziplinären Konsensuskonferenz.* Nucl.-Med., 1996. **35**: p. 42-52.

34. Huang S.C., Yu D.C., Barrio J.R., Grafton S., Melega W.P., Hoffman J.M., Satyamurthy N., Mazziotta J.C. and Phelps M.E., *Kinetics and modeling of L-6-[^{18}F]fluoro-dopa in human positron emission tomographic studies.* J. Cereb. Blood Flow Metab., 1991. **11**: p. 898-913.

35. Wu J.C., Bell K., Najafi A., Widmark C., Keator D., Tang C., Klein E., Bunney B.G., Fallon J. and Bunney W.E., *Decreasing striatal 6-FDOPA uptake with increasing duration of cocaine withdrawal.* Neuropsychopharmacology, 1997. **17**: p. 402-409.

36. Coenen H.H., Kling P. and Stocklin G., *Cerebral metabolism of L-[2-^{18}F]fluorotyrosine, a new PET tracer of protein synthesis.* J. Nucl. Med., 1989. **30**: p. 1367-1372.

37. Meyer G.-J., Waters S.L., Coenen H.H., Luxen A., Maziere B. and Langström B., *PET radiopharmaceuticals in Europe: current use and data relevant for the formulation of summaries of product characteristics (SPCs).* Eur. J. Nucl. Med., 1995. **22**: p. 1420-1432.

38. Halldin C. and Nilsson S.-O., *Carbon-11 radiopharmaceuticals - radiopharmacy aspects*, in *Progress in radiopharmacy*, Schubiger P.A. and Westera G., Editors. 1992, Kluwer Academic Press: Dordrecht. p. 115-129.

39. Knapp W.H., Moser E. and Bares R., *Tumoren*, in *Nuklearmedizin*. Büll U., Biersack H.-J., Knapp W.H., Reiners C. and Schober O., Editors, 1994, Georg Thieme Verlag: Stuttgart. p. 420-452.

40. Schipper R.G., Rutten R.G., Sauerbeck M., Schielen W.J., Adams P.J., Kopitz J., Bohley P., Tesser G.I. and Verhofstad A.A., *Preparation and characterisation of monoclonal antibodies against ornithine decarboxylase.* J. Immunol. Methods, 1993. **161**: p. 205-215.

41. Pegg A.E., McGovern K.A. and Wiest L., *Decarboxylation of alpha-difluoromethylornithine by ornithine decarboxylase.* Biochem. J., 1987. **241**: p. 305-307.

42. Nishiyama M., Matsufuji S., Kanamoto R., Takano M., Murakami Y. and Hayashi S., *Two-step purification of mouse kidney ornithine decarboxylase.* Prep. Biochem., 1988. **18**: p. 227-238.

43. Iwami K., Wang J.Y., Jain R., McCormack S. and Johnson L.R., *Intestinal ornithine decarboxylase: half-life and regulation by putrescine.* Am. J. Physiol., 1990. **258**: p. G308-315.

44. Holinka C.F. and Gurpide E., *Ornithine decarboxylase activity in human endometrium and endometrial cancer cells.* In Vitro Cell Dev. Biol., 1985. **21**: p. 697-706.

45. Gritli Linde A. and Linde A., *Localisation of ornithine decarboxylase in mouse teeth. An in vitro and in vivo study.* Int. J. Dev. Biol., 1994. **38**: p. 107-115.

46. Glass J.R. and Gerner E.W., *Polyamine-mediated turnover of ornithine decarboxylase in Chinese-hamster ovary cells.* Biochem. J., 1986. **236**: p. 351-357.

47. Gaines D.W., Friedman L. and McCann P.P., *Apparent ornithine decarboxylase activity, measured by $^{14}CO_2$ trapping, after frozen storage of rat tissue and rat tissue supernatants.* Anal. Biochem., 1988. **174**: p. 88-96.

48. Bellofatto V., Fairlamb A.H., Henderson G.B. and Cross G.A., *Biochemical changes associated with alpha-difluoromethylornithine uptake and resistance in Trypanosoma brucei.* Mol. Biochem. Parasitol., 1987. **25**: p. 227-238.

49. Anehus S., Emanuelsson H., Persson L., Sundler F., Scheffler I.E. and Heby O., *Localisation of ornithine decarboxylase in mutant CHO cells that overproduce the enzyme. Differences between the intracellular distribution of monospecific ornithine decarboxylase antibodies and radiolabelled alpha-difluoromethylornithine.* Eur. J. Cell Biol., 1984. **35**: p. 264-272.

50. Pegg A.E., McCann P.P. and Sjoerdsma A., *Inhibition of polyamine biosynthesis and function as an approach to drug design*, in *Enzymes as targets for drug design*, Palfreyman M.G., McCann P.P., Lovenberg W.T., Temple Jr. J.G. and Sjoerdsma A., Editors. 1989, Academic Press: San Diego. p. 157-183.

51. Koch-Weser J., Schechter P.J., Bey P., Danzin C., Fozard J.R., Jung M.J., Mamont P.S., Seiler N., Prakash N.J. and Sjoerdsma A., *Potential of ornithine decarboxylase inhibitors as therapeutic agents*, in *Polyamines in biology and medicine*, Morris D.R. and Marton L.J., Editors. 1981, Marcel Dekker Inc.: New York. p. 437-453.

52. Jänne J., Pösö H. and Raina A., *Polyamines in rapid groth and cancer.* Biocim. Biopys. Acta, 1978. **473**: p. 241-293.

53. Westin T., Edstrom S., Lundholm K. and Gustafsson B., *Evaluation of ornithine decarboxylase activity as a marker for tumour growth rate in malignant tumors.* Am. J. Surgery, 1991. **162**: p. 288-293.

54. Bey P., *Substrate-induced irreversible inhibition of alpha-aminoacid decarboxylases. Application to glutamate, aromatic-L-alpha-aminoacid and ornthine decarboxylases*, in *Enzyme-activated irreversible inhibitors*, Seiler N., Jung M.J., and Koch-Weser J., Editors. 1978, Elsevier: Amsterdam. p. 27-42.

55. Metcalf B.W., Bey P., Danzin C., Jung M.J., Casara P. and Vevert J.P., *Catalytic irreversible inhibition of mammalian ornithine decarboxylase (E.C. 4.1.1.17) by substrate and product analogues.* J. Am. Chem. Soc., 1978. **100**: p. 2551-2553.

56. Palfreyman M.G., Danzin C., Bey P., Jung M.J., Ribereau-Gayon G., Aubry M. and Sjoerdsma A., *alpha-Difluoromethyl DOPA, a new enzyme-activated irreversible inhibitor of aromatic L-amino acid aecarboxylase.* J. Neurochem., 1978. **31**: p. 927-932.

57. Bey P., Vevert J.-P., Van Drosselear V. and Kolb M., *Direct synthesis of alpha-halogenomethyl-alpha-amino acids from the parent alpha-amino acids.* J. Org. Chem., 1979. **44**: p. 2732-2742.

58. Bey P. and Vevert J.-P., *Synthesis of alpha-alkyl and alpha-fluoroalkylised methyl-alpha-amino acids.* Tetrahedron Lett., 1977: p. 1455-1458.

59. Bey P. and Vevert J.-P., *New approach to the synthesis of alpha-halogenomethyl-alpha-amino acids.* Tetrahedron Lett., 1978: p. 1215-1218.

60. Abdel-Monem M.M., Newton N.E. and Weeks C.E., *Inhibitors of polyamine biosynthesis. 1. alpha-Methyl-(±)-ornithine, an inhibitor of ornithine decarboxylase.* J. Med. Chem., 1974. **17**: p. 447-451.

61. Golankiewicz K. and Wiewiorowski M., *Chemical equilibrium between ornithine and its lactams.* Acta Biochim. Pol., 1963. **10**: p. 443-448.

62. Abdel-Monem M.M., Newton N.E., Ho B.C. and Weeks C.E., *Potential inhibitors of polyamine biosynthesis. 2. alpha-Alkyl- and benzyl-(±)-ornithine.* J. Med. Chem., 1975. **18**: p. 600-604.

63. Pellegata R., Pinza M. and Pifferi G., *An improved synthesis of gamma-, delta-, and epsilon-lactams.* Synthesis, 1978: p. 614-616.

64. Gerhart F., Higgins W., Tardif C. and Ducep J.-B., *2-(4-Amino-4-carboxybutyl)aziridine-2-carboxylic acid. A potent irreversible inhibitor of diaminopimelic acid epimerase. Spontaneous formation from alpha-(halomethyl)diaminopimelic acids.* J. Med. Chem., 1990. **33**: p. 2157-2162.

65. Angelini G., Speranza M., Shiue C.-Y. and Wolf A.P., *$H^{18}F$ + Sb_2O_3: A new selective radiofluorinating agent.* J. Chem. Soc., Chem. Commun., 1986: p. 924-925.

66. Angelini G., Speranza M., Wolf A.P. and Shiue C.-Y., *Synthesis of N-(alpha,alpha,alpha-tri[^{18}F]fluoro-m-tolyl)piperazine. A potent serotonin agonist.* J. Labelled Cpd. Radiopharm., 1990. **28**: p. 1441-1448.

67. Schirlin D., Ducep J.B., Baltzer S., Bey P., Piriou F., Wagner J., Hornsperger J.M., Heydt J.G., Jung M.J., Danzin C., Weiss R., Fischer J., Mitschler A. and De Cian A., *Synthesis and inhibitory properties of alpha(chlorofluoromethyl)-alpha-amino acids, a novel class of irreversible inactivators of decarboxylases.* J. Chem. Soc. Perkin Trans. 1, 1992: p. 1053-1064.

68. Wagner J., Gaget C., Heintzelmann B. and Wolf E., *Resolution of the enantiomers of various alpha-substituted ornithine and lysine analogs by high-performance liquid chromatography with chiral cluant and by gas chromatography on chiral-val.* Analytical Biochemistry, 1987. **164**: p. 102-116.

69. Wagner J., Wolf E., Heintzelmann B. and Gaget C., *Chiral separation of enantiomers of substituted alpha- and beta- alanine and gamma-aminobutyric acid analogues by gas chromatography and high-performance liquid chromatography.* Journal of Chromatography, 1987. **392**: p. 211-224.

70. Coenen H.H., Klatte B., Knöchel A., Schüller M. and Stöcklin G., *Preparation of n.c.a. [17-^{18}F]-fluoroheptadecanoic acid in high yields via aminopolyether supported, nucleophilic fluoroination.* J. Labelled Cpd. Radiopharm., 1986. **23**: p. 455-466.

71. Luo H., Beets A.L., McAllister M.J., Greenbaum M., McPherson D.W. and Knapp F.F.R.J., *Resolution, in vitro and In vivo evaluation of fluorine-18-labelled isomers of 1-azabicyclo[2.2.2]oct-3-yl alpha-(1-fluoropent-5-yl)-alpha-hydroxy-alpha-phenylacetate (FQNPe) as new PET candidates for the imaging of muscarinic-cholinergic receptor.* J. Labelled Cpd. Radiopharm., 1998. **41**: p. 681-704.

72. Montague K.A., *Catechol compounds in rat tissues and in brains of different animals.* Nature, 1957. **180**: p. 244-245.

73. Carlsson A., Lindqvist M. and Magnusson T., *On the presence of 3-hydroxytyramine in brain.* Science, 1958. **127**: p. 417.

74. Carlsson A. and Waldeck G., *A fluorimetric method for the determination of dopamine (3-hydroxytyramines).* Acta. Physiol. Scan.,, 1958. **44**: p. 293-298.

75. Sibley D.R., Monsma F.J., Jr. and Shen Y., *Molecular neurobiology of dopaminergic receptors.* Int Rev Neurobiol, 1993. **35**: p. 391-415.

76. Shimada S., Kitayama S., Lin C.-L., Patel A., Nanthakumar E., Gregor P., Kuhar M. and Uhl G., *Cloning and expression of a cocaine-sensitive dopamine transporter complementary DNA.* Science, 1991. **254**: p. 576-579.

77. Giros B., el Mestikawy S., Godinot N., Zheng K., Han H., Yang-Feng T. and Caron M.G., *Cloning, pharmacological characterisation, and chromosome assignment of the human dopamine transporter.* Mol. Pharmacol., 1992. **3**: p. 383-390.

78. Hoffman B.J., *Molecular biology of dopamine transporters*, in *Dopamine Receptors and transporters*, Niznik H.B., Editor. 1994, Marcel Dekker, Inc: New York. p. 645-668.

79. Kuhar M.J., Sanchez-Roa P.M., Wong D.F., Dannals R.F., Grigoriadis D.E., Lew R. and Milberger M., *Dopamine transporter: biochemistry, pharmacology and imaging.* Eur. Neurol., 1990. **30**: p. 15-20.

80. Allard P.O., Rinne J. and Marcusson J.O., *Dopamine uptake sites in Parkinson's disease and in dementia of the Alzheimer type.* Brain Res., 1994. **637**: p. 262-266.

81. Hirai M., Kitamura N., Hashimoto T., Nakai T., Mita T., Shirakawa O., Yamadori T., Amano T., Noguchi-Kuno S.A. and Tanaka C., *[^{3}H]GBR-12935 binding sites in human striatal membranes: Binding characteristics and changes in Parkinsonians and Schizophrenics.* Jpn. J. Pharmacol., 1988. **47**: p. 237-243.

82. Janowsky A., Vocci F., Berger P., Angel I., Zelnik N., Kleinmann J.E., Skolnick P. and Paul S.M., *[^{3}H]GBR-12935 Binding to the dopamine transporter Is decreased in the caudate nucleus in Parkinson's disease.* J. Neurochem., 1987. **49**: p. 617-621.

83. Ginovart N., Lundin A., Farde L., Halldin C., Bäckman L., Swahn C.-G., Pauli S. and Sedvall G., *PET study of the pre- and post-synaptic dopaminergic markers for the neurodegenerative process in Huntington's disease.* Brain, 1997. **120**: p. 503-514.

84. Ritz M.C., Lamb R.J., Goldberg S.R. and Kuhar M.J., *Cocaine receptors on dopamine transporters are related to self-administration of cocaine.* Science, 1987. **237**: p. 1219-1223.

85. Volkow N.D., Fowler J.S., Wolf A.P., Wang G.J., Logan J., MacGregor R., Dewey S.L., Schlyer D. and Hitzemann R., *Distribution and kinetics of carbon-11-cocaine in the human body measured with PET.* J Nucl Med, 1992. **33**: p. 521-525.

86. Fowler J.S., Volkow N.D., Wolf A.P., Dewey S.L., Schlyer D.J., Macgregor R.R., Hitzemann R., Logan J., Bendriem B. and Gatley S.J., *Mapping cocaine binding sites in human and baboon brain in vivo.* Synapse, 1989. **4**: p. 371-377.

87. Boja J.W., Kuhar M.J., Kopajtic T., Yang E., Abraham P., Lewin A.H. and Carroll F.I., *Secondary amine analogues of 3beta-(4'sustituted phenyl)tropane-2beta-carboxylic acid esters and N-norcocaine exhibit enhanced affinity for serotonin and norepinephrine transporters.* J. Med. Chem., 1994. **37**: p. 1220-1223.

88. Goodman M.M., Keil R., Shoup T.M.S., Eshima D., Eshima L., Kilts C., Votaw J., Camp V.M., Votaw D., Smith E., Kung M.-P., Malveaux E., Watts R., Huerkamp M., Wu D., Garcia E. and Hoffman J.M., *Fluorine-18-FPCT: a PET radiotracer for imaging dopamine transporters.* J. Nucl. Med., 1997. **38**: p. 119-126.

89. Halldin C., Farde L., Lundkvist C., Ginovart N., Nakashima Y., Karlsson P. and Swahn C.-G., *[^{11}C]beta-CIT-FE, a radioligand for quantitation of the dopamine transporter in the living brain using positron emission tomography.* Synapse, 1996. **22**: p. 386-390.

90. Madras B.K., Meltzer P., C.,, Liang A.Y., Elmaleh D.R., Babich J. and Fischman A.J., *Altropane, a SPECT or PET imaging probe for dopamine neurons: I. Dopamine transporter binding in primate brain.* Synapse, 1998. **29**: p. 93-104.

91. Müller L., Halldin C., Farde L., Karlsson P., Hall H., Swahn C.-G., Neumeyer J., Gao Y. and Milius R., *[^{11}C]beta-CIT, a cocaine analogue. preparation, autoradiography and preliminary PET investigations.* Nucl. Med. Biol, 1993. **20**(3): p. 249-255.

92. Neumeyer J.L., Wang S., Milius R.A., Baldwin R.M., Zea-Ponce Y., Hoffer P.B., Sybirska E., Al-Tikriti M., Charney D.S., Malison R.T., Laruelle M. and Innis R.B., *[^{123}I]-2beta-Carbomethoxy-3beta-(4-iodophenyl)tropane: high-affinity SPECT radiotracer of monoamine reuptake sites.* J. Med. Chem., 1991. **34**: p. 3144-3146.

93. Wong D.F., Yung B., Dannals R.F., Shaya E.K., Ravert H.T., Chen C.A., Chan B., Folio T., Scheffel U., Ricaurte G.A., Neumeyer J.L., Wagner Jr H.N. and Kuhar M.J., *In vivo imaging of baboon and human dopamine transporters by positron emission tomography using [^{11}C]WIN 35,428.* Synapse, 1993. **15**: p. 130-142.

94. Scanley B.E., Al-Tikriti M.S., Gandelman M.S., Laruelle M., Zea-Ponce Y., Baldwi R.M., Zoghbi S.S., Hoffer P.B., Charney D.S., Wang S., Neumeyer J.L. and Innis R.B., *Comparison of [^{123}I]beta-CIT and [^{123}I]IPCIT as single-photon emission tomography radiotracers for the dopamine transporter in nonhuman primates.* Eur. J. Nucl. Med, 1995. **22**: p. 4-11.

95. Guilloteau D., Emond P., Baulieu J.-L., Garreau L., Yves F., Pourcelot L., Mauclaire L., Besnard J.-C. and Chalon S., *Exploration of the dopamine transporter: In vitro and In vivo characterisation of a high-affinity and high-specificy iodinated tropane derivative (E)-N-(3-iodoprop-2-enyl)-2beta-carbomethoxy-3beta-(4'-methylphenyl)nortropane (PE2I).* Nucl. Med. Biol., 1998. **25**: p. 331-337.

96. Bergström K.A., Halldin C., Hall H., Lundkvist C., Ginovart N., Swahn C.-G. and Farde L., *In vitro and in vivo characterisation of nor-beta-CIT: a potential radioligand for visualisation of the serotonin transporter in the brain.* Eur. J. Nucl. Med., 1997. **24**: p. 596-601.

97. Farde L., Halldin C., Müller L., Suhara T., Karlsson P. and Hall H., *PET study of [^{11}C]beta-CIT binding to monoamine transporters in the monkey and human brain.* Synapse, 1994. **16**: p. 93-103.

98. Kotian P., Mascarella S.W., Abraham P., Lewin A.H., Boja J.W., Kuhar M.J. and Carrol F.I., *Synthesis, ligand binding, and quantitative structure-activity relationship study of 3beta-(4'-substituted phenyl)-2beta-heterocyclic tropanes: evidence for an electrostatic interaction at the 2beta-position.* J. Med. Chem., 1996. **39**: p. 2753-2763.

99. Gee A.D., Moldt P. and Gjedde A., *The labelling of a novel tropane derivative [^{11}C]NS 2214 (BMS-204756) - an inhibitor of the dopamine transporter.* J. Labelled Cpd. Radiopharm., 1997. **39**: p. 959-972.

100. Swahn C.-G., Halldin C., Günther I., Patt J. and Ametamey S., *Synthesis of unlabelled, ^{3}H- and ^{125}I-labelled beta-CIT and its omega-fluoroalkyl analogues beta-CIT-FE and beta-CIT-FP, including synthesis of precursors.* J. Labelled Cpd. Radiopharm., 1996. **38**: p. 675-685.

101. Milius R.A., Saha J.K., Madras B.K. and Neumeyer J.L., *Synthesis and receptor binding of N-substituted tropane derivatives. High-affinity ligands for the cocaine receptor.* J. Med. Chem., 1991. **34**: p. 1728-1731.

102. Olofson R.A., *New, useful reactions of novel haloformates and related reagents.* Pure & Appl. Chem., 1988. **60**: p. 1715-1724.

103. Olofson R.A., Martz J.T., Senet J.-P., Piteau M. and Malfroot T., *A new reagent for the selective, high-yield N-dealkylation of tertiary amines: improved syntheses of naltrexone and nalbuthine.* J. Org. Chem., 1984. **49**: p. 2081-2082.

104. Crouzel C., Långstöm B., Pike V.W. and Coenen H.H., *Recommendations for a practical production of [^{11}C]methyl Iodine.* Int. J. Appl. Radiat. Isot., 1987. **38**: p. 601-603.

105. Larsen P., Ulin J. and Dahlstrøm K., *A mew method for production of ^{11}C-labelled methyl iodide from ^{11}C-methane.* J. Labelled Cpd. Radiopharm., 1995. **37**: p. 73-75.

106. Link J.M., Krohn K.A. and Clark J.C., *Production of [^{11}C]CH_3I by single pass reaction of [^{11}C]CH_4 with I_2.* Nucl. Med. Biol., 1997. **24**: p. 93-97.

107. Chaly T., Dhawan V., Kazumata K., Antonini A., Margouleff C., Dahl J.R., Belakhlef A., Margouleff D., Yee A., Wang S., Tamagnan G., Neumeyer J.L. and Eidelberg D., *Radiosynthesis of [^{18}F] N-3-fluoropropyl-2-beta-carbomethoxy-3-beta-(4-iodophenyl) nortropane and the first human study with positron emission tomography.* Nucl. Med. Biol., 1996. **23**: p. 999-1004.

108. Neumeyer J.L., Tamagnan G., Wang S., Gao Y., Milius R.A., Kula N.S. and Baldessarini R.J., *N-Substituted analogs of 2beta-carbomethoxy-3beta-(4'-iodophenyl)tropane (beta-CIT) with selective affinity to dopamine or serotonin transporters in rat forebrain.* J. Med. Chem., 1996. **39**: p. 543-548.

109. Neumeyer J.L., Wang S., Gao Y., Milius R.A., Kula N.S., Campbell A., Baldessarini R.J., Zea-Ponce Y., Baldwin R.M. and Innis R.B., *N-omega-fluoroalkyl analogs of (1R)-2beta-carbomethoxy-3beta-(4-iodophenyl)-tropane (beta-CIT): radiotracers for positron emission tomography and single photon emission computed tomography imaging of dopamine transporters.* J. Med. Chem., 1994. **37**: p. 1558-1561.

110. Middleton W.J., *New fluorinating reagents. Dialkylaminosulfur fluorides.* J. Org. Chem., 1975. **40**: p. 574-578.

111. Gaudette L.E. and Brodie B.B., *Relationship between the lipid solubility of drugs and their oxidation by liver microsomes.* Biochem. Pharmacol., 1959. **2**: p. 89-96.

112. Hansch C., Bjorkroth J.P. and Leo A., *Hydrophobicity and central nervous system agents: on the principle of minimal hydrophobicity in drug design.* J. Pharm. Sci., 1987. **76**: p. 663-687.

113. Leo A., Hansch C. and Elkins D., *Partition coefficients and their uses.* Chem. Rev., 1971: p. 525-555.

114. Strijckmans V., Hunter D.H., Dolle F., Coulon C., Loc'h C. and Mazière B., *Synthesis of a potential M_1 muscarinic agent [^{76}Br]bromo-caramiphen.* J. Labelled Cpd. Radiopharm., 1996. **38**: p. 471-481.

115. Zoghbi S.S., Baldwin R.M., Seibyl J., Charney D.S. and Innis R.B., *A radiotracer technique for determining apparent pKa of receptor-binding ligands.* Abstract book XIIth International symposium on radiopharmaceutical chemistry, Uppsala, June 15-19, 1997. p:136-138

116. Menniken F., Savasta M., Peretti-Renucci R. and Feuerstein C., *Autoradiographic localisation of dopamine uptake sites in the rat brain with ^{3}H-GBR 12935.* J. Neural. Transm., 1992. **87**: p. 1-14.

117. Hitri A., Venable D., Nguyen H.Q., Casanova M.F., Kleinman J.E. and Wyatt R.J., *Characteristics of [^{3}H]GBR 12935 binding in the human and rat frontal cortex.* J. Neurochem., 1991. **56**: p. 1663 -1672.

118. Laruelle M. and Maloteaux J.M., *Regional distribution of serotonergic pre- and postsynaptic markers in human brain.* Acta Psychiatr. Scand. Suppl., 1989. **350**: p. 56-59.

119. Winchell H.S., Baldwin R.M. and Lin T.H., *Development of I-123-labelled amines for brain studies: localisation of I-123 iodophenylalkyl amines in rat brain.* J Nucl Med, 1980. **21**(10): p. 940-946.

120. Mathis C.A., Mason N.S., Holt D.P. and Lopresti B.J., *A sensitive rapid method to quantitate metabolites of (+)- and (-)-[C-11]McN5652.* J. Nucl. Med., 1998. **39**(Abstract No.1053): p. 239.

121. Kuikka J.T., Åkerman K., Bergström K.A., Karhu J., Hiltunen J., Haukka J., Heikkinen J., Tiihonen J., Wang S. and Neumeyer J.L., *Iodine-123 labelled N-(2-fluoroethyl)-2beta-carbomethoxy-3beta-(4-iodophenyl)nor-tropane for dopamine transporter imaging in the living human brain.* Eur. J. Nucl. Med., 1995. **22**: p. 682-686.

122. Kazumata K., Dhawan V., Chaly T., Antonini A., Margouleff C., Belakhlef A., Neumeyer J. and Eidelberg D., *Dopamine transporter imaging with fluorine-18-FPCIT and PET.* J. Nucl. Med., 1998. **39**: p. 1521-1530.

123. Koeppe R.A., Holthoff V.A., Frey K.A., Kilbourn M.R. and Kuhl D.E., *Compartmental analysis of [^{11}C]flumazenil kinetics for the estimation of ligand transport rate and receptor distribution using positron emission tomography.* J Cereb Blood Flow Metab, 1991. **11**(5): p. 735-744.

124. Westera G., Buck A., Burger C., Leenders K.L., von Schulthess G.K. and Schubiger A.P., *Carbon-11 and iodine-123 labelled iomazenil: a direct PET-SPET comparison.* Eur J Nucl Med, 1996. **23**: p. 5-12.

125. Burger C. and Buck A., *Requirements and implementation of a flexible kinetic modeling tool.* J. Nucl. Med., 1997. **38**(11): p. 1818-1823.

126. Buck A., *Quantitative assessment of in vivo physiology with positron emission tomography*, in *Medizinische Fakultät.* 1995, Universität Zürich: Zurich.

127. Mikolajczyk K., Szabatin M., Rudnicki P., Grodzki M. and Burger C., *A JAVA environment for medical image data analysis: initial application for brain PET quantitation.* Med. Inform., 1998. **23**: p. 207-214.

128. Reddy G.N., Haeberli M., Beer H.-F. and Schubiger P.A., *An improved synthesis of no-carrier-added (NCA) 6-[^{18}F]fluoro-L-DOPA and its remote routine production for PET investigations of dopaminergic systems.* Appl. Rad. Isot., 1993. **44**: p. 645-649.

129. Beer H.-F., Haeberli M., Ametamey S. and Schubiger P.A., *Comparison of two synthetic methods to obtain [^{18}F] N-(2-aminoethyl)-5-fluoropyridine-2-carboxamide, a potential MAO-B imaging tracer for PET.* J. Labelled Cpd. Radiopharm., 1995. **36**: p. 933-945.

Appendix

Arbeitsvorschrift Herstellung [C-11]-β-CPPIT

Produkt: **[C-11]-β-CPPIT** 3β-(4'-chlorphenyl)-2β-(3'-phenylisoxazol-5'yl)tropan Code: C-L 7	Registrierung: C-L 7 11	Gültig ab: 11.3.99

Abteilung: Radiopharmazie/ Nuklearmedizin USZ Erstellt von: R. Schönbächler	Kontrolliert von: QUSS H. Stapfer	Seitenzahl: 3
Für die Einhaltung der Vorschrift verantwortlich: T. Cservenyak	Abteilungsleiter: Prof. Dr. P.A. Schubiger ..... (Datum)	

1. Definition

3β-(4'-chlorphenyl)-2β-(3'-phenylisoxazol-5'yl)tropan

in injektabler Lösung.

2. Chemikalien

Siehe Protokoll Herstellung β-CPPIT.

3. Synthesevorbereitung

Die semipräparative HPLC-Säule (Phenomenex Luna, C18, 250x10mm, 5µ, micron) ist mit dem Eluens für die semipräparative HPLC (0,1% Ammoniumformiat 20 / Acetonitril 80), welches alle 4 Wochen frisch hergestellt wird, 0,5 h bei einem Fluss von 0,8 ml/min zu spülen.

Folgende Lösungen werden kurz vor der Synthese frisch angesetzt:

2 mg Desmethyl-β-CPPIT (=Precursor) werden in einem 1,5 ml Reactivial in 300 µl DMF gelöst. Das Reactivial wird mit einem Septum verschlossen und in die Methylierungsanlage eingebaut.

4. Starten der [C-11]Produktion am Zyklotron

C-11-CO_2-dir, 60 Minuten, 60 µA

5. Vorbereitung der Produkt- und Probenfläschchen

Vial **a**: 1 Vial 30 ml (=Produktflasche), steril, mit Radioaktivaufkleber versehen (Beschriftung: [C-11]CPPIT, Chargen-Nr., Datum, Aktivität, Volumen, Kalibrationsdatum, Verfall)
nicht verwendeter Rest = Rückstellmuster.

Vial **b-c**: 2 Vials 10 ml, steril, mit Radioaktivaufkleber versehen (Beschriftung: [C-11]CPPIT, Chargen-Nr., Datum, Art der Probe: Vial b: Sterilität, Vial c: Isotonizität und Pyrogenität).

Vial **d**: 1 Vial 100 ml (NaCl 0,9%-Flasche) für die isotonische Lösung

1 Original-Perfusor®-**Spritze** OPS 50 ml Luer Lock Braun, steril (RN-USZ 850)
1 Connectub 1816P 10 M/F Polyethylen - **Schlauch** 150 cm / 1,0 mm, Laboratoire Plastimed, steril (RN-USZ 851)

Folgendes Material wird in der Laminarflowbox vorgelegt:

	RN-USZ-Nr.
1 Vial 30 ml, steril, mit Radioaktivaufkleber (Vial **a**)	815
1 Injektionsnadel (gelb: 0,9x55mm)	808
1 Filternadel (0,5 µm)	804
1 Sterilfilter (Sterile Vented Millex®-GS - 0,22 µm)	814
1 Injektionsspritze 1 ml	809
1 Injektionsnadel (grün: 0,80x80mm)	805
2 Vials 10 ml, steril, mit Radioaktivaufkleber (Vial **b-c**)	818
2 Filternadeln (0,5 µm)	804
1 Injektionsspritze 5 ml	811
1 Injektionsnadel (gelb: 0,9x55mm)	808
1 Ampulle Aqua ad Injectabilia Ph.H.VII, pyrogenfrei, 10ml	018
1 NaCl-Lösung 0,9%, steril, 100 ml (Vial **d**)	011
1 Messzylinder 100 ml	
1 Eppendorf-Pipette 1 ml	
1 Pipettenspitze blau (100-1000µl)	817
Ethanolum absolutum	003
Tween 80, Ph. Eur.	023

6. Vorbereitung der Lösung zum Aufnehmen des Produktes

Die Arbeitsschritte ist in der Laminarflowbox unter aseptischen Bedingungen durchzuführen.

Vial a: Filternadel einstechen, gelbe Injektionsnadel mit Sterilfilter versehen einstechen.
Vial b: Filternadel einstechen, mit gelber Injektionsnadel und 5ml Spritze 4ml Aqua ad Injectabilia zugeben.

Vial c: Filternadel einstechen.

Vial d: 90 ml NaCl 0,9% und 10 ml Ethanol im 100ml Messzylinder abmessen und zurück in die
100 ml NaCl-Flasche füllen. Mit der Eppendorf Pipette (mit blauer Spitze) 100 µl Tween 80 zugeben. Die so erhaltene Lösung gut schütteln und im Ultraschallbad 5 Minuten entgasen

7. Vorbereitung der Syntheseapparatur und Laden der Synthesesequenz

RN-USZ-Nr.

Material:

Aceton p.a.	400
Acetonitril p.a.	403
Aqua ad Injectabilia	018
Ethanol abs.	003

HPLC-Eluens
Isotonische Lösung zum Aufnehmen des Produktes (=Vial **d**)

1 Spitzkolben 25 ml
sterile Produktflasche mit Sterilfilter und Filternadel (=Vial **a**)

Das Labview-Programm für die CPPIT-Synthese aufstarten. Sequenz starten. Interaktive Anweisungen befolgen.

8. Synthese

Wenn die Bestrahlung beendet ist, beim Zyklotron-Computer Delivery drücken, die Methyliodidsynthese starten (Run drücken bei der Bediener-Konsole - Details siehe Betriebsanleitung GE Mel MicroLab) und mit der CPPIT-Synthese-Sequenz weiterfahren (ok drücken beim Labview-Programm).

Das Endprodukt wird in der Laminarflowbox mit einer Original-Perfusor®-Spritze (versehen mit einem Connectub-Schlauch) aufgezogen.

9. Kontrolle

Die Qualitätskontrolle des Produktes wird gemäß der Arbeitsvorschrift Qualitätskontrolle β-CPPIT durchgeführt.

1.3.99/rs

Protokoll Herstellung [C-11]-β-CPPIT

Registrierung: C-L 7 21

Datum: _____ Charge: _____ Hersteller:_____

Ausgangssubstanzen:	Code	Lieferant	Charge
N_2 / O_2 0.5%	110 RN-USZ	Carbagas	_____
Desmethyl-β-CPPIT	026 RN-USZ	PSI	_____
NaCl-Lösung 0,9%	011 RN-USZ	Braun	_____
Ethanolum absolutum	003 RN-USZ	Riedel de Haen	_____
Tween 80	023 RN-USZ	Fluka	_____

Materialien

Dimethylformamid	407 RN-USZ	Fluka	_____
H_2	105 RN-USZ	Carbagas	_____
Iod	434 RN-USZ	Merck	_____
Ascarite (II) 20-30 mesh	237 RN-USZ	Merck	_____
Molekularsieb 4A 80/100	238 RN-USZ	Alltech	_____
Porapak N 50-80 mesh	623 RN-USZ	Shimadzu	_____
Shimalite-Ni reduziert 80/100	239 RN-USZ	Shimadzu	_____
Millex - GS Filter	814 RN-USZ	Millipore	_____
Penicillinflaschen 10 ml	818 RN-USZ	PSI	_____
Penicillinflaschen 30 ml	815 RN-USZ	Amersham	_____

Laufmittel HPLC Produktion

Acetonitril	403 RN-USZ	Fluka	_____
Ammoniumformiat	246 RN-USZ	Fluka	_____
Wasser	431 RN-USZ	Fresenius	_____

Herstellung:

nach Arbeitsvorschrift Radiopharmazie USZ

Ausbeute

Endvolumen: _____ ml

Eingesetzte Aktivität: Zeit _____ _____ GBq

Erhaltene Aktivität: Zeit _____ _____ GBq

Ausbeute: kalibriert auf Produktionsende _____ %

Kontrolle des Endprodukts:

Sinnesprüfung
pH - Kontrolle Endprodukt
Osmolalitäts-Kontrolle Endprodukt
GC-Kontrolle Endprodukt
HPLC-Kontrolle Endprodukt
Probe Sterilität = 100 µl Endprodukt + 4 ml Aqua ad injectabilia (RN-USZ 18)
Probe Pyrogenität/Isotonizität* = 500 µl Endprodukt

(*Probe wird ins ZRP PSI-Ost geschickt.)

Verteilung: Perfusor-Spritze mit Schlauch (RN-USZ 850 und 851)

Charge	bestellte Aktivität	gelieferte Aktivität	Volumen [ml]	Kalibrationszeit	Visum

1.3.99/rs

Arbeitsvorschrift Qualitätskontrolle [C-11]-β-CPPIT

Produkt:	Registrierung:	gültig ab:
[C-11]-β-CPPIT 3β-(4'-chlorphenyl)-2β-(3'-phenylisoxazol-5'yl)tropan Code: C-L 7	C-L 7 31	11.3.99

Abteilung: Radiopharmazie/ Nuklearmedizin USZ Erstellt von: R. Schönbächler	Kontrolliert von: QUSS H. Stapfer	Seitenzahl: 3
Für die Einhaltung der Vorschrift verantwortlich: P. Pavlicek	Abteilungsleiter: Prof. Dr. P.A. Schubiger ..... (Datum)	

1. Allgemeines / Hilfsstoffe

1.1 Allgemeines

- Prüfung gemäss BAG-Dokumentation
- Kontrollergebnisse / Freigabe:
  Es liegen zu diesem Zeitpunkt die Prüfungen auf Aussehen, pH-Wert, Osmolalität, Identität des Radiotracers (HPLC), radiochemische Reinheit und chemische Reinheit (GC) vor. Die Prüfungen auf Sterilität und Pyrogenfreiheit können erst nach Anwendung des Radiotracers erfolgen.
- Rückhaltemuster werden mindestens 1 Jahr aufbewahrt.

1.2 Ausgangssubstanzen

Neben dem Wirkstoff β-CPPIT (< 0,01 mg/ml)
enthält das Produkt folgende Hilfsstoffe:

NaCl-Lösung 0,9%:	11 RN-USZ	(NaCl: 8,1 mg/ml)
Ethanolum absolutum:	03 RN-USZ	(0,8 mg/ml)
Tween 80:	23 RN-USZ	(1,0 mg/ml)

(Herstellung der isotonischen Lösung siehe AV Herstellung.)

2. Material

2.1 Chemikalien

HPLC-Laufmittel:

Acetonitril	Merck	403 RN-USZ
Triethylamin	Fluka	424 RN-USZ
Wasser Typ 1 Plus	KAZ	019 RN-USZ

2.2 Geräte - und Laborhilfsmaterial

pH-Wert:
pH-Indikatorstäbchen Neutralit®, pH 5-10, Merck Art. 9533 823 RN-USZ

Osmolalität:
Wescor Vapor pressure Osmometer 5500

HPLC:
HPLC - Anlage: LaChrom
Interface D 7000
UV - Detector L 7400
Pumpe L 7100
Autosampler L 7200
Flow count Bio Scan mit Aktivitäts-Detektor
Computer Compaq Deskpro XE 466

Säule: Phenomenex Luna 5µ C18, 250x4,6mm

GC:
GC - Fisons-Instrument
GC 9000 Serie
EL 980
VIC 900
Computer Compaq Deskpro XE 466
Interface D - 6000 A

Säule:
Chromosorb 101-80/100, 1/8 Zoll, Länge 3m, Brechbühler, 621 RN-USZ

3. Prüfung

3.1 Sinnesprüfung
Es wird auf Farbe und allfällige Schwebstoffe geprüft.

3.2 pH-Wert
Der pH-Wert wird mittels pH-Stäbchen Neutralit® ermittelt.

3.3 Osmolalität
Die Osmolalität wird am USZ mit dem Wescor Osmometer gemessen und am ZRP PSI-Ost nachträglich überprüft (weil die Lösung Ethanol enthält).

3.4 Radiotracer-Identität
Erfolgt mittels HPLC:

HPLC:	siehe Punkt 2.2
Säule:	siehe Punkt 2.2
Laufmittel:	0,1% Triethylamin 20 / Acetonitril 80
Injektionsvolumen:	20 µl
Flow:	1,5 ml/min.
Druck:	135 bar
UV:	254 nm
Retentionszeit:	Vergleich mit dem Standard

3.5 Radiochemische Reinheit
Die radiochemische Reinheit wird durch HPLC ermittelt.
Nuklididentität: Diese ist gewährleistet durch Messung der Halbwertszeit (20,4').
Nuklidreinheit: Diese Prüfung entfällt.

3.6 Chemische Reinheit
Mittels GC wird der Gehalt an Acetonitril überprüft. (Für den Standard wurde eine Eichgerade erstellt. Die Genauigkeit derselben wird durch wöchentliche Kontrolle überprüft. Bei einer Abweichung von > 20% wird die Eichung erneuert.)

3.7 Sterilität
Die Prüfung auf Sterilität (100µl Endprodukt in 4ml Aqua ad Injectabilia) erfolgt am ZRP PSI/Ost gemäss KV „Sterilität" Reg. KT - 001.63 innert einer Woche nach Chargenherstellung.

3.8 Pyrogenfreiheit
Die Prüfung auf Pyrogenfreiheit (500 µl Endprodukt) erfolgt am ZRP PSI/OST gemäss KV „Limulustest", Reg. KT - 809.63 innert einer Woche nach Chargenherstellung.

4. Richtwerte / Verfalldatum / Vorbehalte

4.1 Richtwerte

Sinnesprüfung:	klare, farblose, schwebstofffreie Flüssigkeit
pH-Wert:	5-8
Osmolalität:	290 ± 45 mmol/kg
Radiotracer-Identität:	Abweichung der Retentionszeit vom Standard < 10%
Radiochemische Reinheit:	> 95% (zur Kalibrationszeit)
Chemische Reinheit:	< 100 ppm Acetonitril
Sterilität:	steril
Pyrogenfreiheit:	Limulus negativ
Nuklididentität:	i.O.
Nuklidreinheit:	i.O.

4.2 Verfalldatum

3 Stunden nach Kalibration.

4.3 Vorbehalte

Unter Vorbehalt freigegeben werden dürfen Endprodukte mit einer radiochemischen Reinheit > 93% in Anlehnung an andere Vorschriften (z.B. Racloprid). Die semipräparative HPLC-Säule muss dann regeneriert werden.

1.3.99/rs

Kontrollprotokoll [C-11]-β-CPPIT

Produkt (Code): C - L 7.42 **Mikrobiologische Analysen-Nr.:**

Charge:

Chargengrösse: GBq in ml

Herstellungsdatum:

Musterzugsdatum:

Prüfung	Spezifikation	Resultat	Datum/Visum
Aussehen der Lösung	Klar, farblos, schwebstofffrei		
PH-Wert	5-8		
Radionuklididentität	$t_{1/2}$=20,4'		
HPLC	Abweichung t_R < 10% Reinheit > 95%		
GC / Acetonitril	< 100ppm		
Osmolalität	290 ± 45mmol/kg		

Befund (vor Applikation): 0 Sperrung 0 Freigabe

Freigabe - Vorbehalte:

Datum / Visum:

Limulustest	Negativ		
Sterilität	Steril		

Publications

Schönbächler R., Ametamey S. and Schubiger P.A., *Synthesis and ^{11}C-Radiolabelling of a Tropane Derivative Lacking the 2beta-Ester Group: a Potential PET Tracer for the Dopamine Transporter*, J. Labelled Cpd. Radiopharm, 1999. **42**: p. 447–456.

Ametamey S.M., Schönbächler R. , Allemann L. and Schubiger P.A., *Synthesis and first in vivo Results of a New Tropane Derivative Lacking the 2beta-Ester Group: a Potential PET Tracer for Imaging the Dopamine Transporter*, J. Nucl. Med., 1998. **Abstract Book 39**: p. 118.

Gucker P.M., Schönbächler R.D., Vollenweider F.X., Arigoni M., Berthold T., Buck A., Burger C., Schubiger P.A. and Ametamey S.M., *PET Studies with [^{11}C](+)McN-5652 in the Human Brain*, Eur. J. Nucl. Med. (submitted).

Buck A., Gucker P.M., Schönbächler R.D., Arigoni M., Vollenweider F.X., Ametamey S.M. and Burger C., *Evaluation of Serotonergic Transporters Using PET and [^{11}C](+)McN-5652, Assessment of Methods*, J. Cerebr. Blood F. Met. (submitted).

Schönbächler R.D., Gucker P.M., Arigoni M., Kneifel S., Vollenweider F.X., Berthold T., Buck A., Burger C., Schubiger P.A. and Ametamey S.M., *Positron emission tomography imaging of dopamine transporters in the human brain using [^{11}C]β -CPPIT, a new cocaine derivative lacking the 2beta-ester function*, J. Nucl. Med. Bio. (in preparation)

Burger C., Schönbächler R.D., Gucker P.M., Vollenweider F.X., Schubiger P.A., Ametamey S.M. and Buck A., *Modeling alternatives for [C-11]-beta-CPPIT*, J. Cerebr. Blood F. Met. (in preparation)

Presentations

Schönbächler R., *Synthese von ^{11}C- und ^{18}F-markierten Kokainderivaten als potentielle Tracer für den Dopamintransporter*, 5. Arbeitstreffen der Arbeitsgemeinschaft Radiochemie/Radiopharmazie, Wolfsberg CH, 9. - 11.10.1997.

Schönbächler R., *Synthese von ^{11}C- und ^{18}F-markierten Kokainderivaten als potentielle Tracer für den Dopamintransporter*, Aktuelle Forschung Pharmazie ETHZ, Zurich, 22.10.1997.

Schönbächler R., Ametamey S., Allemann L. and Schubiger P. A., *Synthese eines ^{11}C-markierten Kokainderivates als potentieller Tracer für den Dopamintransporter*, 85. Kongress der Schweizerischen Gesellschaft für Medizinische Radiologie, Solothurn CH, 14. - 16. 5.1998.

Curriculum Vitae

Name:	Roland Schönbächler
Born:	7.5.70 in Einsiedeln/SZ
1977-1983	Primary school in Einsiedeln
1983-1985	High school in Einsiedeln
1985 - 1990	Gymnasium in Pfäffikon/SZ
1990 - 1995	Study of Chemistry at the Swiss Federal Institute of Technology Zurich (ETHZ), specialisation on organic chemistry
1994	Dissertation in the Laboratory for organic chemistry of the ETHZ in the group of Prof. Dr. François Diederich (Subject: "Synthese von 1,8-Naphthyridin- und 9,9'-Spirobifluoren-Derivaten als Bausteine für enantioselektive Zucker-Rezeptoren").
1996 - 1999	Thesis at the Center for Radiopharmaceutical Science of PSI, ETHZ and USZ in the division of Prof. Dr. P. August Schubiger (Subject: "Evaluation of Three Cocaine Analogues as PET Tracers for the Dopamine Transporter and Synthetic Approaches to [F-18]-DFMO").